1985

Mississippi Lignite Utilization Stuides -- Task B, Pyrolysis and Gasification of Mississippi Lignites

J. E. Clemmer

Open-File Report 85-lFb

Mississippi Lignite Utilization Studies - Task B
Pyrolysis and Gasification of Mississippi Lignites

J. E. Clemmer and C. W. Williford

1985

The Mississippi Mineral Resources Institute
University, Mississippi 38677

FINAL REPORT

TASK B OF GRANT FOR

MISSISSIPPI LIGNITE UTILIZATION STUDIES

TASK B: Pyrolysis and Gasification of Mississippi Lignite

MMRI-85-1F
(G1144128)

Part A: Gasification of Mississippi Lignite in a Fixed Bed Gasifier

Part B: Rapid Pyrolysis of Mississippi Lignite

Co-Principal Investigators

J.E. Clemmer
C. W. Williford

Chemical Engineering Department
University of Mississippi
University, MS 38677

July 1985

ACKNOWLEDGEMENTS

In addition to MMRI-85-1F, this work was supported by grants from the Mississippi Chemical Corporation and the Department of Chemical Engineering in the form of release time for the Principal Investigators, Ms. Amy Burrow who provided a great deal of clerical support and Mr. Art Bowles who helped us a great deal in construction and maintenance of the equipment.

Mr. David R. Boswell and Ms. Noushin Arab, graduate assistants, who were supported by the above grants, did the majority of the experimental work on this project and are substantially responsible for producing this document.

ABSTRACT

PART A: STEAM GASIFICATION OF MISSISSIPPI LIGNITE IN A FIXED BED GASIFIER

Mississippi lignite samples were gasified in a steam atmosphere at temperatures ranging from 550 to 950°C in a 1 inch diameter fixed bed gasifier. Reaction time was varied from 10 to 50 minutes. Two particle sizes, 0.25 to 0.59 mm and 1.0 to 1.41 mm, were used. Also, runs were made at 870°C using Texas lignite samples (0.25 to 0.59 mm particle size).

Gas production from gasification of Mississippi lignite was found to be roughly 1.4 grams gas produced per gram dry-ash free coal. The gas produced (1-2 atmosphere pressure, steam atmosphere) was approximately 7.5 weight % hydrogen, 63 weight % carbon dioxide, 4.5 weight % methane and 22 weight % carbon monoxide. The gasification rate of Mississippi lignite was found to be comparable to that of North Dakota, Montana and Texas lignite (Big Brown Power Plant, Fairfield, Texas) and greater than Darco lignite. Hydrogen and carbon monoxide concentrations were found to increase at higher temperatures while methane and carbon dioxide concentrations decreased. Hydrogen concentration increases abruptly following pyrolysis and then levels off. The carbon dioxide, methane and carbon monoxide concentrations all decreased slightly and then leveled off.

PART B: RAPID PYROLYSIS OF MISSISSIPPI LIGNITE

Coal has emerged as the principal potential source of the synthetic pipeline gas and fuel gases that may be needed to supplement our rapidly dwindling natural gas reserves and to provide fuel alternatives for electrical utilities and other industries. Coal research pertinent to gasification is not new, and considerable experimental data are dispersed throughout the scientific and technical literature. Unfortunately, the phenomena are so complex that no unifying theory has evolved. The type of coal, the nature of the experiment, and the apparatus each profoundly influence the results; hence, only restricted interpretations have been possible.

The objective of this study is to correlate between devolatilization (weight loss), particle size and temperature.

The rapid devolatilization of Mississippi and Texas lignite was studied by electrically heating in helium. Approximately monolayer samples of small particles supported on wire mesh heating elements. The samples were rapidly brought to a desired temperature, held there for a desired time, and then rapidly cooled.

Weight loss from coals was essentially within a fraction to a few seconds depending upon temperature, and increased with increasing final temperature up to 900°C and decreasing particle size.

The general reaction schemes appears to involve thermal decomposition forming volatiles and initiating a sequence of secondary polymerization and char-forming reactions. The secondary reactions can be prevented by hydrogasification resulting in more volatile matter particularly methane.

We hope to find more ways to produce energy out to coal to replace our dwindling natural gas reserves.

TABLE OF CONTENTS

LIST OF TABLES FOR PART A; Gasification of Mississippi Lignite In a Fixed Bed Gasifier

LIST OF TABLES FOR PART B: Rapid Pyrolysis of Mississippi Lignite

LIST OF FIGURES FOR PART A: Gasification of Mississippi Lignite In a Fixed Bed Gasifier

LIST OF FIGURES FOR PART B: Rapid Pyrolysis of Mississippi Lignite

Page

Page

PART A

GASIFICATION OF MISSISSIPPI LIGNITE IN A FIXED BED GASIFIER

CHAPTER I

INTRODUCTION

Approximately twenty-two billion tons of recoverable lignite deposits lie beneath the surface of the gulf coast states. Recoverable deposits are defined as those in seams greater than three feet thick at depths less than 200 feet. Mississippi is second only to Texas in total tonnage with approximately twenty-five percent of these deposits. Figure 1 points out these deposits in the gulf coast states, while Figure 2 shows the deposits in Mississippi. Although about twenty million tons per year (15) of lignite are being combusted for electricity production in Texas, the lignite reserves have been essentially undeveloped in other southern states.

With the current prevailing energy costs, Mississippi lignite is probably not competive with coal from other states or other sources of energy. However, should energy become relatively more expensive in the future, development of Mississippi lignite may become feasible.(23)

Coal can be gasified in the presence of steam and oxygen (or air) to produce a medium (or low) BTU gas consisting of carbon monoxide, carbon dioxide, hydrogen, nitrogen (air

gasification), methane, and other light hydrocarbons. The principle reactions that take place during gasification may be represented as:

Gasification	$\Delta H_r°$, 298 cal/gmole
$C + H_2O \rightarrow CO + H_2$	+ 31,380
$CO + H_2O \rightarrow CO_2 + H_2$	- 9,840
$C + 1/2\ O_2 \rightarrow CO$	- 26,420
Methanation	
$CO + 3\ H_2 \rightarrow CH_4 + CO_2$	- 49,720

Since the steam carbon reaction is highly endothermic, the heat of reaction must supplied either externally or internally by partial combustion of a portion of the coal in air or oxygen. Gasification temperatures are normally in the range of 800° - 1200°C, depending on several factors, one of the more important of which is coal rank.(9) Lignites have a higher gasification rate than higher rank coals, allowing a lower temperature to be used. The upper temperature limit for gasification usually is the point at which the ash softens and agglomerates forming clinkers.

The product gas produced by coal gasification has many potential uses. The product, low or medium BTU gas, may be used "as is" for on-site industrial boilers. If oxygen is used as an oxidant, rather than air, medium BTU gas is produced.

Medium BTU gas may be used as boiler fuel, or, if the methane content is low, as synthesis gas. Synthesis gas, primarily a mixture of carbon monoxide and hydrogen, may be used in the petrochemical industry for methanol, acetic acid and complex alcohol production. Syngas may be used to produce high purity hydrogen which may be used in petroleum refining or in ammonia production. Syngas may also be used to manufacture synthetic crude oil, through the Fischer-Tropsch process. Medium BTU gas may be upgraded by purification and catalytic methanation to produce high BTU gas, also called synthetic natural gas (SNG) (19).

In this study, steam gasification will be studied with time, temperature and particle size as variables. Kinetics of the gasification process will be studied along with gas production data.

CHAPTER II

LITERATURE SURVEY

A. SURVEY OF COAL GASIFICATION

Gasification processes are frequently grouped together into three main categories: fixed bed, fluidized bed, and entrained bed.

Fixed bed gasification processes date back to the 1870's. These early methods were used to provide low BTU "town gas" before natural gas and oil became inexpensive and plentiful in the 1920's. Pressurized fixed bed reactors which could be operated semi-continuously were developed in Germany in the 1930's by Lurgi. In this fixed bed process, coal as solid lumps is fed at the top of the gasifier through a coal lock and moves slowly downward at a rate which is controlled by the amount of gasification agents, oxygen (or air) and steam supplied. As the coal flows downward, oxygen (or air) together with steam supplied at or near the bottom of the gasifier moves upward through the bed. The coal is converted to ash and gas by passing through the gasification and oxidation zones. The ash exits at the bottom of the gasifier. Temperatures must be kept below the softening or initial deformation temperature of the ash to prevent formation of ash clinkers and slag. (22)

in a fluidized bed reactor, carefully sized particles of crushed coal are suspended within the reaction vessel by the upflow of oxidant, gasified products from the coal, and temperature moderators such as steam. Feed coal is added intermittently at the top or middle of the fluidized bed and spent coal and ash are withdrawn from the reactor's base. Raw product gas is taken from the top of the reactor. The prevention of clinker formation is even more important in fluidized beds, since the formation of large clinkers may seriously affect the fluidization of the bed. Dust particles in the product gas are another serious problem in this process. Examples of this process are the Winkler pressurized fluidized bed process, the CO_2 acceptor method (Conoco) and the Exxon catalytic method (3).

Entrained flow gasifiers differ from the previous designs in that oxidant and finely ground coal particles flow concurrently as opposed to the counter current flow of fixed and fluidized bed reactors. Flow in these gasifiers may be upward or downward and more than one stage may be employed. Two of the most commonly used entrained flow processes are the Koppers-Totzek process and the Texaco slurry method. Some companies have experimented with molten bath gasifiers. In these designs, coal, oxidant, and steam are injected into a hot liquid pool of molten salt, iron or ash. Product gases rise from the bath's surface while ash and other by-products

remain behind. Research concerning underground ("in situ") coal gasification is proceeding at several sites in the United States (19).

B. LIGNITE PROPERTIES AND PARAMETERS FOR GASIFICATION

Lignite (or brown coal) is the lowest rank in the metamorphic development of a coal substance. Coals may be ranked in ascending order of carbon content to form a continuous coal series :

peat -> lignite -> subbituminous coal -> bituminous coal -> anthracite

Chemical composition of coal is defined in terms of proximate analysis. This analytical procedure divides the coal content into four categories: moisture (includes bulk and physically adsorbed water), volatile matter (that matter which is lost from a dry sample when heated at a specified temperature for a specified time in an inert atmosphere, ASTM standards prescribe 7 min. at 950°C (3)), ash (material left behind when all organic material has been burned off), and fixed carbon (organic material which was not lost in the devolatilization step). Proximate analysis data for five lignites including Mississippi lignite is included in Table 3. Also, occasionally reported with proximate analysis of coal is the fuel ratio. This is the ratio of fixed carbon to volatile matter. An ultimate or elemental analysis reports

percentages of carbon, hydrogen, nitrogen, sulfur and oxygen in the coal. Ultimate analyses of five lignites are given in Table 7. A mineral analysis may also be done on the remaining ash.

Many properties of Mississippi lignite must be recognized when considering its utilization. High moisture (approximately 40% as received) and ash (10-30%) content contribute to high mining, transportion, and drying costs. Also the fuel ratio is very low, causing a smoky flame if combusted and increasing the possibility of spontaneous combustion during storage. Heating value is low, at approximately 6000 Btu/lb compared to bituminous coal at 10-15000 Btu/lb (3). The coal is friable with a large fraction reduced to dust during crushing. Some processes may have problems handling the fines produced during crushing. This is not a problem, however, in the methods which use an oil or water slurry (4). Also, the Lurgi Company has developed methods of agglomerating coal fines for gasification in a fixed bed (22). Not all of the properties of the Mississippi lignite are poor, however. Sulfur content is moderate, 0.5 - 2.0%. Also, lignites in general have a higher activity in gasification than higher rank coals. High gasification activities are important because lowering of the gasification temperature makes possible substantial improvements in thermal efficiencies. (9)

Lignites have a low caking tendency. A tendency of many coals to cake under gasification conditions can cause problems in some commercial processes (22).

Several explanations have been proposed for the increased activity of lignites in gasification. Alkali and other metal compounds are effective catalysts for the steam carbon reaction. Studies showing the catalytic effect of cesium, potassium, calcium, rubidium, sodium, lithium, cobalt, iron and other transition metals have been found in the literature (14, 10, 13, 21, 29, 24, 17, 18, 11). Examples of these catalysts appearing naturally in the Mississippi lignite ash (see Table 4 for ash mineral analysis) are calcium, potassium, sodium and iron. The order of catalytic activity for the alkali metals is Cs > K > Na > Rb > Li (11). For transition metals the order is Rh > Ru > Ir > Ni >> Pd > Co > Fe (10). Another factor believed to contribute to the high gasification activity is the high concentration of carbon sites active for gasification. It has been reported that the concentration of carbon sites active to gasification increases with decreasing rank, and the accessibility of reactant gases to the active sites may also increase with decreasing rank. (9,12)

As temperature increases, gasification rate also increases. The reaction rate of steam gasification has been shown to fit the first order kinetic model shown in Equation 1 (16, 13, 27, 30) .

$$\frac{dX}{dt} = \kappa (1 - X) \quad (1)$$

where X = carbon conversion

κ = 1st order rate constant

t = time

The temperature dependence of the gasification rate follows the Arrhenius relation shown in equation 2 (30, 6, 18, 10, 21, 24) .

$$k = k_o \exp(- E/RT) \quad (2)$$

where k_Q = frequency factor

E = activation energy

R = gas constant

T = absolute temperature

Pressure and component partial pressure (particularly hydrogen) are important parameters in the gasification process. Zabranský and Nandi (30) report little, if any, effect of pressure on the rate of gasification in steam in the range studied (14.6 - 41.8 atm). The atmosphere I used was steam at near atmospheric pressure (1-2 atm). The hydrogen partial pressure, however, is important if the gasification is taking place in a hydrogen atmosphere. Gasification rate increases with increasing hydrogen partial pressure (30,2). Increasing the hydrogen partial pressure also increases the concentration of methane in the product gas. Researchers have investigated many different atmospheres for the gasification

process. In commercial processes, air (or oxygen) is generally used as an oxidant to produce heat for the reaction with steam added as a temperature moderator and to produce carbon monoxide and hydrogen. The amounts of each injected may be used to control the temperature and products produced. Atmospheres investigated by laboratory researchers are pure steam (30, 20, 18, 11, 6), hydrogen (30, 2), steam-hydrogen mixtures (30), air (8, 20) and combinations of these with additional inert gases such as nitrogen, helium and oxygen (7,8).

Very little experimental evidence has been obtained on the effect of particle size on gasification behavior. Anthony et al. (2) varied particle size over the range of 53 to 1000 pM in both hydrogasification and pyrolysis experiments. The effect of particle size was found to be substantial for Pittsburgh seam bituminous coal in hydrogen atmosphere but small for helium. In the case of Montana lignite, no significant effect of particle size was observed in either hydrogen or helium. It has also been proposed that resistance to mass transfer increases with increased rank. Drying and devolatilization may open up the pore structure of the lignite particle (1) increasing mass transfer within the particle.

Previous similar work done using Mississippi lignite includes a micro pulverization study (4), studies on drying

and devolatilization (1) and a study on pyrolysis in a fixed bed (5). The work done on pyrolysis was done using the same equipment and was the background step for this study. Some of the conclusions of this study follow. Volatile content removed was found to increase for increased temperatures below 700 degrees C and constant over 700 degrees. Production (grams per gram DAF) of carbon monoxide, methane and hydrogen was found to increase in increasing temperatures. Carbon dioxide production was approximately constant. The molecular weight of the gas was found to decrease with increasing temperature. Also gas produced was found to increase with respect to temperature.

CHAPTER III

EXPERIMENTAL APPARATUS

The apparatus used in this study is basically the same as that used by Farage (5) except for modifications necessary to introduce steam into the reactor.

The reactor and support analysis equipment used in the devolatilization experiments will be presented in three major sections: (a) The gasification unit, (b) the gas chromatograph, and (c) the proximate analysis coal analyzer. All of this information will be given in as much detail as is practical and necessary. Appendix B contains all the supporting figures referred to in this and following chapters.

A. DEVOLATILIZATION UNIT GENERAL

A basic diagram of the unit has been provided in Figure 3 to aid in the respective location of each section. All tubing components are made of either 304 or 316 stainless steel if they are exposed to the reactor gases or tars. The Swagelok fittings and the tube sizes ranged from one inch for the reactor, one-eighth inch for product gas lines to one-sixteenth inch lines in the gas chromatograph. The only section of the system that does not have metal tubing is the portion of the gas network going from the sample system to the glass saturator

bottles and on to the wet test meter (Figure 3). This section of tubing is very short and is TYGON plastic tubing.

I

B. GAS AND COAL INPUT SYSTEM

The helium carrier gas for the unit is supplied in bottled form and is regulated once from the bottle for bulk flow to the system and the coal hopper. It is regulated again for accurate flow control to a rotameter. The rotameter is used in line to check the rough flow rate of the purge gas through the reactor. The helium rate is fine-tuned by the use of the wet test meter and accurately measured before each run with a bubble tube.

The coal is measured and placed in the hopper on top of the reactor. The hopper can be purged of air and pressurized with helium for sample injection. The sample is held from the reactor by a one-half inch ball valve below the hopper.

Both the coal and the helium flow downward into the heated zone to the reactor through one-half inch tubing.

C. STEAM GENERATOR

The steam generator consists of a coil of 1/4 inch stainless steel tubing (8 turns, 9 inches long by 2% inches in diameter) which passes through a Mellon electric furnace (inside dimensions - 14^ inches long by 3 1/4 inches in diameter). This preheater is capable of heating the enclosed tubing to over 550°C. The furnace is controlled by a type K Love

controller. Water is added at a measured rate using a Lapp Microflo Pulsafeeder metering pump. The water along with the helium carrier is heated and vaporized in the coils in the preheater. Following the preheater the tube diameter is increased to *h* inch. Five inches of the tubing between the preheater and the reactor is filled with stainless steel wool to prevent entraining of water droplets. All tubing between the preheater and the reactor is wrapped with electric heating tape to prevent condensation of the steam.

D. REACTOR AND FURNACE SYSTEM

The reactor, from the top, consists of a one-half inch tube that joins a Swagelok reducing union which brings the reactor to one inch tubing (Figure 3). Both ends of the 28 inch reactor tubes have identical reducing unions and are kept outside the heated zone to prevent gauling. The lower union has been bored to allow the one-half inch tube to enter the one inch tube. On the end of the one-half inch tube is placed a specially machined sleeve welded reducing union that has not been welded in place (Figure 3). A 100 mesh stainless steel screen fits snuggly atop the one inch end of the welded union. By sliding the tubing up into the bottom union, the welded union and screen can be placed in the lower edge of the middle section of the furnace. With the screwed fittings outside the furnace we are allowed access to the screen and

the reactor internals for examination. If these parts were inside the furnace then they would be hopelessly welded together after the first run.

The furnace is a three zone, 2000 watt Marshall model 20235 split furnace. It is mounted vertically on a rail car which allows for easy removal of the furnace at the end of a run. Each zone of the furnace has its own type K Love controller. This helps achieve even heating down the furnace.

The exit gas temperature is measured by a type K thermocouple stationed just below the reactor screen. This thermocouple is connected to a model 400 Trendicator temperature indicator.

E. TAR COLLECTION SYSTEM

Both the hot tars and gas leave the bottom of the reactor through one-half inch tubing which is reduced to one-quarter inch tubing before entering the first tar trap. The traps are constructed using a one inch cap fitting. The cap has a center tapped hole bored in it with a rounded one-quarter inch union silver soldered in place. To one side of the center, a one-eighth inch hole was bored and a section of the same size tubing was also silver soldered in the hole to allow the gases to leave. The center union has been center bored to allow the one-quarter inch tube from the reactor to pass down into a 25 mm x 100 mm pyrex culture tube. The culture tube is

sealed to the cap by a one inch nut and teflon ferrei set. The first tube is fitted with a nut and cap at the bottom. A 1/4 inch tube leads from the cap to a valve which allows draining of water from the trap preceding each run. The second tube has a closed bottom. Both of those tubes are placed in an ice bath for an experiment. This successfully stops all tar and water from reaching the gas sampling system.

F. SAMPLES AND VOLUME MEASUREMENT SYSTEM

The cleaned gas from the reactor and tar traps now must be sampled for composition and its volume measured. In Figure 3, the piping arrangement of the sample network can be viewed graphically more simply than it can be explained verbally. The sample network allows the evacuation of each sample bottle and separate sample collection. This is done independently of the other sample bottles. The sample bottles are only about 30 milliliters in volume and are constructed of tubing and fittings. All bottles were thoroughly leak tested. Each bomb connects to the network by means of a quick-connect fitting. This feature lets us capture a sample, seal it, and later inject it to the gas chromatograph for composition analysis.

The remainder of the gas now passes through a short section of TYGON tubing to two glass saturator bottles. These bottles are arranged so that if a vacuum is placed on the gas

network by accident, no water will enter the sample network.

The saturated gas now enters a Precision Scientific three liter Wet Test Meter. The wet test meter has a thermometer and a mercury manometer attached to it for monitoring gas temperature and pressure. Gas leaving the wet test meter is vented to the atmosphere.

G. GAS CHROMATOGRAPH SYSTEM

The gas composition from each sample of a run is analyzed with a Carle 111H Gas Chromatograph (GC) which is equipped with a palladium hydrogen transfer tube. This feature will separate the hydrogen in the sample from the rest of the gas and the helium carrier gas. The GC is equipped with a thermal conductivity detector using thermistors. The GC has been calibrated against a standard gas containing hydrogen, carbon dioxide, oxygen, nitrogen, methane, and carbon monoxide. The other gases are approximated using an estimate of their proportionality factor.

In order to calibrate the GC we assumed that carbon monoxide possessed a K, a proportionality factor, equal to one. This was caused by a limitation on the number of degrees of freedom on the set of equations used for the calibration. The basic equation used is:

$$Vo_1 \quad \Gamma\ /\tau\lambda - \frac{K(I) * A(I)}{K(I) * A(l)+K(2) * \ddot{A}(\ 2) + \cdots+K(N) * A(N)}$$

where KI), Volume % (I), and A(I) are the component proportionality constant, volume percent and the relative area for the 1-th component of N components. We know all the areas, the volume percents and the value of K for carbon monoxide. With this knowledge we can solve a set of five equations and five unknowns using simple linear algebra. The value of K has been placed in tabular form in Appendix A, Table 5.

The gas samples are injected into the one milliliter sample loop by first evacuating the sample system and sealing it off at about 29 inches of vacuum. The sample can then be sent into the loop and injected without fear of contamination.

The GC uses a Houston Instruments Model 150 strip chart recorder with a sweep integrator. This allows each peak to be integrated and placed into the GC mass balance computer program.

H. COAL ANALYSIS SYSTEM

The coal sample and the char samples were analyzed for proximate analysis values with a Model 490 Fischer Coal Analyzer. We used 10 milliliter Airtight Quartz crucibles that release volatiles, but do not allow oxygen back into the crucible during devolatilization. The analyzer is equipped with a microprocessor that controls all functions on the unit. The analyzer has separate programs for sparking and nonsparking coal devolatilization, ASTM ash, and Fischer ash preset

programs. It also allows for user programmable volatiles and ash analysis.

The nonsparking volatiles program was used to analyze the lignite and char for volatile content. This program heats the oven dried sample to 950 degrees Centigrade at 35 degrees Centigrade per minute and hold for seven minutes. The crucible covers are left on to keep the oxygen away from the sample. The furnace fan is off to reduce the air current which might enter the crucibles.

The Fischer ash program was used since we had already devolatilized our sample before checking the ash content. The devolatilized samples are heated to 750 degrees Centigrade at 35 degrees Centigrade per minute and held at that temperature for three hours with the crucible covers off. Also, the furnace fan is on to allow for improved air circulation.

Each char sample and one coal sample was submitted to Galbraith Laboratories for a carbon hydrogen analysis (char sample) or ultimate analysis (coal sample).

CHAPTER IV

EXPERIMENTAL PROCEDURE

The procedures for the operation of the unit and the analysis of the lignite, char and gas can be separated into proximate analysis, run of the experiment, and analysis of products. The data from some of these procedures are only useful for an individual experiment, but some will be used over a series of runs.

A. PROXIMATE ANALYSIS

Preliminary analysis of the lignite must be done for use with the other gasification data and to know the fraction of water, volatiles, fixed carbon, and ash. The analysis of the lignite and char was performed per the instructions with the Model 490 Fischer Coal Analyzer, Manual No. 43661. The lignite and char were dried in the oven at 107 degrees Centigrade for one hour. The volatiles were released using the nonsparking volatiles program with a furnace hold time of seven minutes. Thefixed carbon and ash were determined using the Fischer Ash program with the crucible covers off as opposed to the volatiles analysis with the crucibles covered. The lignite proximate analysis was only done for several samples to begin with and was checked periodically for changes.

B. DETAILS OF GASIFICATION EXPERIMENT

The actual run of the experiment can be accomplished in approximately four hours, if no technical problems arise. The reactor must first be leak tested under pressure with the bottom of the reactor capped. After this the furnace can be put into place and the power turned on to begin heating the reactor. The helium is regulated to a maximum of 20 pounds per square inch (gauge) into the rotameter choke valve. The rotameter is adjusted for approximately 100 milliliters per minute of flow to purge the reactor and the rest of the system of air. When all the air is gone, in about ten to fifteen minutes, the flow rate should be set to ten milliliters per minute during the rest of the heating period.

While the reactor is heating, the lignite sample that has been ground to 0.25 mm to 0.59 mm (or 1.00 to 1.41 mm) particle size should be measured for use in the experiment. The sample size is very important. If the sample size is allowed to vary drastically, then the heat transfer characteristics of the lignite may change. Our goal was to use a sample size of 15 grams. This would make the bed size in the reactor 8.5 centimeters in depth. The sample is now sealed in a flask and set aside until time for sample injection.

The helium flow rate is verified by use of the wet test meter (WTM) over a five to ten minute period of time due to the slow rate of flow of the carrier gas.

As the furnace begins to equilibrate, the final temperature should be checked and adjusted to the desired value. Next, a temperature probe is inserted to check the temperature profile of the furnace through the three thermocouple ports. Adjustments are made on the temperature controllers to bring all three zones of the furnace to the same temperature.

All gas sample bombs are attached to the sampling network and evacuated. This allows for rapid sampling of the product gas during the run. Approximately thirty minutes before the start of the run, the preheater furnace is switched on and heated to approximately 500°C. The power is also switched on to the heating tape heating it up to approximately 275°C.

The unit is now ready for the sample to be placed in the hopper. The hopper must be purged of as much air as is possible by bleeding helium pressurized gases out of the hopper. The hopper is placed under positive helium pressure of 30 pounds per square inch (gauge) until sample injection. This will amount to approximately 0.28 liters of helium that will be subtracted from the total gas production.

Ice is now placed around the tar traps and the wet test meter is zeroed for the beginning of the experiment. The pulsafeeder pump is then started to begin steam flow to the reactor. When the reactor and furnace temperatures are stable, then the run is ready to begin.

All helium flow to the hopper is stopped, the water is drained from the tar traps, the hopper dump valve is opened, the timer is started and run data is collected. Since much oí the gas is evolved in the first few minutes for the medium and high temperature experiments, short interval data gathering is important. The reactor temperature, reactor pressure, water input and gas volumes are all checked every fifteen seconds for the first five minutes. After five minutes, readings are taken at intervals of thirty seconds. After ten minutes, the readings are taken at one minute intervals.

Gas samples are taken at different times during the run. Generally five samples were taken for the 10 minute runs, six for the 20 minute runs, and seven for 30 minute or longer runs. Sample taking was concentrated during the first few minutes of the run since the gas production was greatest during this period. This technique of gas sampling is used to estimate the average gas composition and thereby the average molecular weight of the gas produced.

The samples are taken by closing the vacuum manifold valve and opening the sample manifold valve. Next, the bomb valve is closed and the sample bomb feeder line is evacuated by re-opening the vacuum manifold valve for a moment. The sample may now be removed at the quick-connect fitting. This fitting will allow the sample to be attached to the gas chromatograph See Figure 4 for more information on the sample valve arrange-ment .

At the end of the run the furnace is turned off and rolled away from the reactor. Helium flow is turned up to about 3 liter/min to purge the reactor of reactants and quench the reaction. Cooling occurs rapidly after the furnace is removed. As soon as possible, after the reactor is below 200 degrees Centigrade, the tar traps are removed and the reactor is sealed with a cap fitting. The helium carrier is turned off. The tar traps are removed together and are sealed for later weight analysis. When the reactor is below 100 degrees Centigrade, we open the reactor and pour the granular char into a pre-weighed screw top bottle. The char will be re-weighed in the bottle to obtain the weight of the char. All of the materials are now collected and now must be analyzed.

C. PRODUCT ANALYSIS

The products are in three forms: char, tar and gas. These will be discussed, in order, with emphasis on the gas chromatography procedures.

The char from each run is weighed and subjected to a full proximate analysis to determine the amount of volatiles remaining, the fixed carbon content, and the weight of ash. The procedure for this is referenced in this chapter under the preliminary analysis section for the lignite proximate analysis.

First the water is decanted and weighed. The tar traps are disassembled and each piece is weighed with the tar still in

place. Then the parts are cleaned with methylene chloride and methanol. After each part is cleaned, it is air dried and reweighed. The sum of the difference is the amount of tar from that run.

The gas in each sample bomb must also be analyzed for the composition of the gas. The Carle Model 111H Analytical Gas Chromatograph is operated as per the operating procedures in the Carle manual for this unit, Part Number 30491. The operation of the sample injection system is not complex, but must be understood to be operated properly and accurately.

The injection system is drawn in Figure 4. The sample loop consists of the one milliliter internal gas chromatograph loop, the vent line to the valve, the sample line to the sample bomb quick-connect, and the sample line to the standard gas valve. All of the sample loop must first be evacuated by opening the vacuum line valve. After the loop is fully evacuated, the vacuum valve may be closed. The sample bomb valve is cracked to allow the gas to bleed into the sample loop. The sample must be the same in size. This is accomplished by bleeding the sample into the evacuated sample loop until the pressure is 15 inches mercury of vacuum. At this time, the sample is ready to be injected. The valve switching for the GC may be found in the previously mentioned Carle manual.

CHAPTER V

RESULTS AND DISCUSSION

Data from nineteen usable steam gasification runs (outlined in Table 6) will be presented in tabular form in Appendix A and in graphical form in Appendix B. The variables were time, temperature and particle size for the Mississippi lignite and one series of runs was made with Texas lignite. The data will be discussed in two sections. The first is carbon conversion, which will also contain gasification kinetics. The second section will be a presentation of the material balance data, principally the gas content and make up.

The experimental results for carbon conversion in this work have been presented using three different methods. The first is fixed carbon conversion. The fraction of fixed carbon conversion, X_f, is defined by equation 1.

$$X_f = \frac{y_C C_O - y_T C_T}{y_C C_O} = \frac{\text{fixed carbon gasified}}{\text{fixed carbon in feed}} \qquad (1)$$

where y_O = fraction fixed carbon in the lignite (dry basis)

y_T = fraction fixed carbon in the char (dry basis)

C_O = lignite charged to the reactor (dry basis)

C_T = char recovered (dry basis)

Conversion data calculated in this manner was compared with data for carbon conversion collected by Zabranský and Nandi (29). They calculated base carbon conversion as shown in equation 2.

$$X_b = \frac{\text{base carbon gasified}}{\text{base carbon in feed}} = \frac{C - C^o}{C_b} \qquad (2)$$

where C^o - carbon in the fixed carbon fraction of the feed

C_b - carbon in the fixed carbon fraction of the char

Calculations using proximate analysis and carbon content data of the raw lignite and two samples of devolatilization chars showed that essentially all of the fixed carbon fraction of the lignite is actually carbon. Therefore, X_b should be approximately equal to X_c, making it valid to compare the values for base carbon conversion from Zabranský and Nandi (29) with those found for fixed carbon conversion in this study.

Conversion data was also calculated on a basis of the fraction of carbon converted. This calculation was done using carbon content analyses of the lignite used and for each char. The fraction carbon converted is defined by equation 3.

$$Y_c = \frac{\text{carbon gasified}}{\text{carbon in feed}} \qquad (3)$$

Another way of considering the coal conversion was to take into consideration all the carbonaceous material removed, i.e. the fraction of volatiles and fixed carbon removed. The fraction carbonaceous material converted is defined by equation 4.

$$X_{cm} = \frac{\text{Vol. 8 F.C. gasified}}{\text{Vol. 8 F.C. in feed}} \qquad (4)$$

The temperature reported for each run is the final bed temperature after the fluctuations caused by sample injection have ceased. After the initial temperature drop, the temperature generally returned to near the final value within 3 - 3.5 minutes. Temperature and gas volume history for all runs appear in Figures 17-34.

Figure 5 shows the fraction of fixed carbon converted versus reaction time. Only one run was made at 550 degrees Centigrade because it was decided that the reaction rate at this temperature was very slow.

In the 30 minute run at 550 degrees Centigrade, the fixed carbon conversion fraction was 0.205. The data from the 750 degree Centigrade run was smoothed by linear regression on a TI 55-11 and the regressed values ranged from 0.582 at 30 minutes to 0.693 at 50 minutes. The duration of the runs was reduced for the 870 and 950 degree runs to 10, 20 and 30 minutes. Conversion at 870 degrees Centigrade ranged from Xf = 0.921 at 10 minutes to Xr = 0.989 at 30 minutes. At

950 degrees Centigrade, fixed carbon conversion was 0.955 in 10 minutes. Gasification neared completion (X_c = 1.00) at 20 and 30 minutes. Although a small amount of carbon was found on the char by ultimate analysis, the fixed carbon content was not great enough to be detected when the proximate analysis was done. Figures 6 and 7 show the fractions of carbonaceous material converted and the fraction of carbon converted respectively, plotted versus time for each of the temperatures investigated.

Figures 8, 9 and 10 are plots of conversion versus reaction time for data taken at approximately 870 degrees Centigrade and using 30-60 mesh Texas lignite (TX), 30 - 60 mesh Mississippi lignite (MS), and 14-18 mesh Mississippi lignite (LG). From these plots, it appears that Mississippi lignite is slightly more reactive to gasification than the Texas lignite. Also, the larger particles of Mississippi lignite appear to be more reactive than the smaller particles. The first observation is expected, since the activity of coals generally increases as coal rank decreases. The larger particles of Mississippi lignite were expected, however, to have an equal or lower activity than the smaller particles. The small difference between the curves for the large and smaller particles is probably not significant. Also, the 10-minute run with large particles was a small sample size.

This could have caused the values for conversion which were higher than expected.

Figure 11 is a comparison of fractional conversion of Mississippi and Texas lignite and those lignites found in the Zabranský, Nandi study (30). Since the conversion data was taken at different time intervals, little comparison can be drawn without some type of model.

In order to compare kinetic data with that found in the literature, the data must be fit to some kinetic model. The model chosen is the first order reaction model proposed by Van Heek et al. (27) and used by Kayembe, Pulsifer (6) and Zabranský, Nandi (30).

The first order reaction model for fixed carbon (or base carbon) conversion is:

$$\frac{dX}{dt} = \kappa\ (1 - X) \qquad (5)$$

or, in integrated form

$$-\ \mathrm{In}\ (1 - X) = kt \qquad (6)$$

Thus, a plot of - In(1-X) versus t should yield a straight line through the origin with Slope k. Data for -ln(1-X) was first corrected for temperature using the Arrhenius relation (see Table 10). The activation energy used is found on Figure 18. The point (0,0) is included in all plots of - in (1-X) versus t. Figure 13 shows the data plotted and fit to a regression line forced through the origin. Data for

North Dakota, Montana and Darco lignites was drawn from Zabranský and Nandi (Fig. 14). Although it can be seen from Figure 12, that the data fits regression lines quite well, when the line is forced through the origin there is not a very good fit. This can be explained by Figure 14. At higher carbon conversion (above X 0.78), the data deviates from the model much more than at lower conversion. Fixed carbon conversion for Mississippi lignite at 10 minutes and 870 degrees Centigrade was 0.921. At 10 minutes and 950 degrees Centigrade, fixed carbon conversion was 0.995. So, all the data taken at 870 and 950 degrees is in the region ($X > 0.78$) where the model fit is poor. The data taken at 750 degrees fits the model quite well with a correlation factor of 0.974 for the regression line. The 870 degree data fits the regression line through it with a correlation factor of 0.92. There is not sufficient data to plot $-\ln(1-X)$ versus t at 550 degrees Centigrade. At 950 degrees the conversion fraction is too close to one to construct a plot. The 870 degree data for Texas lignite fit the first order model with a correlation factor of 0.94. The data used for the first order model is found in Table 10, with the rate constants calculated from this data in Tables 11 and 12. Table 12 shows the rate constants, (870 degees Centigrade) in order of magnitude, for North Dakota Lignite, 0.22;

Montana lignite, 0.16; Mississippi lignite, 0.14; Texas lignite, 0.12; and Darco lignite, 0.089.

The Arrhenius equation

$$\kappa = k_0 \exp(-E/RT) \qquad (7)$$

was used to find a relationship between the rate constant, k, and temperature. Manipulating the Arrhenius equation to the form

$$\text{in } k = \text{in } k_0 - E/RT \qquad (8)$$

shows that a plot of In k versus 1/T should yield a straight line with a slope of -E/R and intercept of In k . The rate constant k is obtained from the first order model

$$\kappa = - \frac{\ln(1 - x)}{t} \qquad (9)$$

Table 10 shows the κ values found for the runs at each temperature. Figure 18 is an Arrhenius plot for 30-60 mesh Mississippi lignite in the range of 550-870 degrees Centigrade. The regression line for these points has a correlation factor of R = 0.916. From this plot the frequency factor, κ_0, was found to be 3463 min^{-1} and the activation energy was 95.6 kJ/mole. From this relation, the rate constant, k, at 870 degrees is 0.15 min^{-1}. Therefore, there is fairly good agreement between the rate constant found using the Arrhenius relation and data at several temperatures (0.15) and the rate constant found using the first-order

model and only 870 degrees Centigrade data. It should again be noted, however, that more data taken at lower conversion fractions is needed to confirm the rate constants for Mississippi and Texas lignite.

Gas production during the gasification process was on the order of 1.Ц grams gas per gram dry ash free coal charged to the reactor. This value was found by averaging the gas production in each of the runs with fixed carbon conversion greater than 95% (all the 870 and 950 degree runs). Gas production for each of the runs may be found in the material balance data, Table 10.

Figures 19-23 show gas production versus time on a basis of ml. gas produced per gram dry ash-free coal, with the exception of Figure 21, which was done on a dry coal basis. After 30 minutes, gas production was essentially complete for the 870 and 950 degree runs as seen in Figure 15. The slope of the curve for the 750 degree run at 30 minutes indicates that there is still significant gas production. After 50 minutes (Figure 22), the gas volume curve appears to have leveled off indicating completion of gasification. It can be seen from Figure 19 that gas production at 550 degrees Centigrade is very slow. The slight upward slope at 30 minutes indicates, however, that the reaction is still proceeding. Figures 20 and 21 compare the gas volume produced

by the two sizes of Mississippi lignite used and Texas lignite. These plots indicate no difference in gas production between the two particle sizes. Also, gas production on a dry ash-free basis for the Texas lignite is only slightly greater than the Mississippi lignite. The greater slope in the Mississippi lignite curves indicates a slightly higher gasification rate. Since the Texas lignite has a smaller ash content than the Mississippi lignite, its gas production on a dry basis is much greater than that of the Mississippi lignite, as shown in Figure 21.

Since gas samples were taken at 5-7 different times during the run, a weighted average concentration could be found by weighting each sample's value according to the gas flow rate at the time it was taken. From this, the molecular weight of the gas may be calculated. From the molecular weight and volume the gas weight may be calculated. Table 15 shows the concentration of each of the components measured by gas chromatography for each of the runs. Table 16 shows the production of each component in g/gDAF coal. Figures 25-28 show hydrogen, carbon dioxide, methane, and carbon monoxide concentrations plotted versus temperature. These plots show that hydrogen, carbon monoxide and methane concentration decreases with temperature. A similar concentration shift in pyrolysis is suggested by Wen and Dutta (30). The CO2 concentration could be decreasing in

concentration at higher temperatures due to dilution by CO and H2 which are being produced at a greater rate at higher temperatures.

Figure 29 shows the gas composition plotted versus time for a typical run. Hydrogen composition increases substantially after the first minute of the run and then levels off. Methane composition drops drastically early in the run and also levels off. Carbon dioxide and carbon monoxide both drop slightly and then begin to increase. These changes appear to be due to pyrolysis occurring in the early stages of the run followed by gasification.

The gas volume versus time data was also used to model the kinetic behavior of Mississippi lignite in gasification. The model used assumes that pyrolysis ends at a certain time, decided on from pyrolysis data (5). At this time (4 min. for 750°C runs and 2 min for 870 and 950 °C runs), gasification is assumed to begin. The model assumes first order reaction.

$$\frac{d(V/V_{max})}{dt} = k\left(\frac{V - V_o}{V_{max} - V_o}\right)$$

Integrated and symplified this becomes: $-\ln(1-y) = kt$ *

where V_o = volume produced at start of pyrolysis

V = volume produced at any time

V_{max} = maximum volume produced

t^* = time from end of pyrolysis

$y = (V-V_o)/(V_{max}-V_o)$.

Plots of -ln(1-y) versus t, κ values for each, an Arrhenius plot and predicted value of kg70 from Arrhenius relation are included in Figures 31, 32, 33 and 34.

The overall material balance data is given in Table 13 followed by carbon balance data in Table 14. The materials accounted for are gas, tar, char and water. Table 14 presents carbon balance data as a fraction of total carbon injected so that the total should equal to .one for the material balance to close. Coal carbon was determined by ultimate analysis (Table 7) while a carbon-hydrogen analysis was done on each of the chars. The tar was determined, by carbon-hydrogen analysis, to be 81.45% carbon and 7.08% hydrogen. Much of the error in the carbon balance may be attributed to the inaccurate method of tar weighing. Due to this, an average tar production was calculated and used for the carbon balance. Since the tar is found during pyrolysis, it is reasonable to assume an equal amount of carbon (g/g DAF) is released for each run. This assumption is consistent with the pyrolysis data of Farage (5) on the same equipment. Table 14 presents the actual tar measured and the average tar produced. When the average is used, carbon balance error is reasonable.

CHAPTER VI

CONCLUSIONS

1. Gas Production from steam gasification of Mississippi lignite is roughly 1.4 g. gas/g. DAP coal gasified.
2. Gas composition at approximately 1-2 atm pressure in steam atmosphere is:

	WEIGHT %
H_2 -	7.5%
CO_2 -	63 %
CH_U -	4.5%
CO -	22 %

3. Mississippi lignite favorably compares to other lignites in gasification activity (k value (min ^) $^{-}$ in parenthesis).

   North Dakota (0.22) > Montana (0.16) > Mississippi (0.14) > Texas (0.12) > Darco (0.089)

4. Hydrogen and carbon monoxide concentrations increase with temperature while carbon-dioxide and methane concentrations decrease with temperature.
5. Hydrogen concentration increases abrubtly after pyrolysis and then remains constant. Carbon dioxide, methane, and carbon monoxide concentrations all decrease slightly and then remain fairly constant.

CHAPTER VII

RECOMMENDATIONS

The results of this study indicate the need for the following recommendations for further research:

1. Run experiments using larger particles to study mass transfer limitations;
2. Gasify char which has been previously devolatilized to study gasification kinetics;
3. Make runs at lower temperature and/or reaction time to see if the kinetic model fit is better at lower carbon conversion; and
4. Using the same equipment, study other lignites to compare results with that found in the literature.

BIBLIOGRAPHY

1. . Agarwal, P.K., Genetti, W.E. , Lee, Y.Y., and Prasad, S.N., "Model For Drying During Fluidized Bed Combustion of Wet Low Rank Fuels", Fuel, 63, p. 1020 (1984).

2. Anthony, D.B. and Howard, J.B., "Coal Devolatilization and Hydrogasification", AIChE Journal, 22(4), p. 641 (1975) .

3. Berkowitz, N., An Introduction to Coal Technology, Academic Press, New York, 1979, pp. 250-298.

4. Bouchillon , C.W., Steele, W.G., Clippend, J.A., Burnett, J.D., "Evalution of the Micropulverization, Drying and Benefication of Lignite", Mississippi State University.

5. Farage, D., Clemmer, J.E., Williford, C.W., "Pyrolysis and Gasification of Mississippi Lignite in a Fixed Bed Gasifer", Subtask C of Grant "Development of Mississippi Lignites and Zeolites", MMRI-84-7F.

6. Kayembe , N. and Pulsifer, A.H., "Kinetics and Catalysis of the Reaction of Coal Char and Steam", Fuel, 55, p. 211, (1976).

7. Fung, D.P.C., "Laboratory Gasification of Five Canadian Coals", Fuel, 61, p. 139 (1982).

8. Fung, D.P.C., "Laboratory Gasification Study of Canadian Coals: 2. Chemical Reactivity and Coal Rank", Fuel, 62, p. 1337 (1983).

9. Haynes, H.W., "Gasification of Mississippi Lignites", Proposal to Mississippi Mineral Resources Institute, Sept. 1979.

10. Holstein, W.L. and Boudart, M., "Transition Metal and Metal Oxide Catalysed Gasification of Carbon By Oxgyen, Water, and Carbon Dioxide", Fuel, 6 2, pp. 162 (1983).

11. Huhn, F. , Klein, J. and Juntgen, H., "Investigations on the Alkali-Catalysed Steam Gasification of Coal: Kinetics and Interactions of Alkali Catalyst With Carbon", Fuel, 61(2), p. 196 (1983).

12. Jenkins, R.G., Nandi, S.P. and Walker, P.C., Jr., "Reaction of Heat Treated Coals in Air At 500°C," Fuel, 52 , p. 288 (1973) .

13. Juntgen, H., "Application of Catalysts to Coal Gasification Processes: Incentives and Perspectives", Fuel, 62, p. 274 (1983).

14. Kayembe, N. and Pulsifer, A.H., "Kinetics and Catalysis of the Reaction of Coal Char and Steam", Fuel, 55, p. 211 (1976).

15. Lacy, J.C. and White, D.B., "The Future of Texas Lignite," paper presented at the Tenth Biennial Lignite Symposium, Grand Forks, North Dakota, May 30-31, 1979.

16. Luppens, J.H., "Exploration for Gulf Coast United States Lignite Deposits: Their Distribution, Quality and Reserves", paper presented at the Second International Coal Exploration Symposium, Denver, Colorado, October 1-4, 1978.

17. McKee, D.W., "Mechanism of the Alkali Metal Catalyzed Gasification of Carbon," Fuel, 6 2 , p. 170 (1983).

18. McKee, D.W., Spiro, C.L., et.al., "The Catalysis of Coal Gasification," Chemtech, Oct., 1983, p. 624.

19. Moss, S.H. and Schlinger, W.G., "Coal Gasification," Lubrication, 66(3), p. 25 (1980).

20. Otto, K. , Bartosiewicz, L. and Sholet, M., "Catalytic Steam Gasification of Graphite: Effects of Calcium Strontium, and Burium With and Without Sulfur", Carbon, Г7, p. 351 (1979).

21. Radovič, L.R., Walker, P.C., and Jenkins, R.G., "Catalytic Coal Gasification: Use of Calcium vs. Potassium," Fuel, 63 , p. 1028 (1984).

22. Schad, M.K. and Hafke, C.F., "Recent Developments in Coal Gasification," Chemical Engineering Progress, May, 1983, p. 45.

23. Shull, S.C., Namovato, M.V. and Clayton, M., "Analysis of the Economic Impact on the Producing Counties and on the State of Development of Mississippi's Lignite Reserves", Report to Mississippi Mineral Resources

Institute and Bureau of Business and Economic Research, July 1984.

24. Spiro, C.L., McKee, D.W. et al., "Catalytic co,-(Gasification of Graphite vs. Coal Char", Fuel, 62, p. 180, (1983).

25. "Synfuels Future Hinges on Capital, Cooperation," Oil 8 Gas Journal, 78(24) p. 55-61 (June 10 , 1980).

26. Van Der Heijden S.P.N. and Verma, A., "Gasification of Western Lignite Coals", Canadian Journal of Chemical Engineering, 59, p. 325 (June 1981) .

27. Van Heek, K.H., Jungten, H. and Peters, W., J. Institute Fuel, 4 6, p. 249 (1973).

28. Wen, C.Y. and Dutta, S., "Solid-Gas Reactions in Coal Conversion Processes," Coal Process Technology, April 1978, p. 40.

29. Wigmans, T., Haringer, H. and Moulijn, "Nature, Activity and Stability of Active Sites During Alkali Metal Carbonate-Catalyszed Gasification Reactions of Coal Char", Fuel, 62, p. 185 (1983).

30. Zabranský, R.F. and Nandi, S.P., "Effects of the Preparation Procedure on the Reactivity of Lignite Chars," paper presented at AIChE 1983 Spring National Meeting, Houston, Texas, March 27-31, 1983.

APPENDIX A

TABLES

TABLE 1

PROXIMATE ANALYSIS - MISSISSIPPI LIGNITE

	MOISTURE	VOLATILES	ASH	F.C.
	4.18	40.11	42.92	16.97
	4.42	41.69	40.92	17.39
	8.01	43.72	32.60	23.68
	7.70	43.66	32.89	23.45
	7.72	46.00	31.37	22.63
	5.09	55.30	31.07	13.63
	3.29	47.38	23.70	28.92
	7.16	43.95	23.74	22.31
	7.50	49.43	29.20	21.37
	3.25	47.67	31.86	20.47
	11.92	53.59	24.22	22.19
	8.61	46.35	27.83	25.52
	8.73	46.92	27.91	25.17
	8.60	45.94	28.40	25.66
	8.79	47.09	28.02	24.89
	8.71	46.74	28.13	25.13
Avg.	8.15	46.13	30.18	23.69

LARGE PARTICLES

	MOISTURE	VOLATILES	ASH	F.C.
	7.56	45.25	31.69	23.06
	7.59	45.32	30.93	23.75
	7.76	45.43	30.02	24.55
	7.42	43.85	32.56	23.59
	7.65	45.11	30.96	23.93
Avg.	7.60	44.99	31.23	23.78

TABLE 2

PROXIMATE ANALYSIS - TEXAS LIGNITE

MOISTURE	VOLATILES	ASH	F.C,
14.29	47.92	11.81	40.27
13.94	47.69	11.92	40.39
13.79	47.97	12.57	39.46
13.90	47.50	12.06	40.44
AVG. 13.98	47.71	12.09	40.14

TABLE 3

PROXIMATE ANALYSIS - FIVE LIGNITES

SAMPLE	ASH	U.M.	F.C.
North Dakota(30)	6.7	43.7	49.6
Montana (30)	5.1	43.6	51.3
Mississippi	30.2	46.1	23.7
Texas	12.1	47.8	40.1
Darco (30)	8.4	46.6	44.9

TABLE 4

MINERAL ANALYSIS OF MISSISSIPPI LIGNITE SAMPLE

% Phos. Pentoxide, P2O5	0.05
% Silica, Si O2	76.77
% Ferric Oxide, Fc2O^	3.66
% Alumina, A^O^	7.12
% Titania, TÍO2	2.08
% Lime, CoO	2.80
% Magnesia, M_SO	0.52
% Sulfur Trioxide, SO3	3.02
% Potassium Oxide, K2O	0.36
% Sodium Oxide, Na20	0.11

TABLE 5

GAS CHROMATOGRAPH PROPORTIONALITY CONSTANTS

GAS	CONSTANTS
HYDROGEN	8.93
CARBON DIOXIDE	1.54
ETHYLENE	0.87
ETHANE	0.66
ACETYLENE	0.69
HYDROGEN SULFIDE	0.68
OXYGEN	1.09
NITROGEN	0.99
METHANE	1.12
CARBON MONOXIDE	1.00

TABLE 6

CONVERSION DATA

Run	t (min)	T (°C)	Fixed Carbon Conversion	Carbon Conversion	Carbon-aceous Mat . Converted
			30-60 Mesh Mississippi Lignite		
1	50	730	.732	.787	.877
2	50	751	. 616	.887	.868
3	30	728	. 544	.760	.830
4	40	746	.715	.803	.880
6	30	566	.205	.402	.360
8	30	953	1.00	. 996	1.00
9	20	967	1.00	.993	.996
10	10	951	.495	. 973	. 985
11	20	870	. 976	. 960	. 966
12	10	863	. 884	. 898	. 939
13	10	865	. 947	.894	. 944
15	30	868	.978	. 970	. 980
			14-18 Mesh Mississippi Lignite		
19	10	879	. 978	.928	.955
20	20	876	. 970	. 940	. 967
21	30	877	. 999	.977	. 946
			30-•60 Mesh Texas Lignite		
16	20	867	. 947	. 916	.959
17	10	851	.879	.810	.843
18	20	865	.950	.934	. 948
22	30	870	. 973	.970	. 976

TABLE 7

ULTIMATE ANALYSIS - FIVE LIGNITES

Wt. % Dry

Sample	C	H	N	S	O	ASH
North Dakota (30)	62.90	4.27	0.97	1.10	24.09	6.67
Montana (30)	65.13	4.13	0.89	0.57	24.20	5 .08
Mississippi	46.71	4.19	0.61	0. 59	16.06	31.84
Texas	61.68	4.56	1.20	1.38	17.20	13.98
Darco (30)	64.38	4.19	1.20	1.22	20.11	8.50

TABLE 8

PROXIMATE ANALYSIS OF CHARS

RUN	MOISTURE	VOLATILES	ASH	F.C.
1	2.31	4.46	82.79	12.75
2	1.38	4.22	80.37	15.41
3	2.06	5.08	7 0.87	24.05
4	0.67	4.3 9	81.85	13.76
6	0 .36	11.33	60.70	27.97
8	12.96	0	100.00	0
9	0.08	0.78	99.22	0
10	. 04	2.22	97.48	0 . 30
11	.65	4. 38	94.10	1.52
12	.38	3 .58	90.00	6.42
13	.63	5 . 77	91.11	3.06
15	.36	3.03	95.21	1.76
16	.47	9.41	77.22	13.37
17	0.86	12.42	46.56	41.02
18	0.74	14.52	74.22	11.2 5
19	6 .55	7 .23	91.29	1.48
20	1.52	4.89	92.87	2 . 24
21	0.15	1.04	98.87	0 .09
22	0.22	7.48	84.80	7 . 72

TABLE 9

CHAR CARBON-HYDROGEN ANALYSIS

RUN	CARBON	HYDROGEN
1	19.93	0. 24
2	11.20	0.23
3	24.92	0 .76
4	19.76	0.47
6	41.41	1.61
8	0.18	*
9	0.87	*
10	3.06	*
11	4.67	0.34
12	11.09	0.23
13	10.72	0.11
15	4.80	0.11
16	24.73	0.43
17	52 . 51	0.80
18	26.17	0.17
19	9.34	0.02
20	8.61	0.10
21	3.19	0.12
22	14.92	0.02

* less than 0.2%

TABLE 10

KINETIC DATA - MISSISSIPPI 8 TEXAS LIGNITE

Mississippi Lignite

t	T(°C)	-ln(1-X)	κ	In κ
30	566	0.230	0.00767	- 4.87
30	728	0.912	0.026	- 3.65
40	746	1.2 8 *	0.031	- 3.47
50	751	1.51 *	0.026	- 3.63
50	730	0.957 *	0.019	-3.96
10	863	2.2 3 **	0.215	- 1.53
10	865	2.97 **	0.285	- 1.26
20	820	3.7 2 **	0.186	- 1.68
30	868	3.8 7 **	0.128	-2.06

Texas Lignite

10	851	2.30 **	0.211
20	867	3.00 **	0.147
20	865	3.08 **	0.150
30	870	3.6 3 **	0.121

* These values were corrected to 750°C using the Arrhenius relation.

** These values were corrected to 870°C using the Arrhenius relation

Example : $$k_{750} = - \frac{k_{728}\ \exp\left(-\frac{E}{R}(750 + 273)\right)}{\exp\left(-\frac{E}{R}(728 + 273)\right)}$$

$$-\ln(1-X)_{750} \qquad k_{750} \text{ "} t$$

TABLE 11

RATE CONSTANTS FOR FIRST-ORDER MODEL
MISSISSIPPI LIGNITE

Temperature	κ (min -1)	by Arrhenius Fit
550 °C	0.0077	0.0030
750°C	0.030	0.046
870 °C	0.13	0.15

* one data point

TABLE 12

RATE CONSTANTS FOR FIRST-ORDER MODEL
870°C

Lignite Type	k /(min)1
Darco	0.089
Texas	0.12
Mississippi	0.14
Montana	0.16
North Dakota	0 .22

TABLE 13

OVERALL MATERIAL BALANCE
(grams)

Ruri	Coal Injected	Steam Input	Total Input	Gas Produced	Char Recvd.	Water Recvd.	Tar Recvd.	Total Recvd.	% Err.
1	19.76	40.1	59.86	14.41	9.06	35.1	1.85	60.42	+ 0.93
2	19.94	55.3	75.24	14.81	8.63	48.4	1.90	73.74	- 1.99
3	15.90	28.2	44.10	9.66	6.56	29.6	0.9	46.72	5.90
4	20.19	34.3	54.49	13.27	8.64	29.4	2.4	53.71	- 1.43
6	19.18	42.1	61.28	1.93	11.89	34.0	3.2	51.02	-16.79
8	5.18	31.1	36.28	3.92	4.37	19.2	2.65	30.14	-16.97
9	14.82	28.7	43.52	10.69	4.82	30.6	2.6	48.71	11.92
10	11.88	15.0	26.88	9.96	4.49	9.4	3.3	27.15	1.00
11	10.06	27.9	37.96	7.98	3.72	23.9	2.45	38.05	0.24
12	11.22	14.1	25.32	—	4.41	—	—	—	—
13	6.60	14.1	20.70	6.35	2.71	13.1	1.9	24.06	16.23
15	12.61	43.2	55.81	13.19	3.36	35.6	3.95	56.10	0.52
16	20.19	28.5	48.69	16.76	2.76	24.5	2.5	46.52	- 4.46
17	13.43	13.9	27.33	10.93	3.00	10.1	3.0	27.03	- 1.10
18	12.72	28.3	41.02	17.43	1.96	21.9	0.8	42.09	2.61
19	4.35	14.2	18.55	4.08	1.43	14.8	1.2	21.41	15.42
20	11.65	28.0	39.65	11.59	3.46	24.5	3.85	43.40	9.46
21	9.76	43.3	53.06	9.76	2.96	34.2	2.5	49.42	- 6.86
22	20.59	43.4	63.99	27.05	2.51	31.4	4.2	65.16	1.83

TABLE 14

CARBON BALANCE

Ran	Cin Coal (g)	Char C Coal C	Gas C Coal C	Tar C Coal C	C Recvd. Coal C	Est. Tar C Coal C	C Recvd Coal C
1	8.48	0.21	0.34	.18	.73	.35	.90
2	8.56	0.11	0.34	.18	.63	.35	.80
3	6.52	0.24	0.35	.11	.70	.35	.94
4	8.66	0.20	0.32	.22	.74	.35	.87
6	8.22	0.60	0.16	.32	1.08	.35	1.11
8	2.22	0.003	0.58	.97	1.55	.35	.93
9	6.36	0.007	0.51	.33	.85	.35	.87
10	5.10	0.03	0.63	.53	1.19	.35	1.01
11	4.32	0.04	0.55	.46	1.05	.35	.94
13	2.83	0.11	0.64	.55	1.30	.35	1.10
15	5.41	0.03	0.76	.60	1.39	.35	1.14
16*	12.42	0.08	0.43	.16	.67	.35	0.86
17*	8.27	0.19	0.43	.30	.72	.35	.97
18*	7.83	0.07	0.68	.08	.83	.35	1.10
19**	1.87	0.07	0.69	.52	1.28	.35	1.11
20**	5.00	0.06	0.69	.63	1.38	.35	1.10
21**	4.18	0.02	0.70	.49	1.21	.35	1.07
22*	12.68	0.03	0.66	.27	.96	.35	1.04
				Avg. .35			

* Texas

** Large

TABLE 15

GAS COMPONENT WEIGHT PERCENT

Run	H_2	CO_2	C_2H_4	C_2H_6	H_2S	N_2	CH_4	CO
1	7.0	52.3	1.1	0.82	0.13	3.4	7.4	27.8
2	7.1	69.4	0.8	0.7	0.2	1.1	5.5	15.2
3	8.16	72.8	0.4	0.4	0.1	1.4	4.0	12.6
4	7.82	68.8	0.4	0.4	0.1	0.7	4.3	17.5
6	3.77	70.7	0.6	1.0	0.3	1.8	8.8	13.0
8	12.5	41.3	2.4	0.3	0.1	2.7	6.4	30.1
9	10.0	48.8	.15	0.01	.003	2.6	1.0	37.4
10	7.6	49.0	1.9	0.3	.03	3.8	3.9	33.6
11	7.9	60.9	0.9	0.2	0.02	3.3	2.8	23.9
13	6.4	76.1	0.5	0.06	0.1	0.5	1.7	14.7
15	7.5	60.9	0.9	0.2	0.08	1.26	3.10	26.0
16	7.9	55.9	0.5	0.2	0.11	0.74	3.33	31.3
17	6.83	57.3	0.7	0.2	.13	1.00	4.88	29.0
18	7.37	60.9	0.3	0.1	0.10	0.89	2.43	27.8
19	8.16	62.5	1.6	.2	.09	1.04	5.37	21.0
20	7.33	60.3	.9	.2	.10	4.45	3.48	23.17
21	7.57	64.0	1.1	0.3	0.10	2.30	3.41	21.2
22	8.00	56.6	.12	.11	.11	1.28	2.19	31.6

TABLE 16

COMPONENT GAS PRODUCTION (g prod/gDAF coal)

Run	H_2	CO_2	C_2H_4	C_2H_2	H_2S	1	CH_4	CO
1	.061	.456	.010	.007	.001	.030	.064	.243
2	.066	.646	.007	.006	.002	0.010	.051	.141
3	.084	.759	.004	.004	.001	.014	.041	.132
4	.070	.618	.004	.003	.001	.006	.038	.157
6	.013	.245	.002	.003	.001	.006	.03	.045
8	.053	.175	.010	.001	.0005	.011	.022	.145
9	.122	.595	.002	.0001	.00001	.032	.012	.456
10	.108	.695	.026	.004	.0004	.053	.055	.476
11	.106	.817	.012	.024	.0003	.044	.038	.321
13	.098	1.16	.007	.0008	.001	.007	.026	.223
15	0.119	0.970	0.015	0.004	0.001	.020	.049	.413
16	0.099	0.707	0.006	0.003	0.001	.009	.042	.395
17	0.098	0.825	0.009	0.004	0.002	0.014	.070	.417
18	.153	1.26	.007	.003	.002	.018	.050	.577
19	.116	.891	.023	.004	.001	.015	„077	.299
20	.115	.944	.014	.003	.001	.070	.054	.363
21	.119	1.01	.018	.004	.002	.036	.053	.383
22	.157	1.11	.002	.002	.002	.025	.043	.624

TABLE 17

RUN 1 TEMPERATURE AND VOLUME HISTORY

Time (min)	Volume (ml. STP/g.DAF coal)	Reactor T (°C)
0.00	0.00	716
1.00	30.00	665
2.00	82.19	667
3.00	136.50	684
4.00	180.81	714
5.00	210.11	716
10.00	315.16	719
15.00	557.43	729
20.25	798.09	730
25.25	1004.63	729
30.00	1152.03	729
35.00	1262.08	728
40.00	1310.68	727
45.00	1367.85	723
50.50	1403.23	720

TABLE 18

RUN 2 TEMPERATURE AND VOLUME HISTORY

Time (min)	Volume (ml. STP/g.DAF coal)	Reactor T (°C)
0.00		754
0.25		748
0.50		74 8
1.00	18.38	754
2.00	84 . 81	754
3 .00	146.30	755
4.00	203.55	757
5.00	273.52	757
10.00	566.84	758
15.00	778.87	757
20.00	941.43	758
25.00	1072.19	758
30.00	1185.27	757
35.00	1266.55	756
40.00	1335.11	758
45 . 00	1383.87	757
50.00	1423.46	757

TABLE 19

RUN 3 TEMPERATURE AND VOLUME HISTORY

Time (min)	Volume (ml. STP/g.DAF coal)	Reactor T (°C)
0.00	0.00	740
0.25		594
1.00	36.34	
2.00	97.49	
3 . 00	167.50	
4 . 00	264.10	
5.00	350.07	
10.00	648.73	728
15.00	883.59	728
20.00	1069.70	728
25.00	1220.36	728
30.00	1340.01	728

TABLE 20

RUN 4 TEMPERATURE AND VOLUME HISTORY

Time (min)	Volume (ml. STP/g.DAF coal)	Reactor T (°C)
0.00		74 8
0 .25		532
0.50		561
0.75		617
1.00	43.28	664
2.00	112.39	585
3.00	191.96	662
4.00	271.54	720
5.00	340.65	737
10.00	658.26	745
15.00	888.62	746
20.00	1077.09	746
25.00	1227.17	746
30.00	1347.93	746
35.00	1443.56	747
40. 00	1516.16	748

TABLE 21

RUN 6 TEMPERATURE AND VOLUME HISTORY

Time (min)	Volume (ml. STP/g.DAF coal)	Reactor T (°C)
0.00		569
0.25		444
0.50		477
0.75		528
1.00	0.00	523
2.00	0.00	534
3.00	11.86	477
4.00	23.72	478
5.00	36 . 31	529
10.00	94.86	564
15.00	124.50	565
20.00	145.25	566
25.00	161.55	567
30.00	174.15	568

TABLE 22

RUN 8 TEMPERATURE AND VOLUME HISTORY

Time (min)	Volume (ml. STP/g.DAF coal)	Reactor T (°C)
0.00		947
0.25		909
0.50		913
0.75		919
1.00	181.21	922
2. 00	356.92	936
3.00	738 . 55	940
U .00	1079.00	941
5. 00	1295.89	943
10.00	1913.64	952
15.00	2078 . 37	952
20.00	2157.99	954
25.00	2193.69	953
30.00	2223.89	953

TABLE 23

RUN 9 TEMPERATURE AND VOLUME HISTORY

Time (min)	Volume (ml. STP/g.DAF coal)	Reactór T (°C)
0.00		985
0.25		905
0. 50		918
0.75		927
1.00	368.57	932
2.00	586.41	951
3 . 00	731.31	958
4.00	832.44	960
5.00	957.89	960
10.00	1414.96	962
15.00	1696.98	959
20.00	1867.16	967

TABLE 24

RUN 10 TEMPERATURE AND VOLUME HISTORY

Time (min)	Volume (ml . STP/g.DAF coal)	Reactor T (°C)
0.00		956
0.25		841
0.50		830
0.75		849
1.00	385.36	858
2.00	745.44	912
3 .00	1003.15	929
4.00	1158.50	938
5 . 00	1362.02	939
7 . 50	1675.73	947
10.00	1847.34	951

TABLE 25

RUN 11 TEMPERATURE AND VOLUME HISTORY

Time (min)	Volume (ml. STP/g.DAF coal)	Reactor T (°C)
0.00		877
0.25		807
0.50		809
0.75		810
1.00	242.47	813
2 . 00	482.10	823
3.00	718.90	854
U .00	901.81	857
5.00	1053.53	859
10.00	1527.12	870
15.00	1715.71	869
20.00	1782.35	870

TABLE 26

RUN 13 TEMPERATURE AND VOLUME HISTORY

Time (min)	Volume (ml. STP/g.DAF coal)	Reactor T (°C)
0 .00		872
0.25		783
0 .50		806
0.75		800
1.00	199.25	804
2.00	498.12	843
3 . 00	820.81	851
4.00	1037.39	855
5 .00	1262.62	858
7 .50	1521.43	862
10.00	1682.78	865

TABLE 2 7

RUN 15 TEMPERATURE AND VOLUME HISTORY

Time (min)	Volume (ml. STP/g.DAF coal)	Reactor T (°C)
0.00		878
0.25		737
0.50		758
0.75		761
1.00	174.27	765
2.00	416.44	827
3.00	675.59	849
4.00	855.52	854
5.00	1024.13	856
10.00	1589.95	859
15.00	1921.51	862
20.00	2104.84	865
25.00	2196.50	867
30. 00	2255 . 34	868

TABLE 28

RUN 16 TEMPERATURE AND VOLUME HISTORY

Time (min)	Volume (ml. STP/g.DAF coal)	Reactor T (°C)
0 .00		874
0.25		740
0.50		748
0.75		747
1.00	66.61	738
2.00	183.78	792
3.00	273.58	839
4.00	487.10	828
5.00	653.04	842
10.00	1097.91	853
15.00	1402.42	860
20.00	1593.33	867

TABLE 29

RUN 17 TEMPERATURE AND VOLUME HISTORY

Time (min)	Volume (ml. STP/g. DAE coal)	Reactor T (°C)
0.00		875
0.25		690
0 . 50		730
0.75		725
1.00	115.39	720
2.00	315.47	781
3.00	536.72	829
4.00	789.73	825
5 . 00	1021.56	835
7 . 50	1410.60	850
10.00	1683.20	851

TABLE 30

RUN 18 TEMPERATURE AND VOLUME HISTORY

Time (min)	Volume (ml. STP/g. DAF coal)	Reactor T (°C)
0. 00		875
0 .25		808
0 . 50		807
0.75		803
1.00	115.79	800
2.00	318.90	821
3 .00	536.25	845
4.00	767.83	849
5. 00	999.41	84 8
10.00	1715.04	858
15.00	2198.13	861
20.00	2495.20	865

TABLE 31

RUN 19 TEMPERATURE AND VOLUME HISTORY

Time (min)	Volume (ml. STP/g.DAF coal)	Reactor T (°C)
0.00		880
0.25		847
0.50		848
0.75		842
1.00	86.01	842
2 .00	426.75	860
3 .00	926.27	862
4.00	1326.56	867
5.00	1614.37	870
7 . 50	1999.76	877
10.00	2150.28	879

TABLE 32

RUN 20 TEMPERATURE AND VOLUME HISTORY

Time (min)	Volume (ml. STP/g. DAF coal)	Reactor T (°C)
0.00		892
0.25		773
0 .50		783
0.75		767
1.00	81.57	786
2.00	278.08	811
3 .00	524.03	850
4.00	800.87	854
5.00	1034.46	857
10.00	1658.59	867
15.00	2004.64	873
20.00	2138.12	876

TABLE 33

RUN 21 TEMPERATURE AND VOLUME HISTORY

Time (min)	Volume (ml. STP/g. DAF coal)	Reactor T (°C)
0.00		873
0.25		744
0 .50		757
0.75		759
1.00	87.88	763
2 .00	243.19	808
3.00	428.14	843
4.00	621.26	845
5.00	773.51	853
10.00	1214.93	864
15.00	1398.86	871
20.00	1472.42	874
25.00	1490.82	874
30.00	1505.12	877

TABLE 34

RUN 22 TEMPERATURE AND VOLUME HISTORY

Time (min)	Volume (ml. STP/g. DAF coal)	Reactor T (°C)
0.00		878
0.25		799
0.50		789
0.75		772
1.00	98.45	766
2.00	254.64	780
3.00	419.58	824
4.00	560.82	845
5 .00	680.92	852
10.00	1168.53	856
15.00	1583.47	858
20.00	1882.44	861
25.00	2097.90	866
30.00	2233.47	870

APPENDIX B

FIGURES

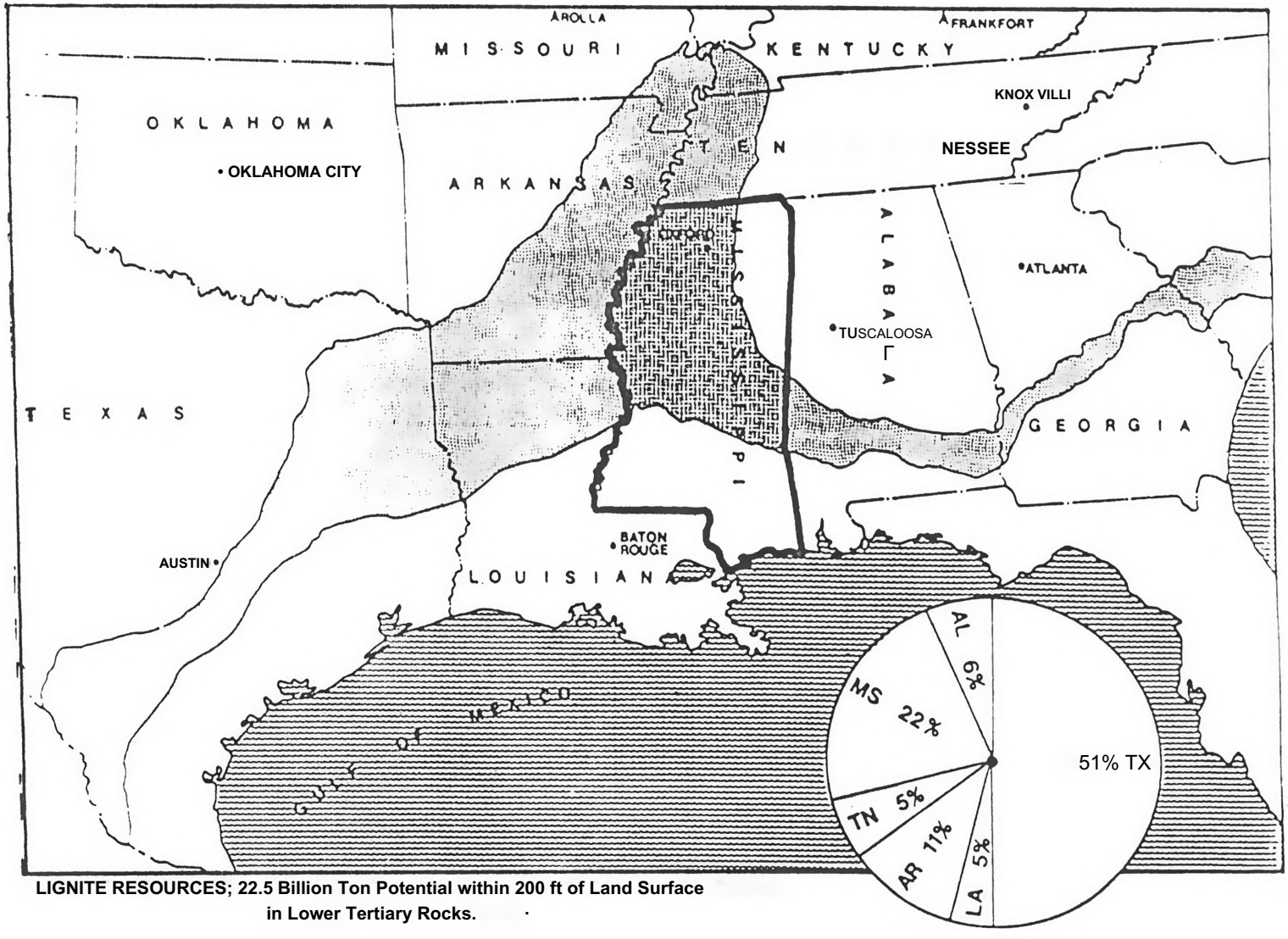

LIGNITE RESOURCES; 22.5 Billion Ton Potential within 200 ft of Land Surface in Lower Tertiary Rocks.

Figure 1. Gulf State Lignite Resources

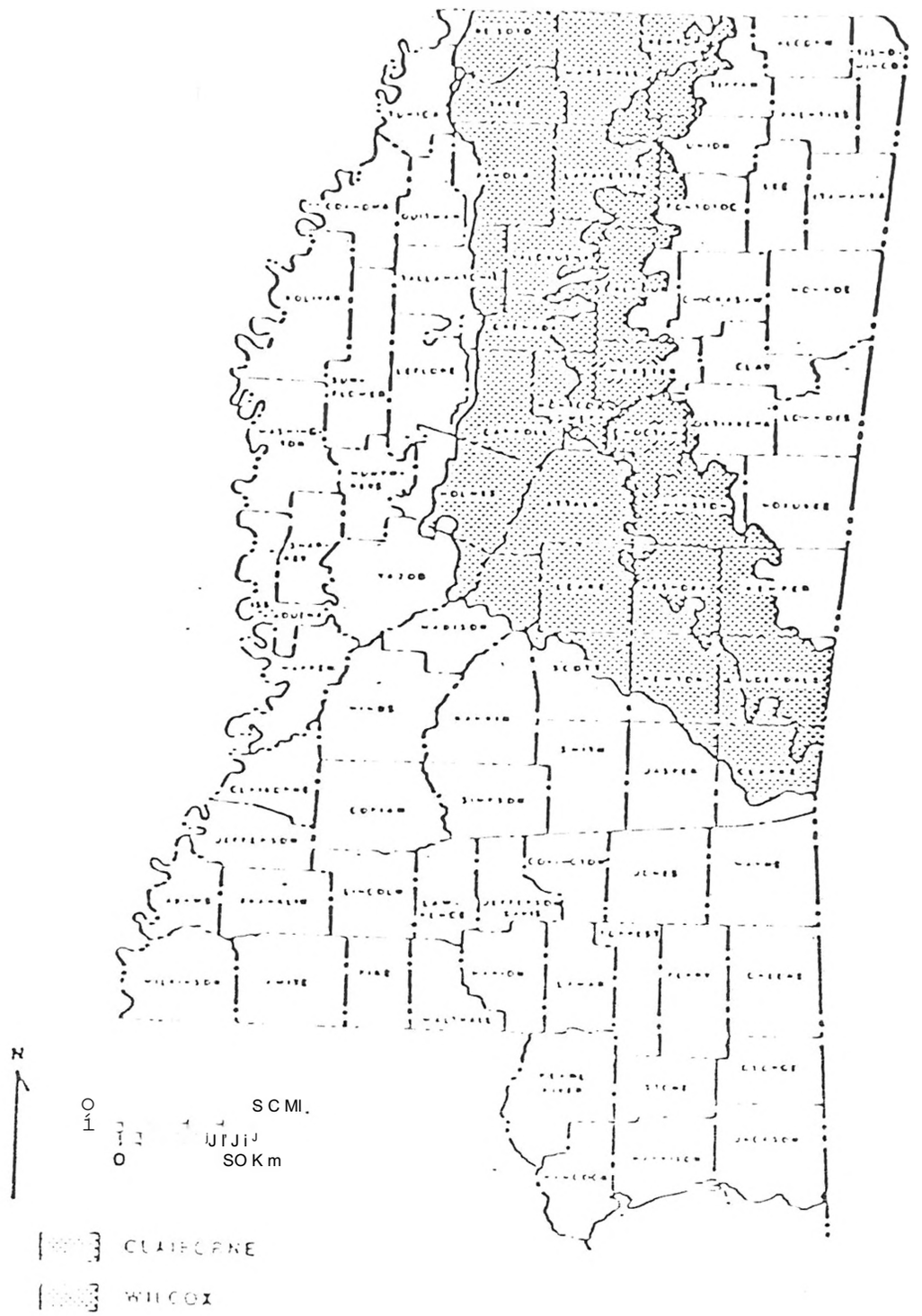

Figure 2. Mississippi's Principal Lignite Seams

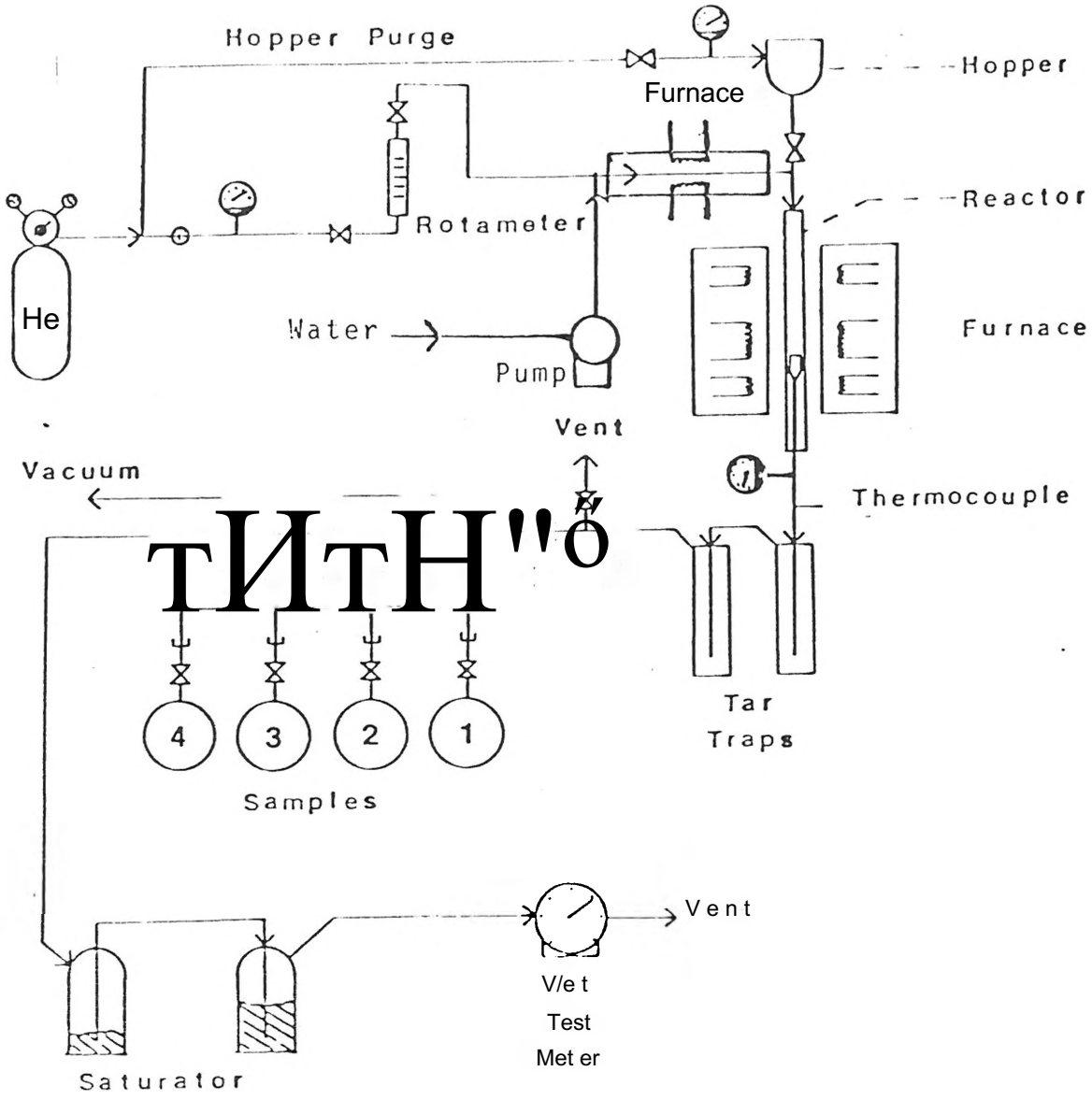

Figure 3 . Reactor Piping Flowchart

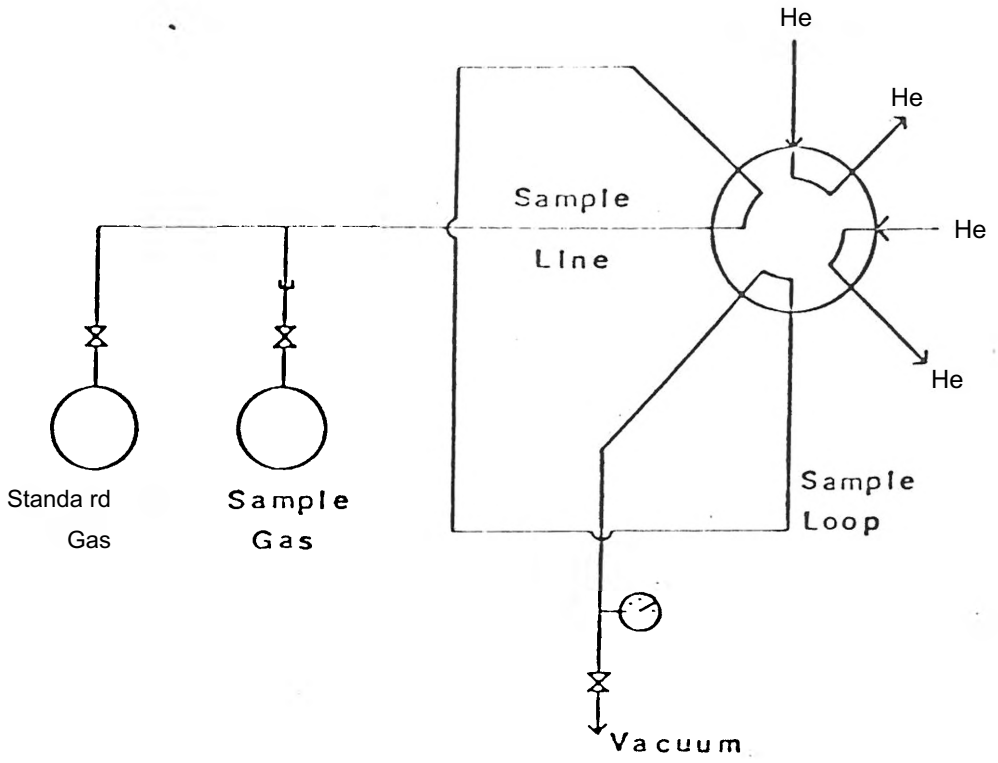

Figure 4. Eight Port Gas Chromatograph Valve Shown in Counter Clockwise Position (Sample). Sample Injection by Switching Valve to Clockwise Position (Inject).

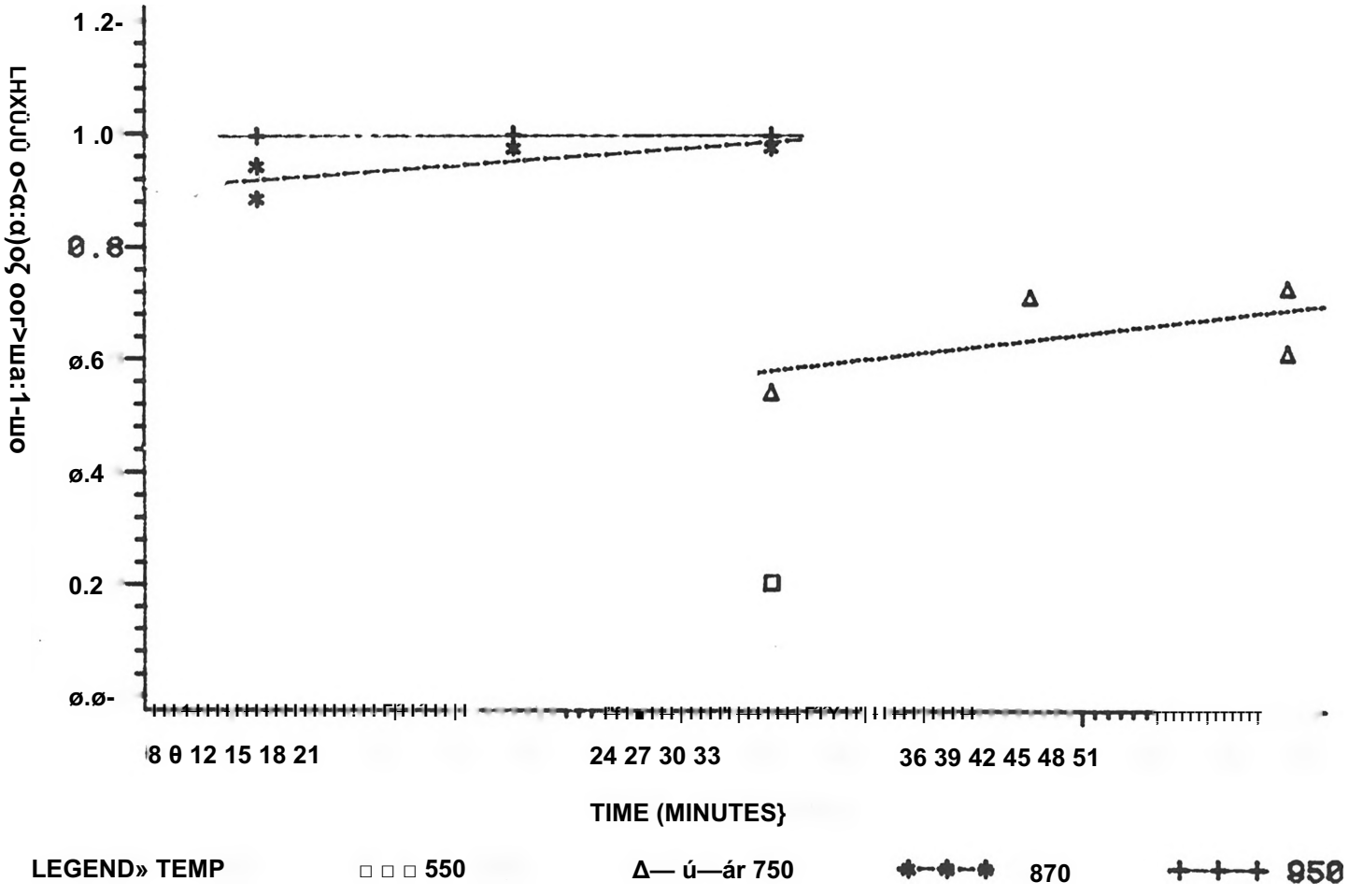

Figure 5. Fraction of Fixed Carbon Converted vs. Time

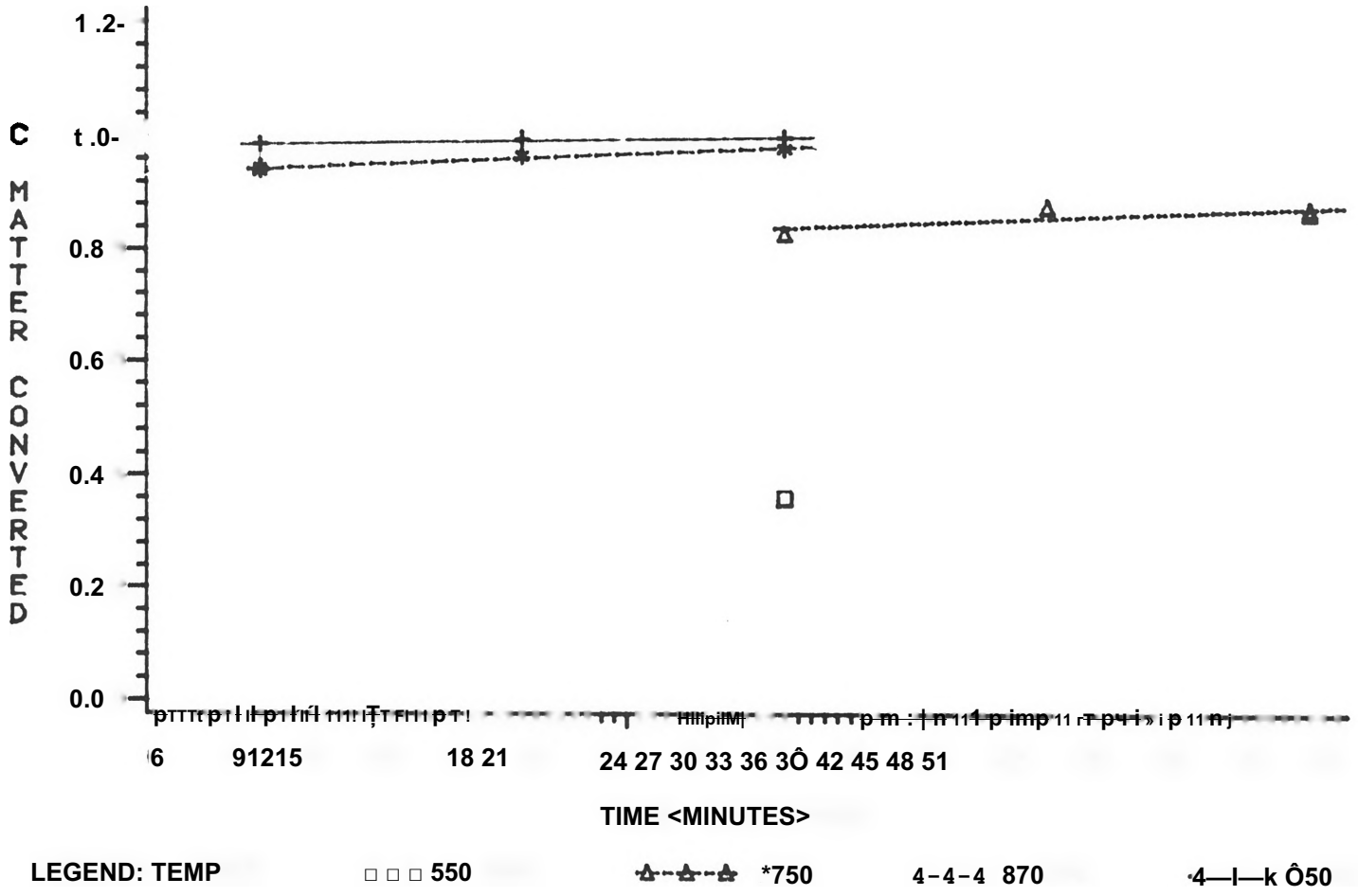

Figure 6. Carbonaceouse Material Converted vs. Time

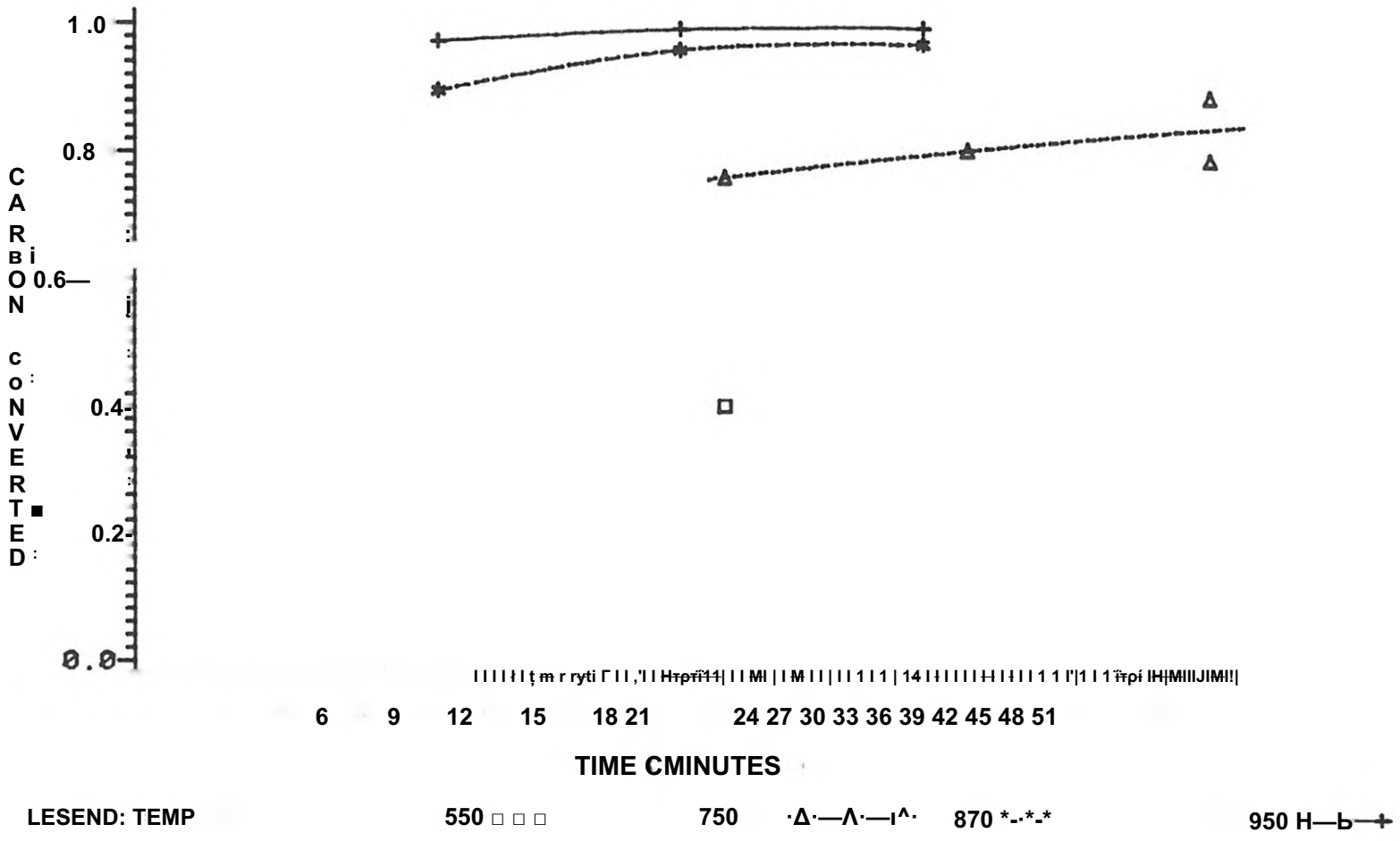

Figure 7. Fraction of Carbon Converted vs. Time

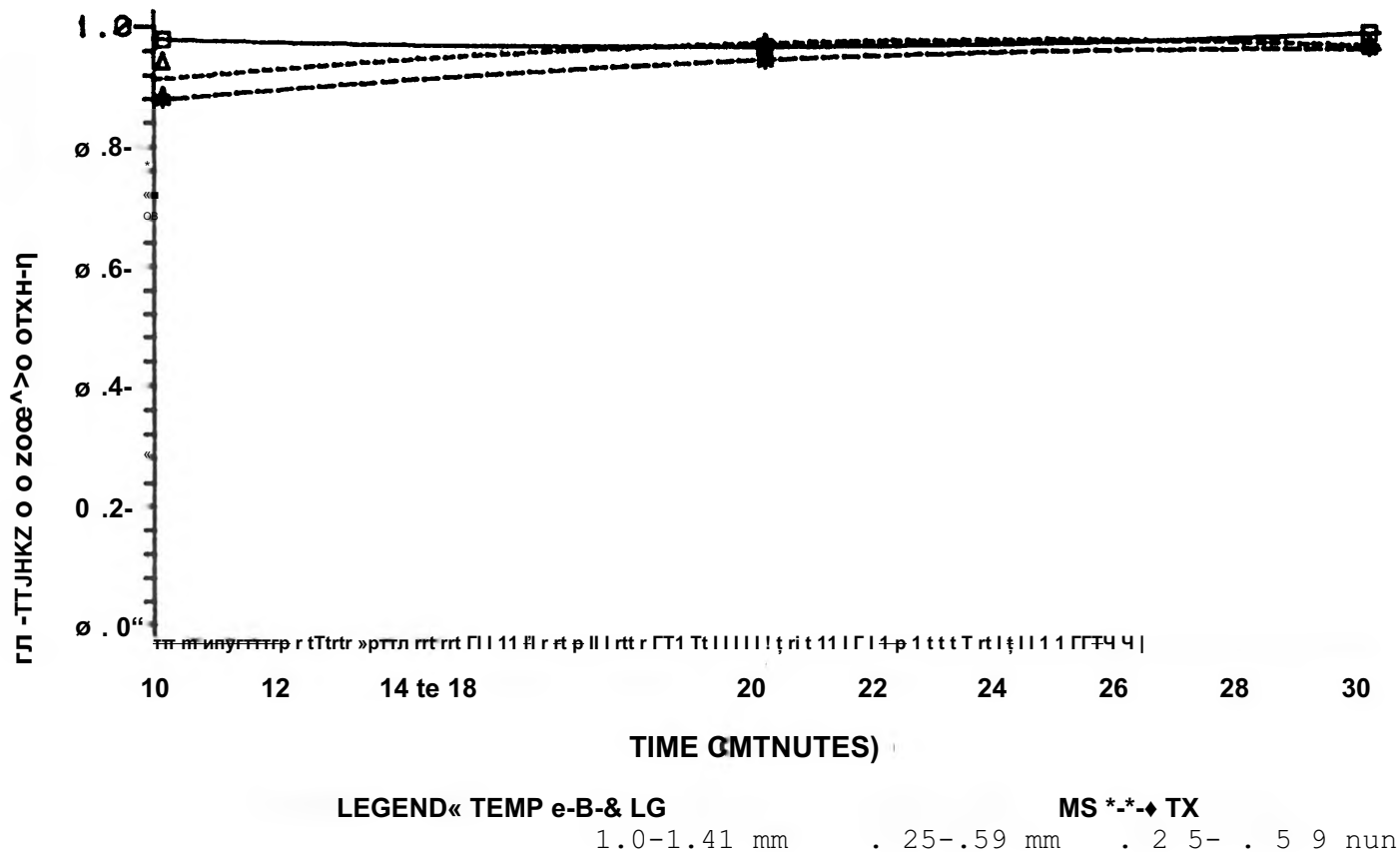

Figure 8. Fraction of Fixed Carbon Converted vs. Time 870 Degrees Centigrade

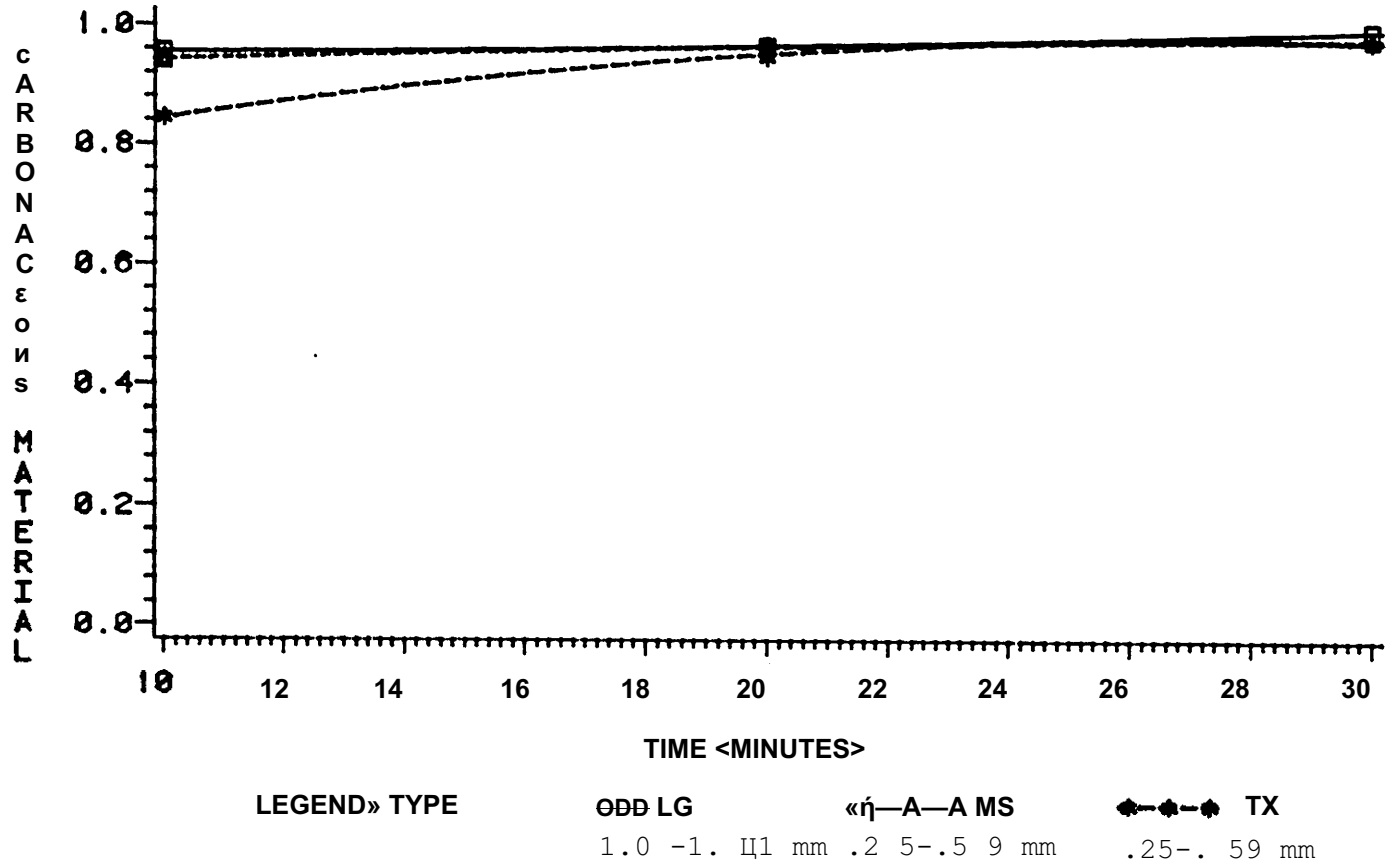

Figure 9. Fraction of Carbonaceous Material Converted vs. Time 870 Degrees Centigrade

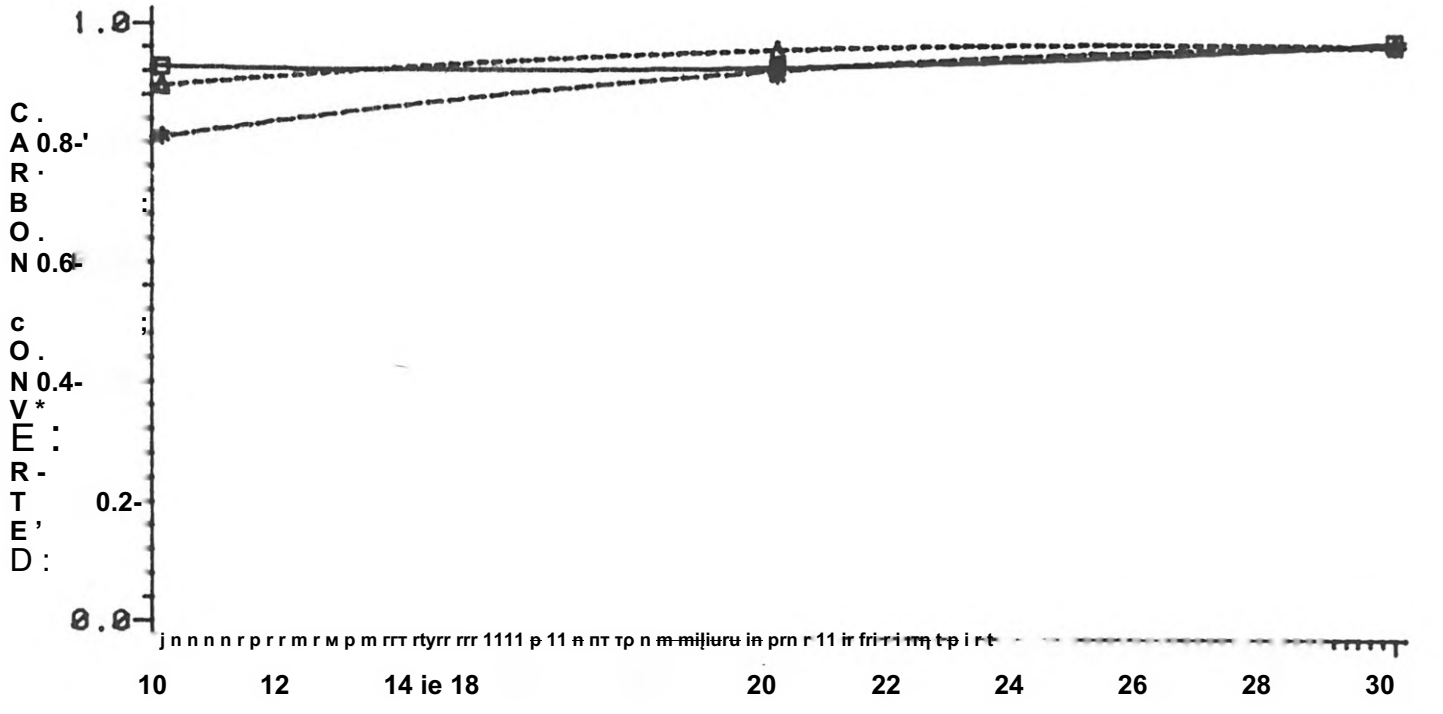

Figure 10. Fraction of Carbon Converted vs. Time
870 Degrees Centigrade

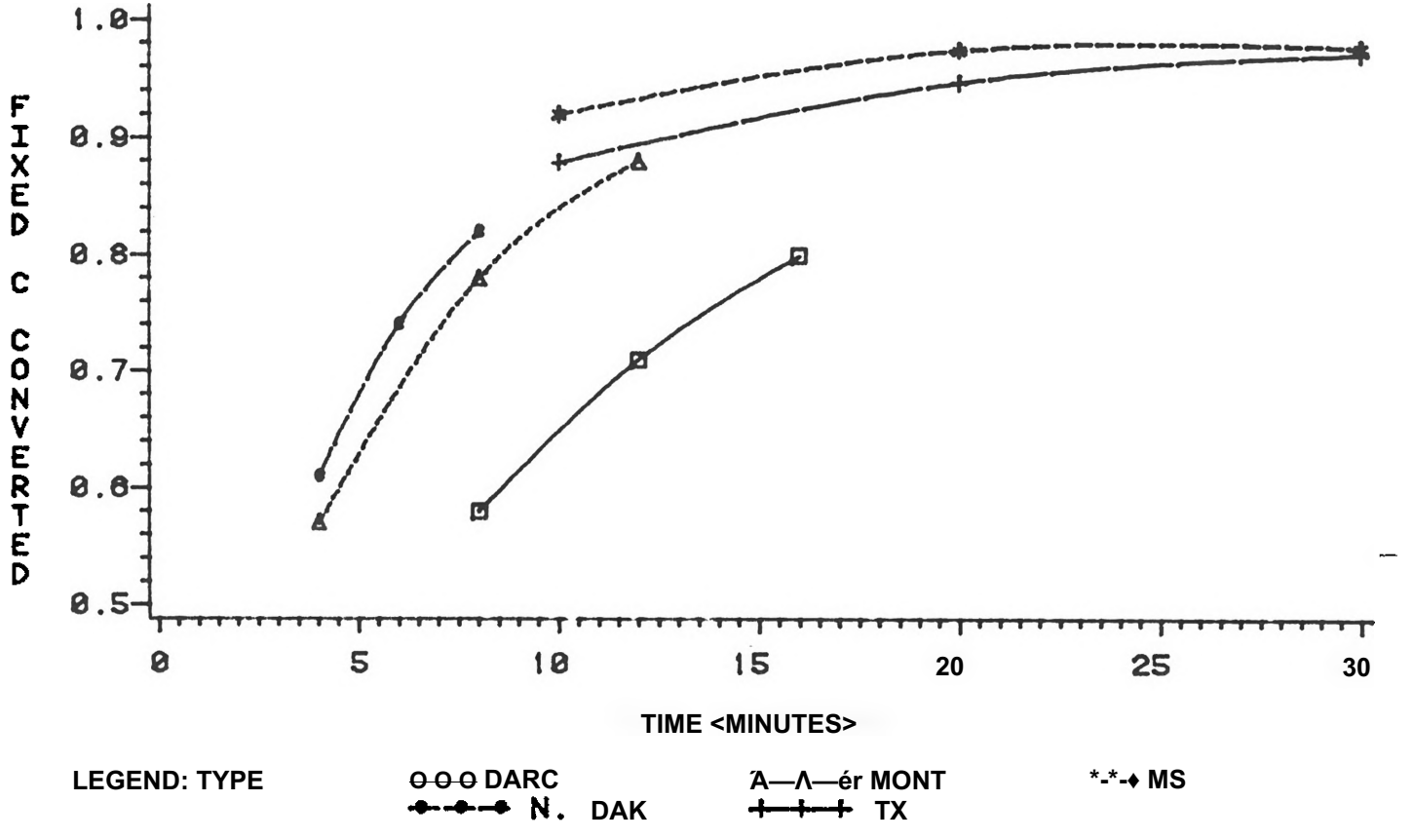

Figure 11. Fixed Carbon Conversion vs. Time
870 Degrees Centigrade

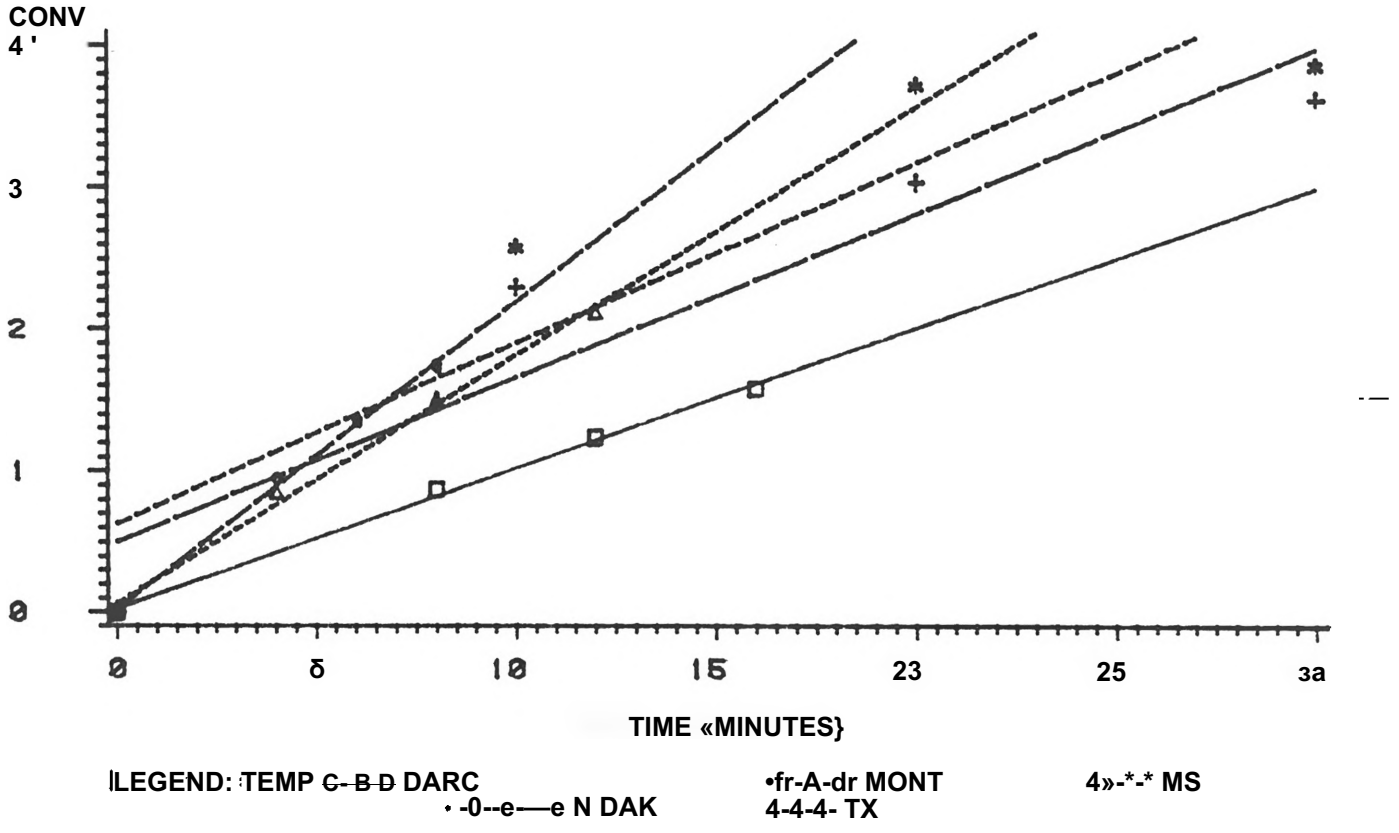

Figure 12. -ln(1-X) vs. Time
870 Degrees Centigrade

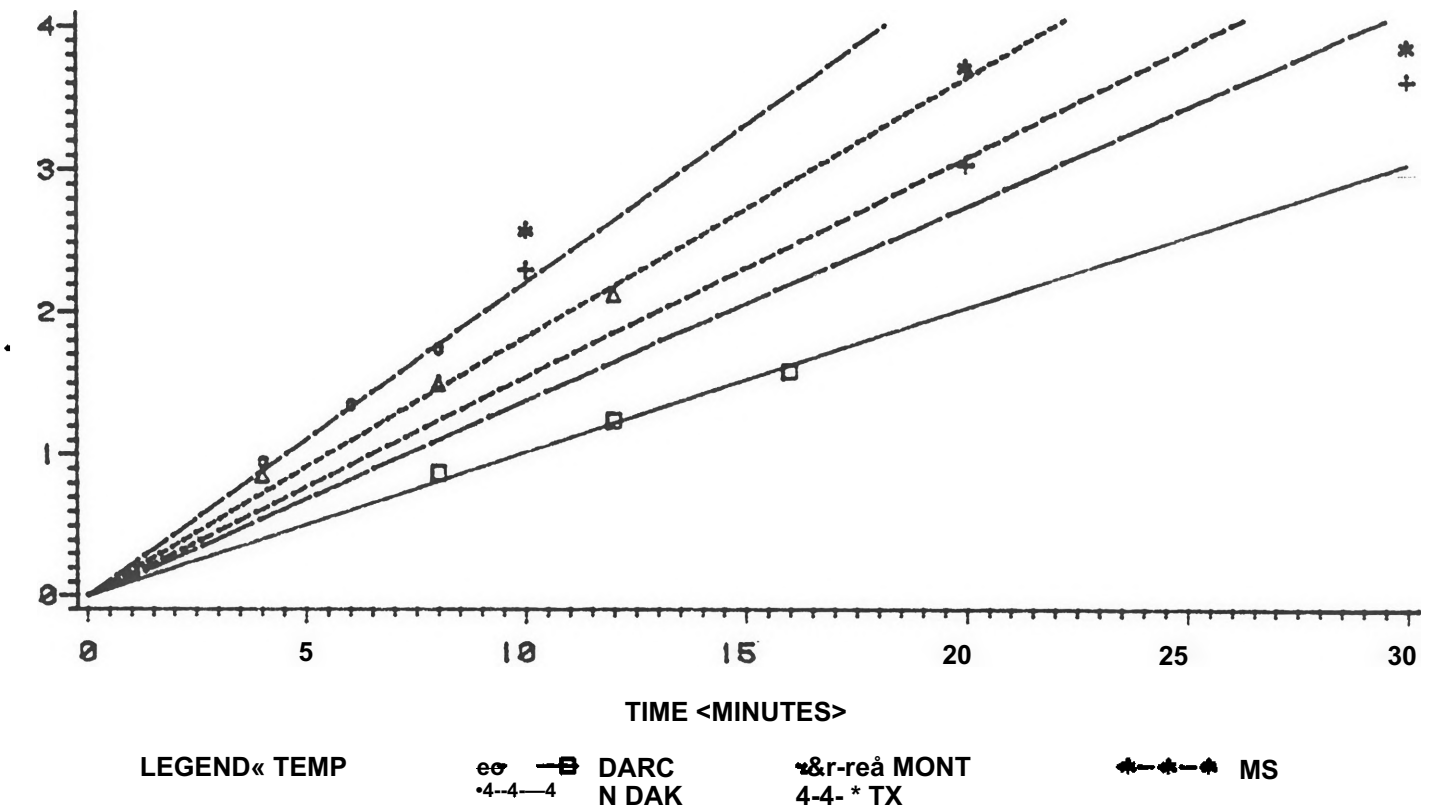

Figure 13. -ln(l-X) vs. Time
870 Degrees Centigrade

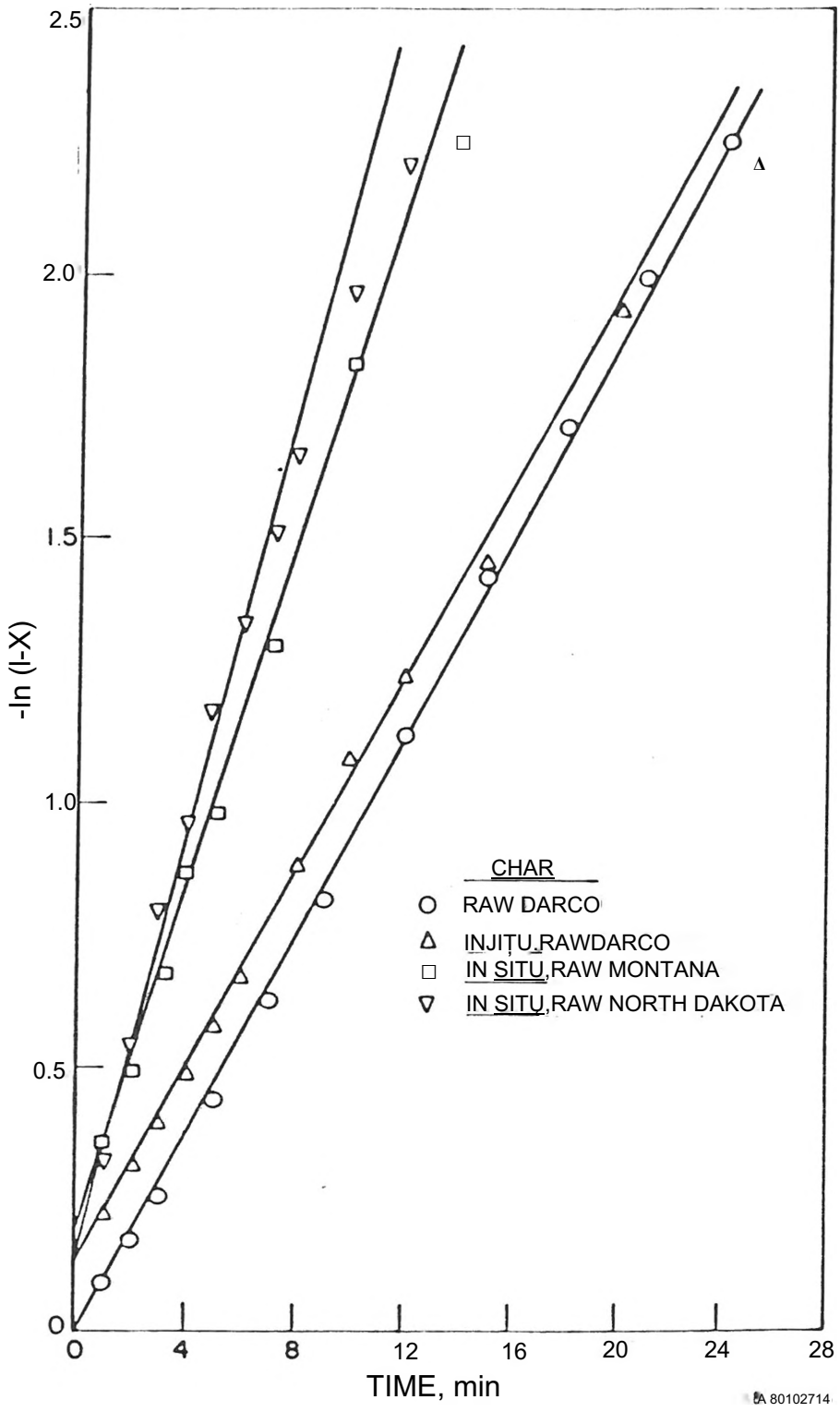

Figure 1U. GASIFICATION OF CHARS IN STEAM AT 1600°F
(Reproduced from Zabranský 8 Nandi) (30)

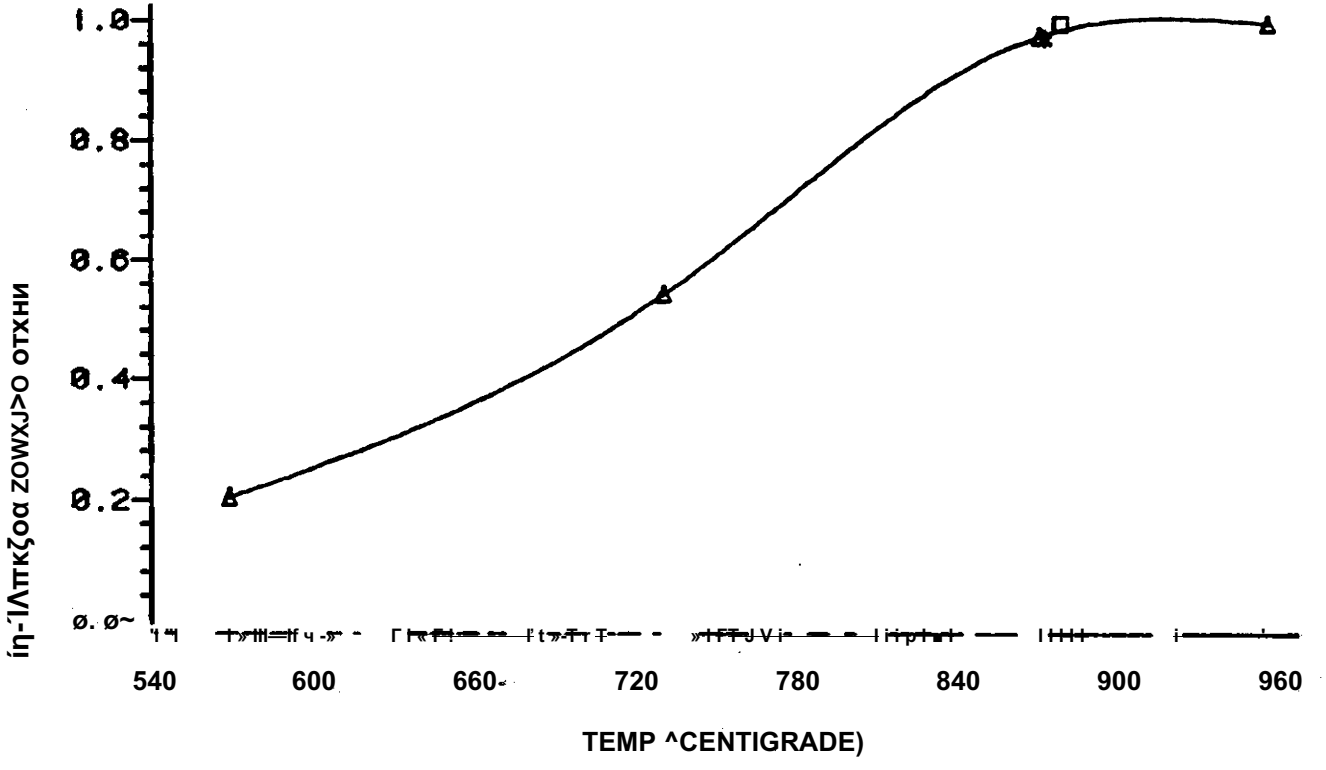

Figure 15. Fraction Fixed Carbon Converted vs. Temperature (30 minute runs)

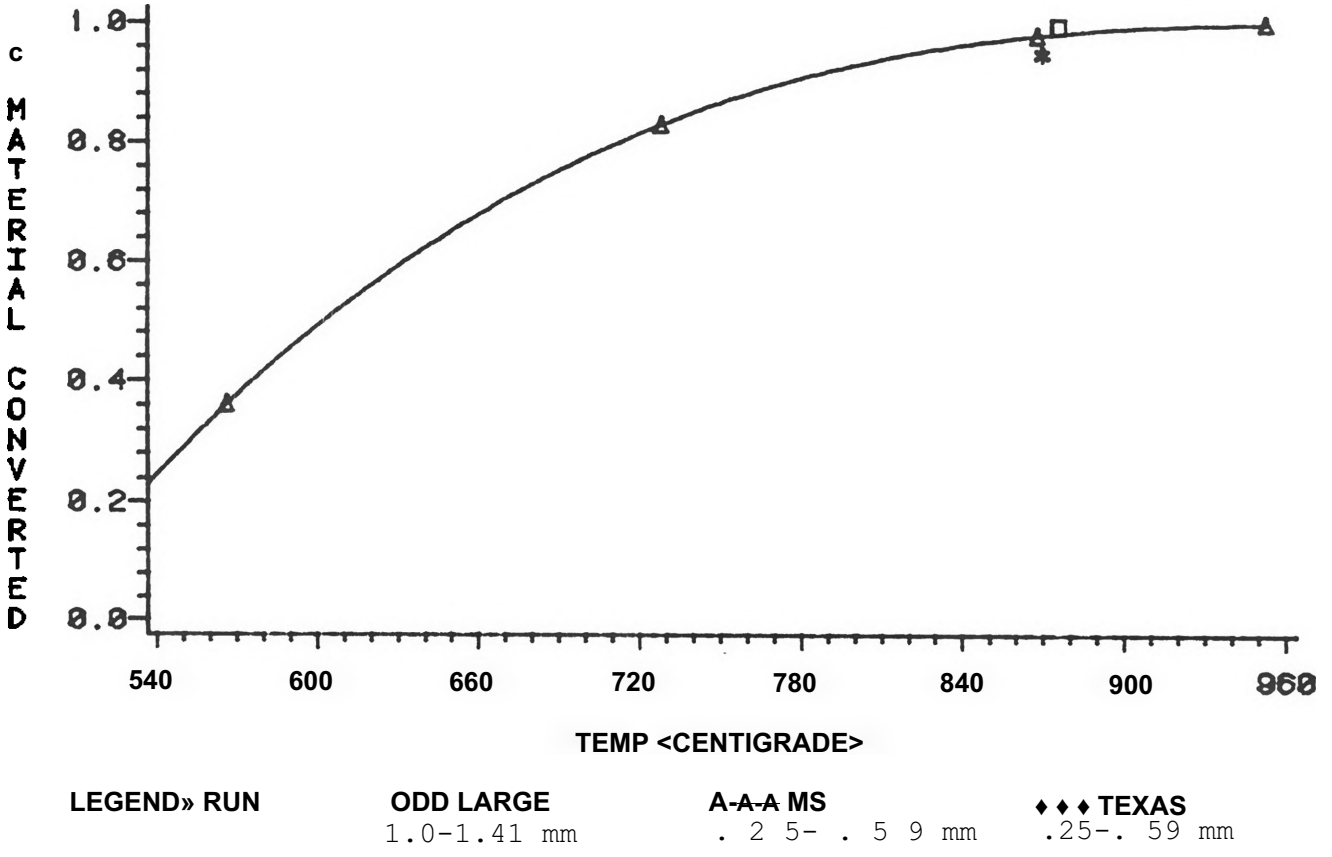

Figure 16. Fraction Carbonaceous Material Converted vs. Temperature (30 minute runs)

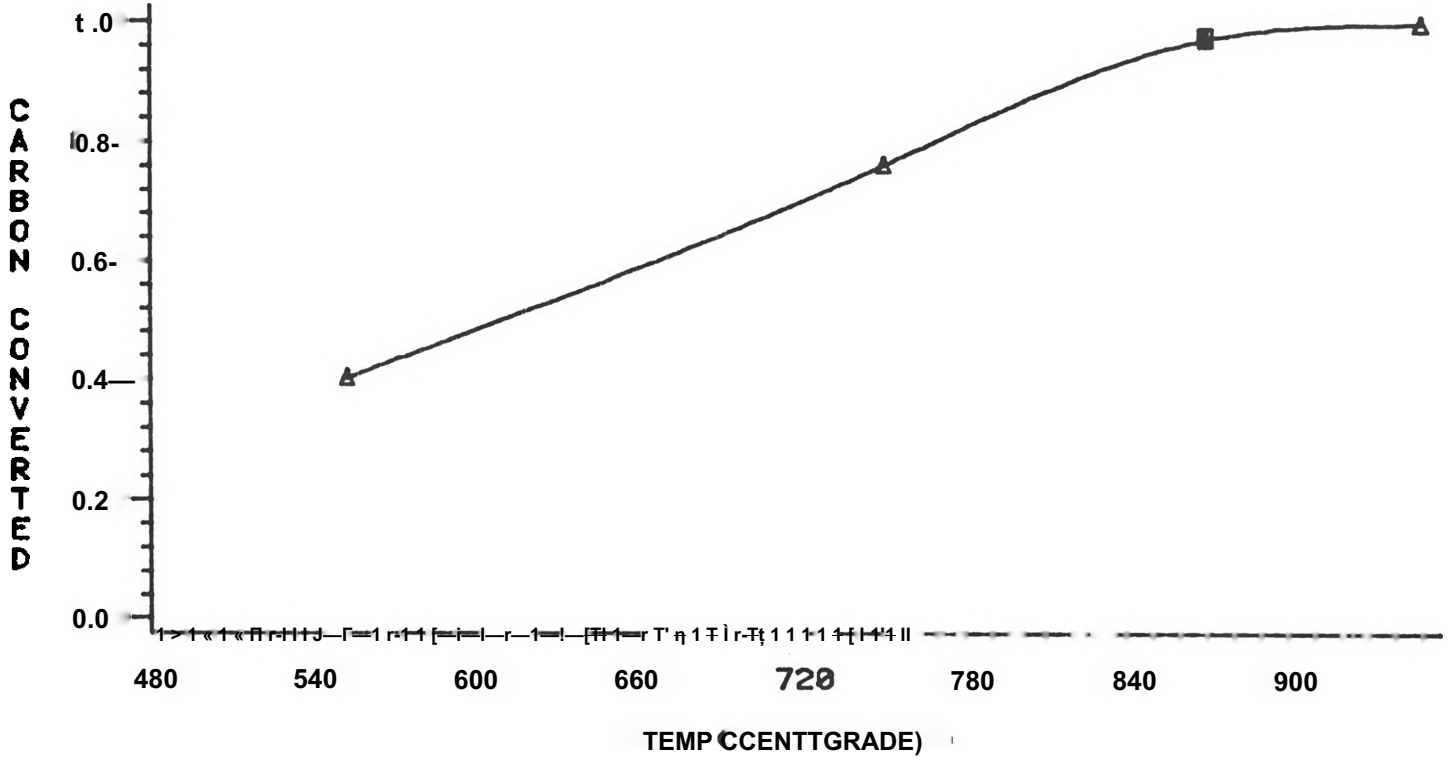

Figure 17. Fraction Carbon Converted vs. Temperature
(30 minute runs)

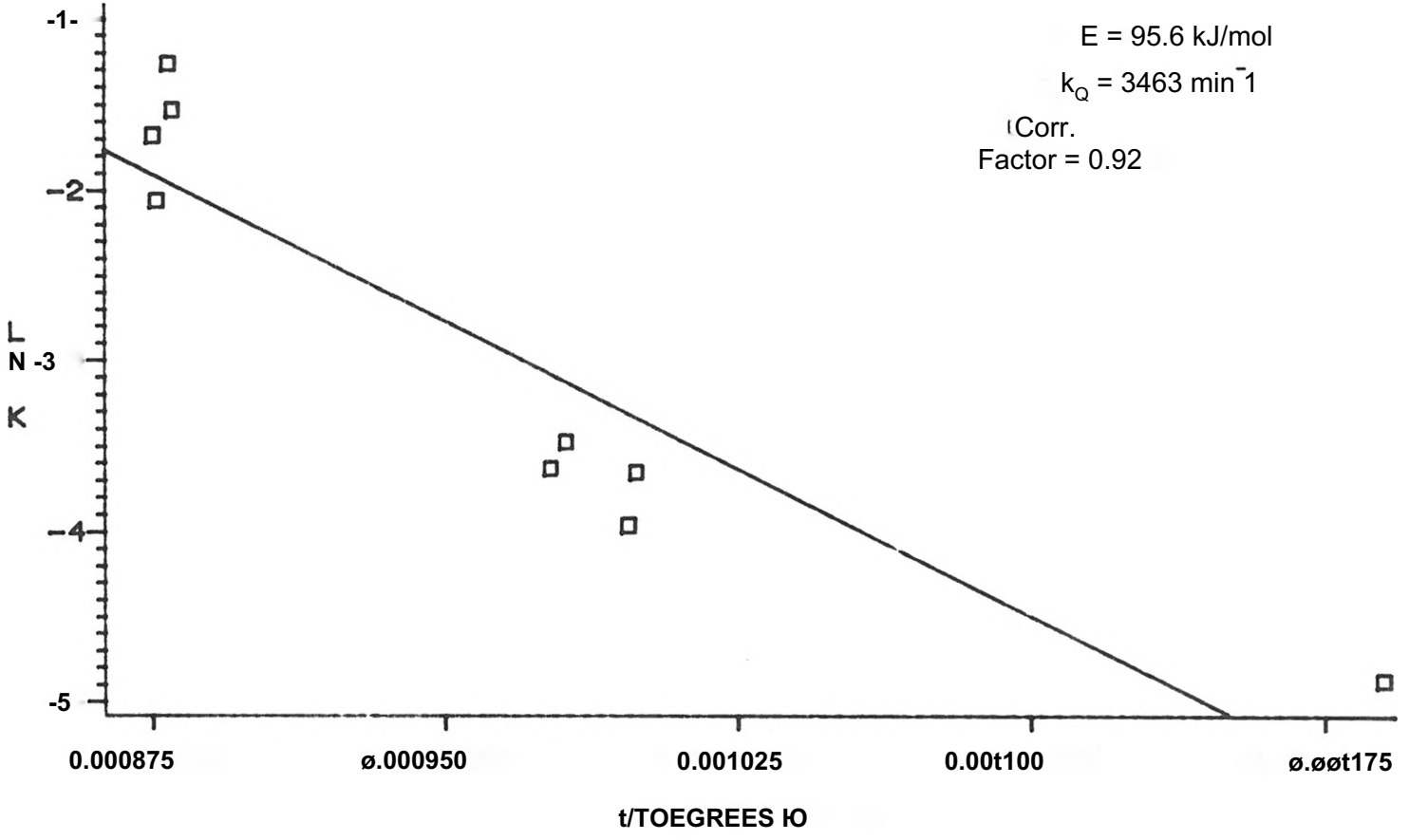

Figure 18. ln(k) vs. 1/T

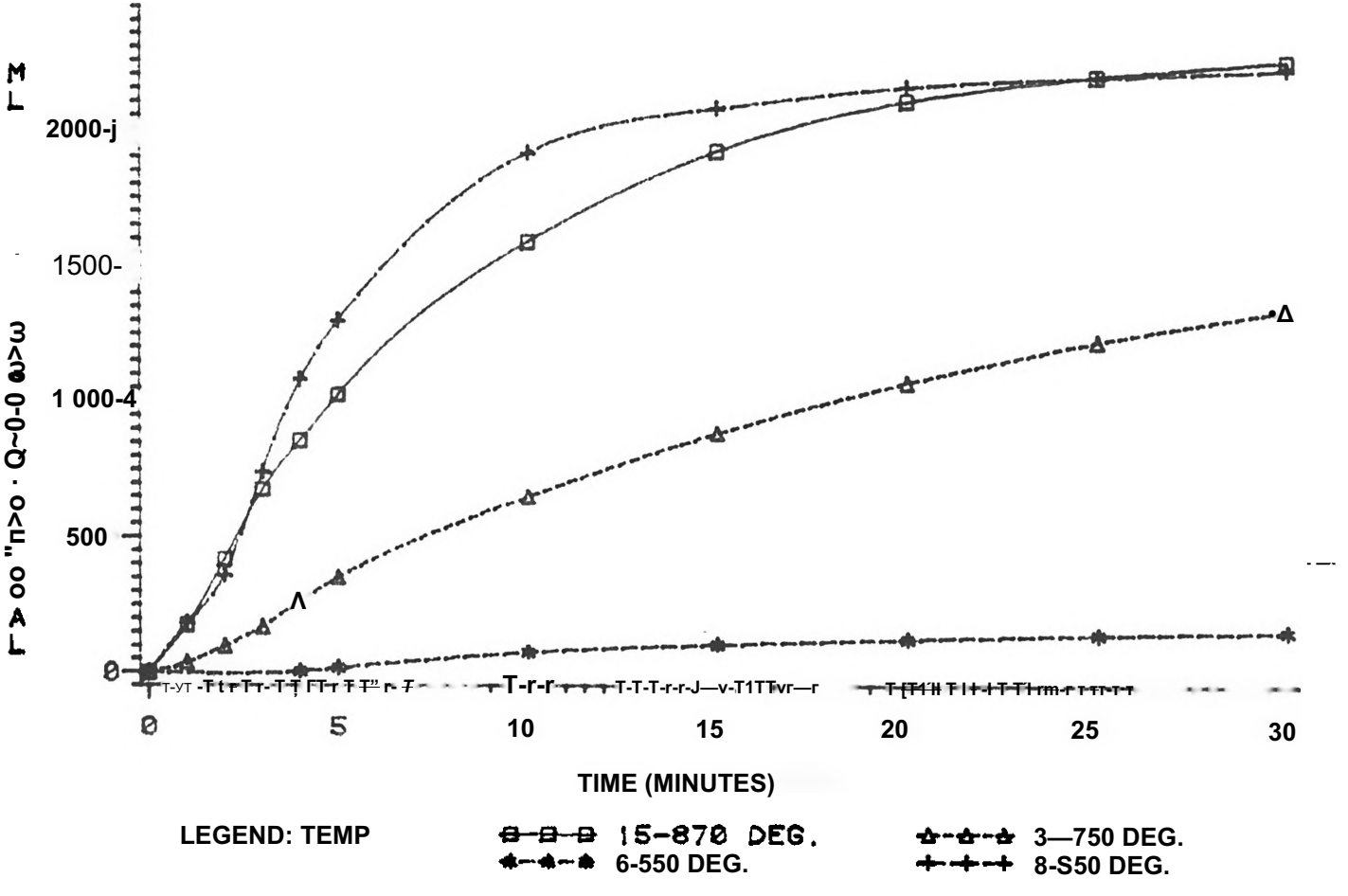

Figure 19. Gas Volume vs. Time

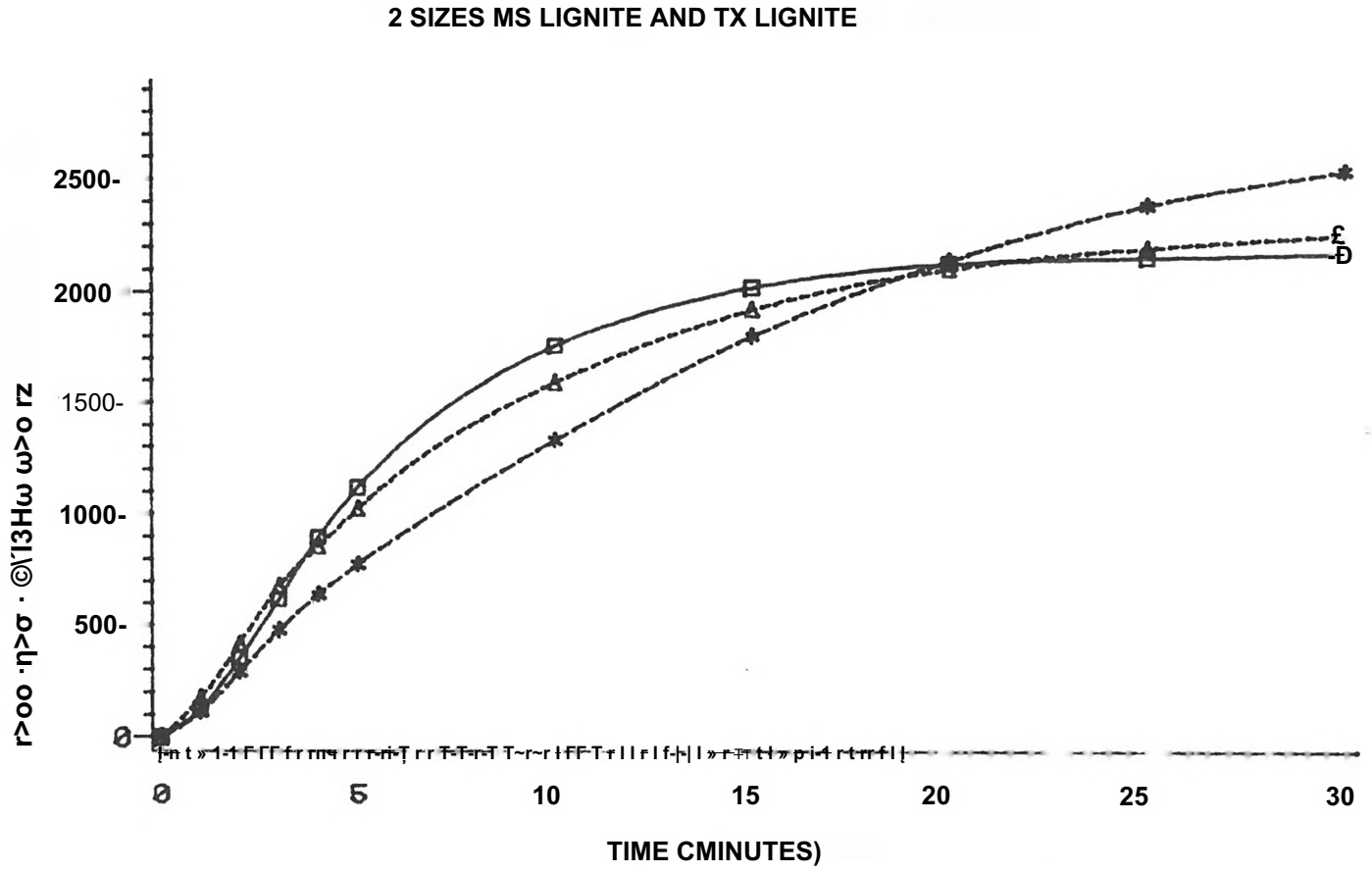

Figure 20. Gas Volume vs. Time
870 Degree Centigrade Runs

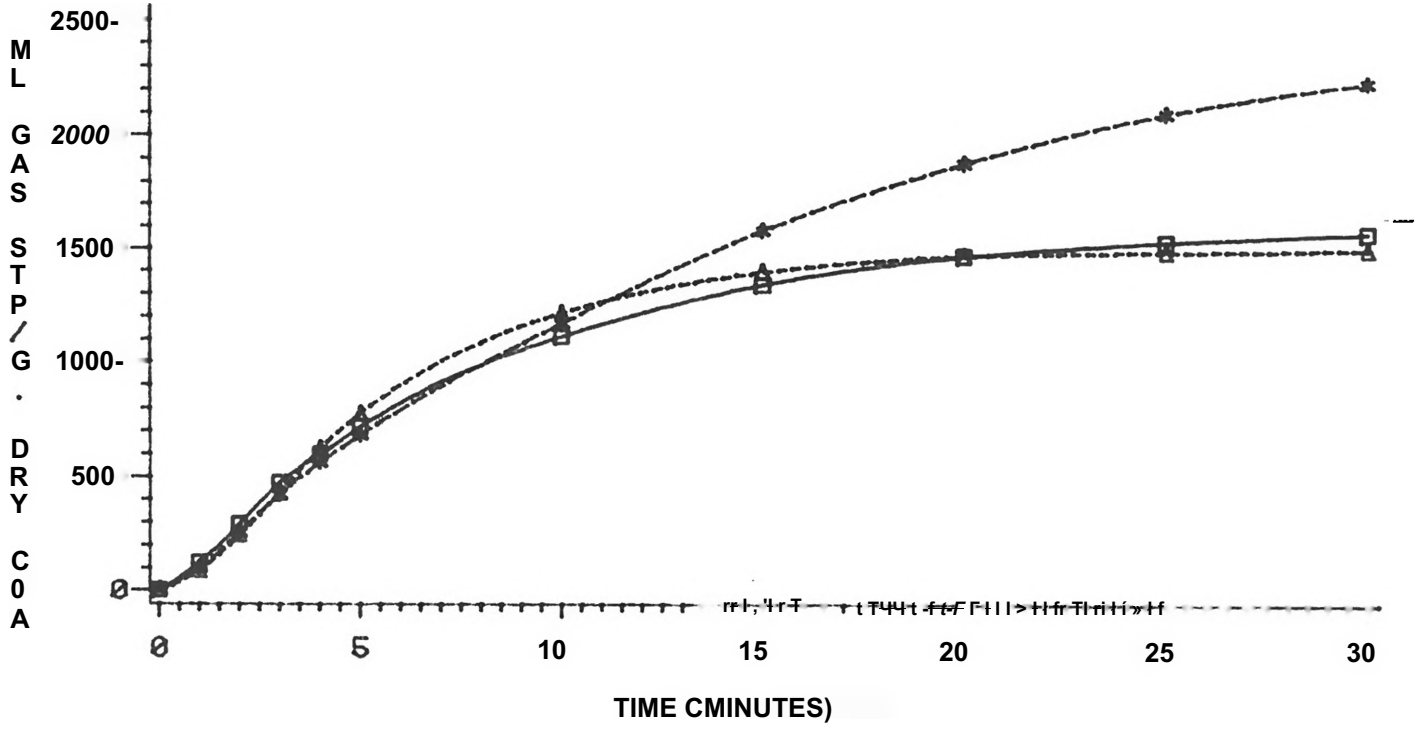

Figure 21. Gas Volume vs. Time
Dry Basis
870 Degree Centigrade Runs

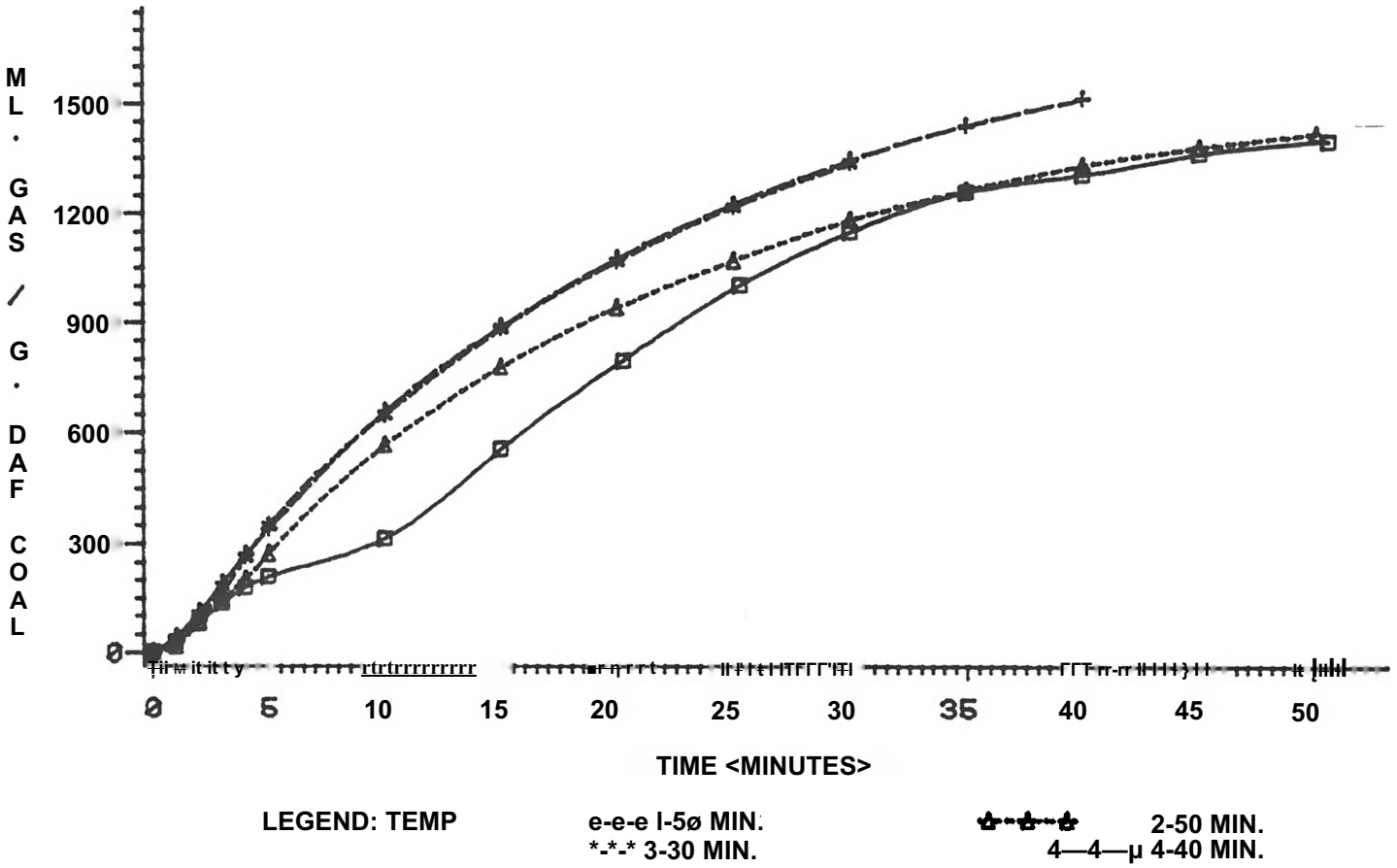

Figure 22. Gas Volume vs. Time
750 Degree Centigrade Runs

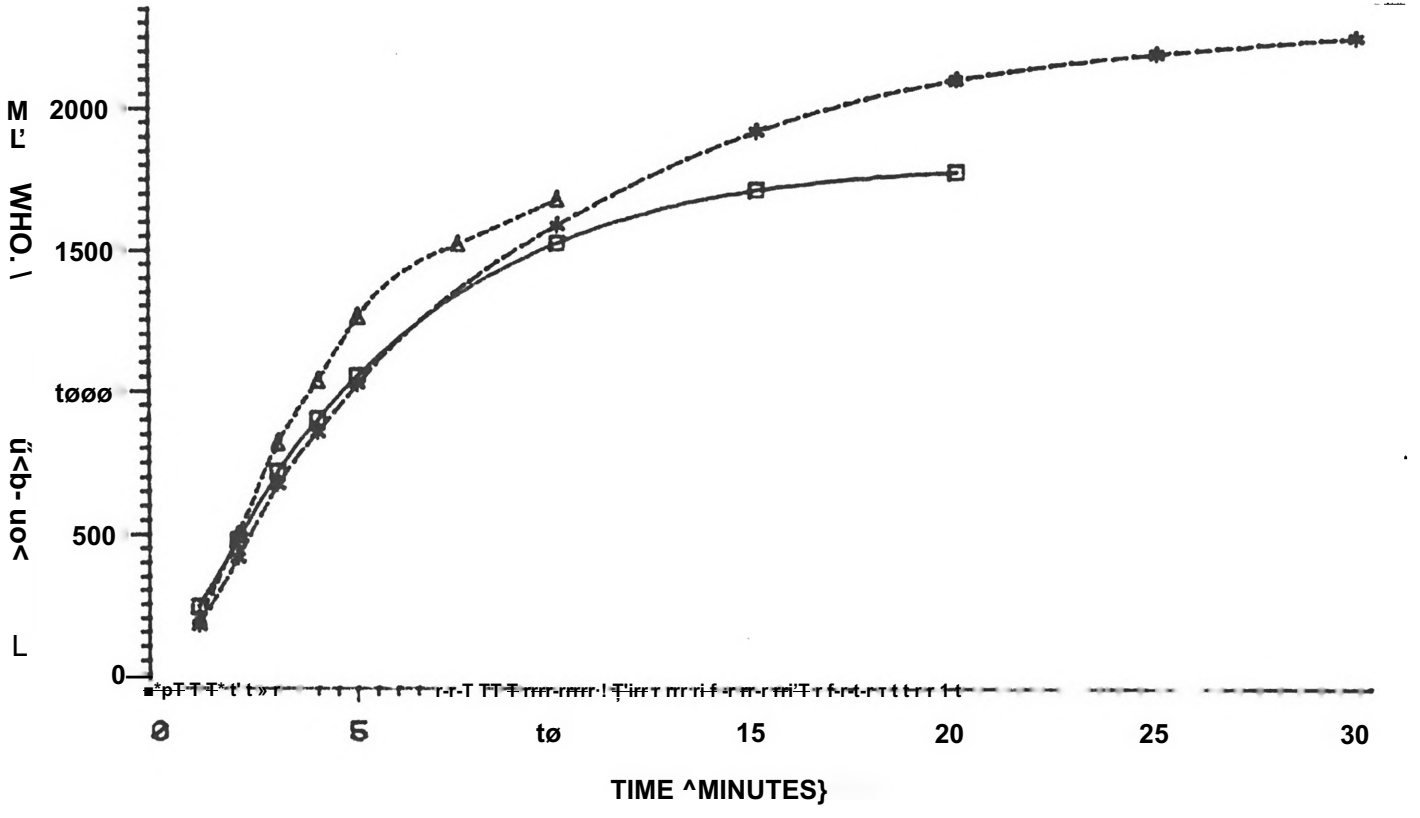

Figure 23. Gas Production vs. Time
870 Degree Centigrade Runs

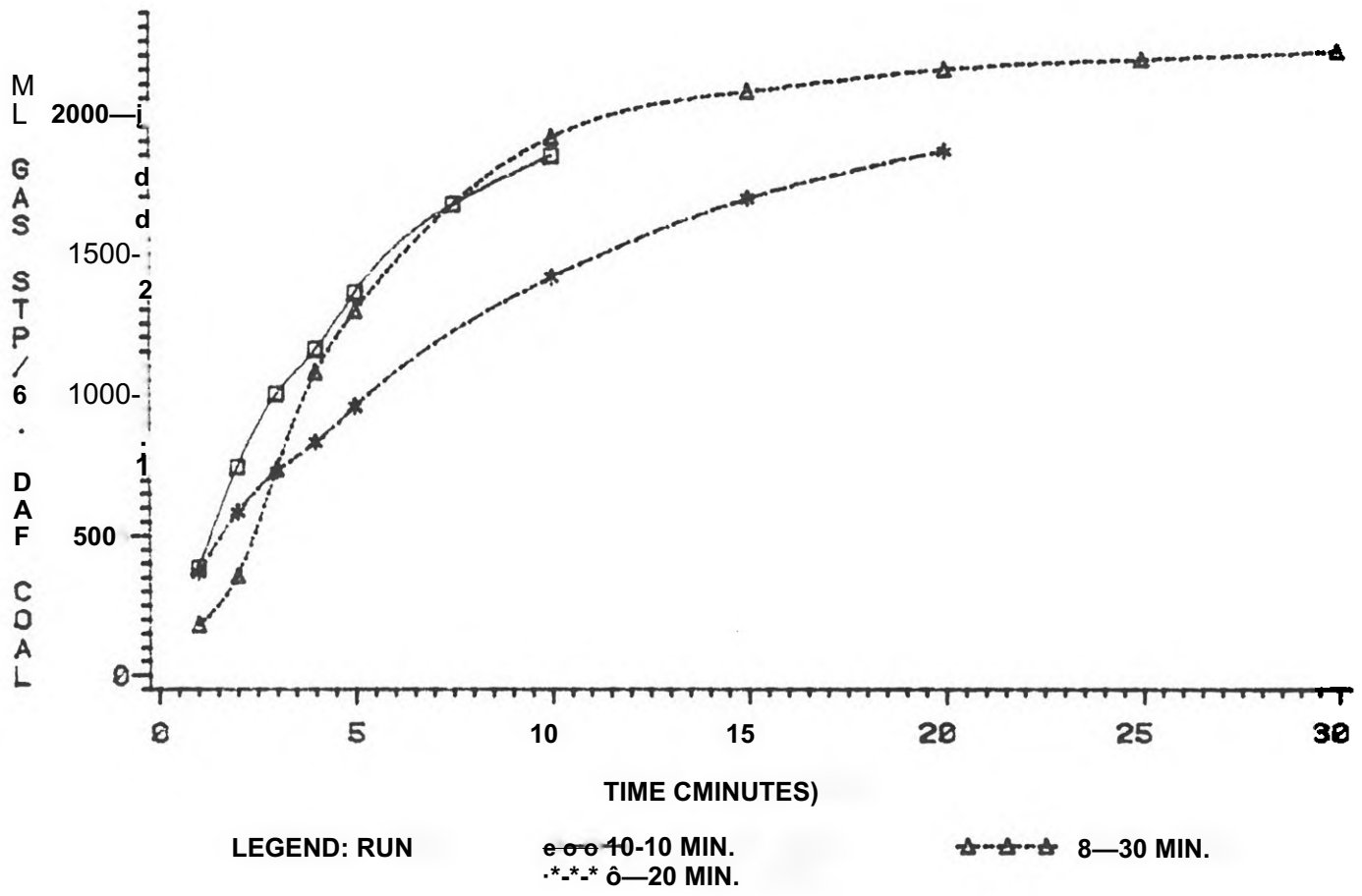

Figure 24. Gas Volume vs. Time
950 Degree Centigrade Runs

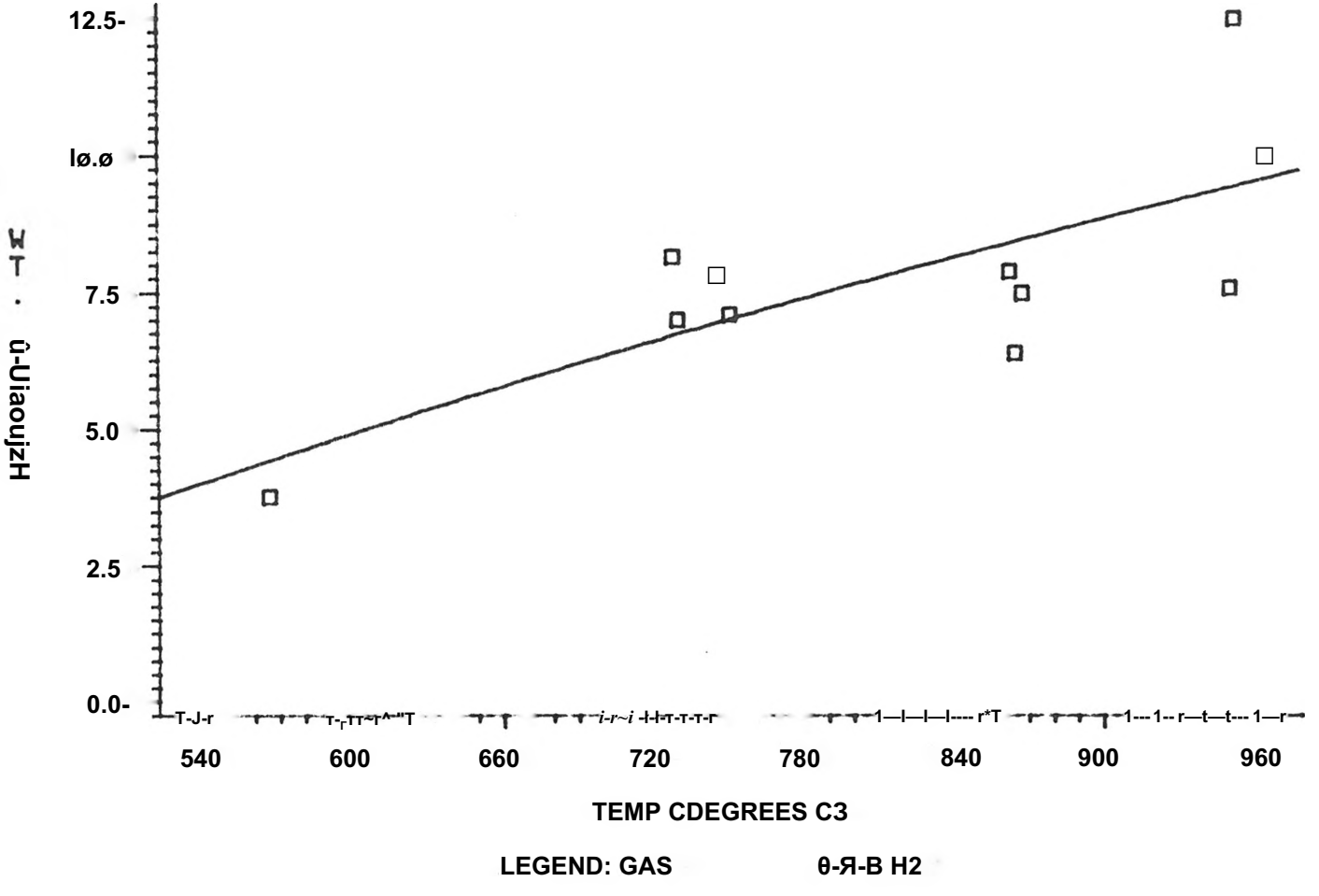

Figure 25. Hydrogen Content vs. Temperature

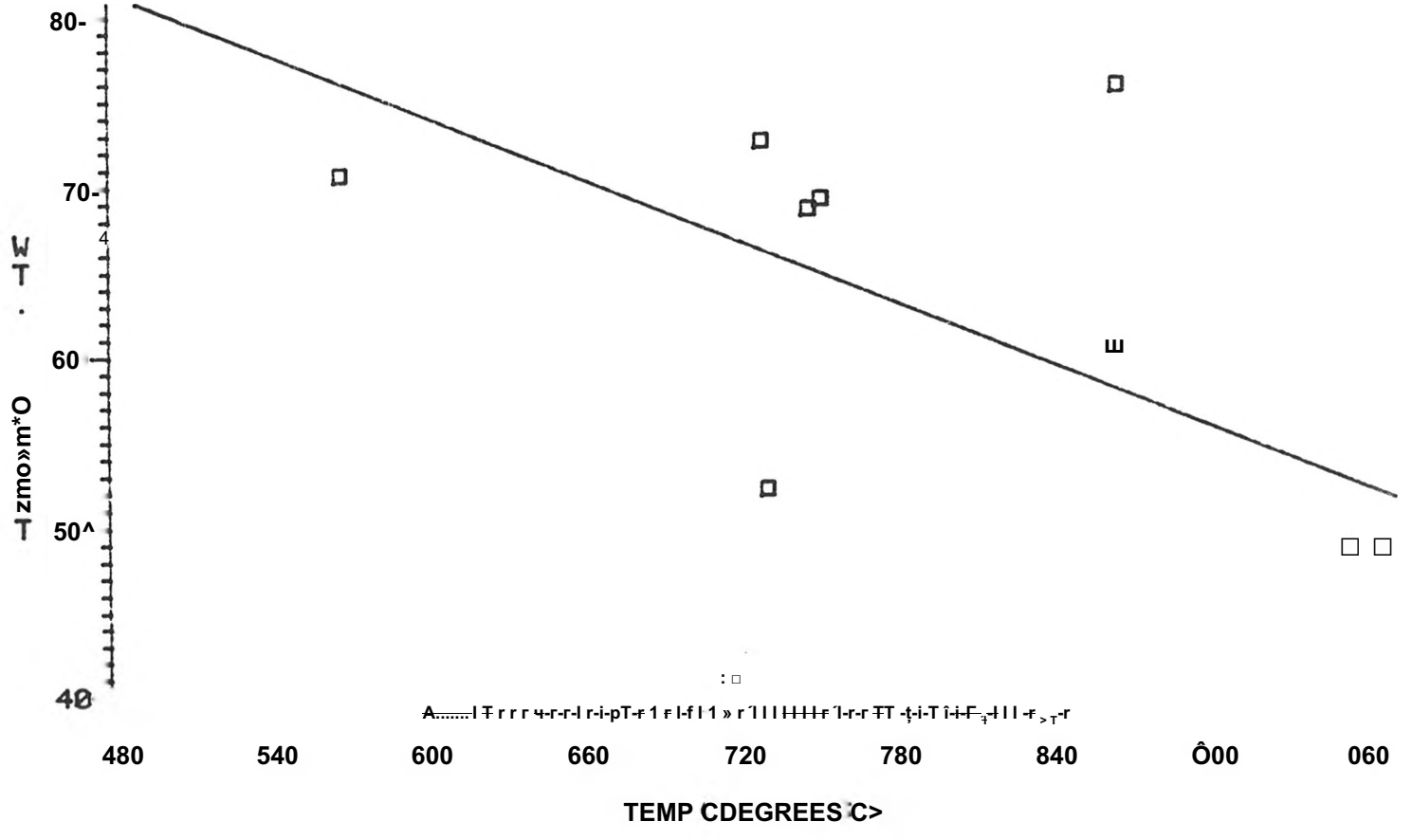

Figure 26. CO_2 Content vs. Temperature

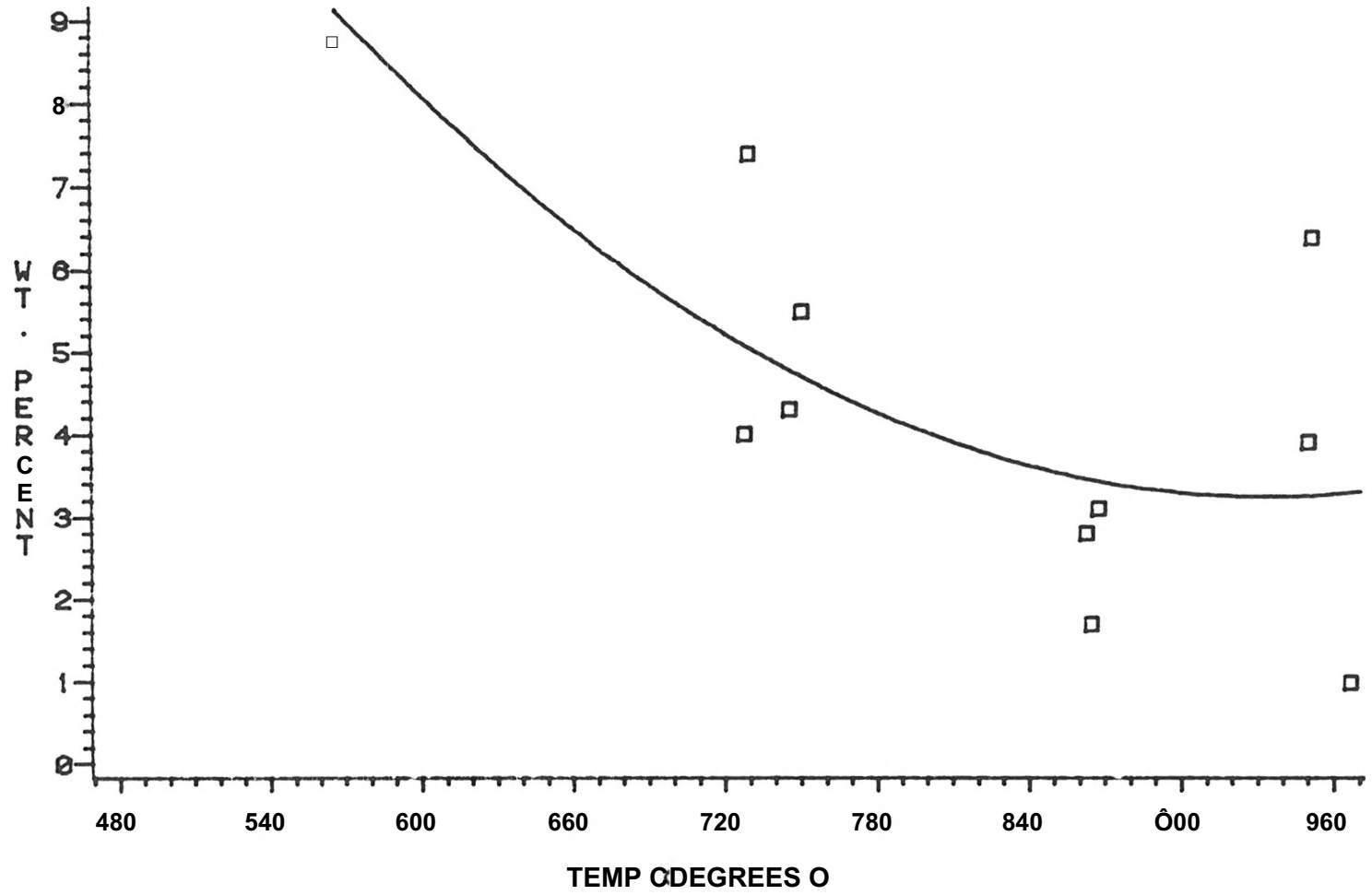

Figure 27. Methane Content vs. Temperature

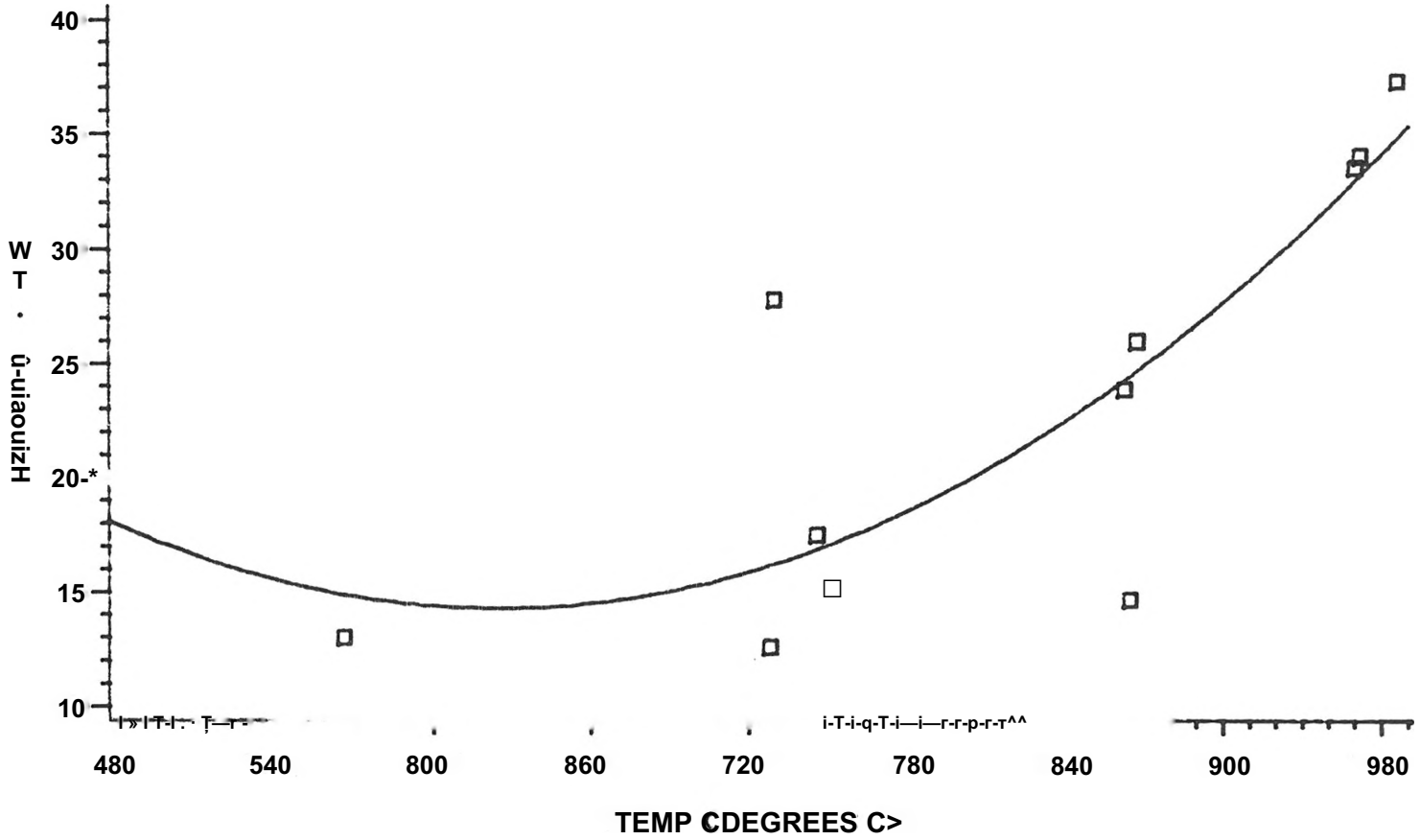

Figure 28. Carbon Monoxide Content vs. Temperature

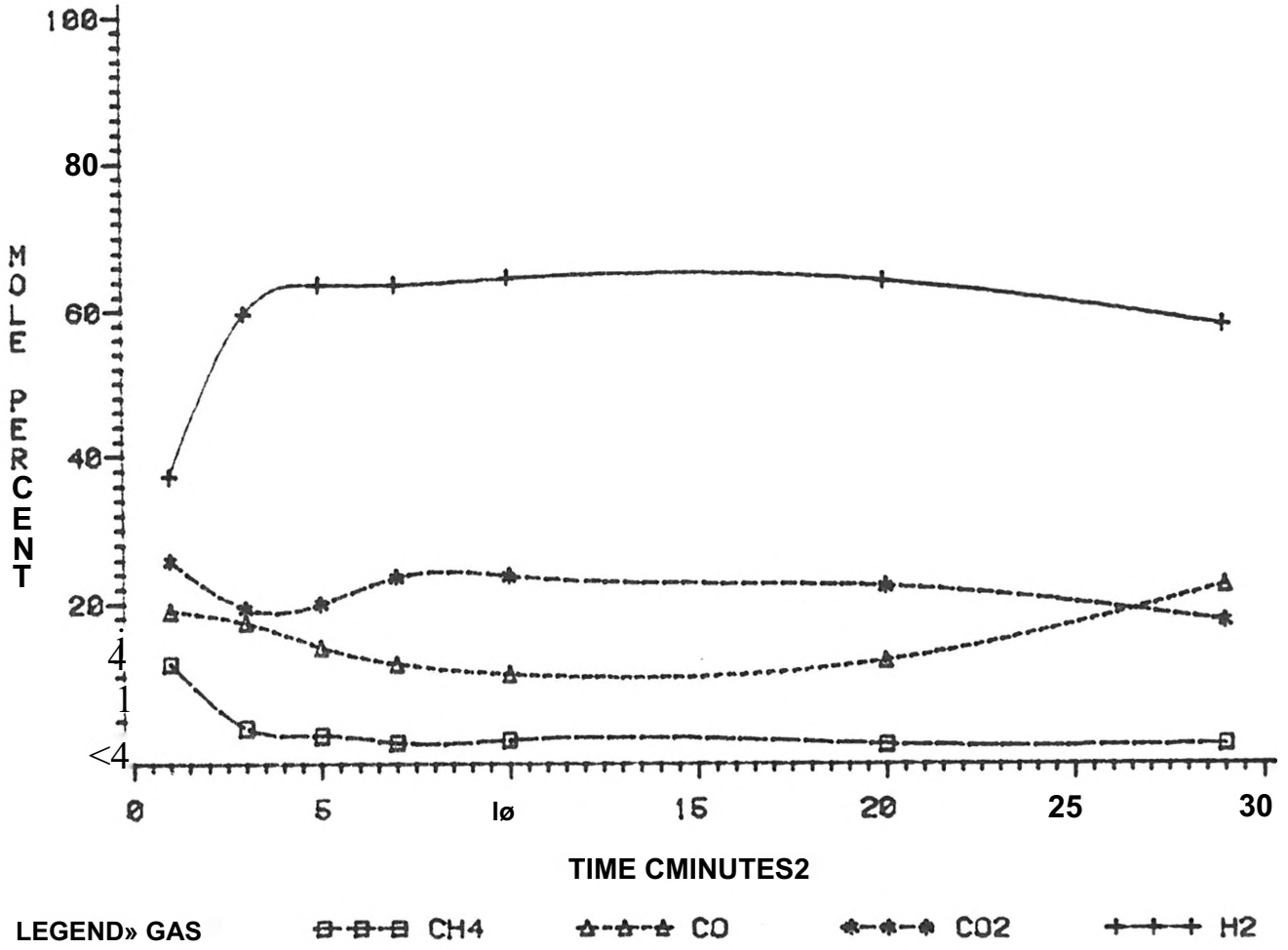

Figure 29. Gas Composition vs. Time (Mole Percent)

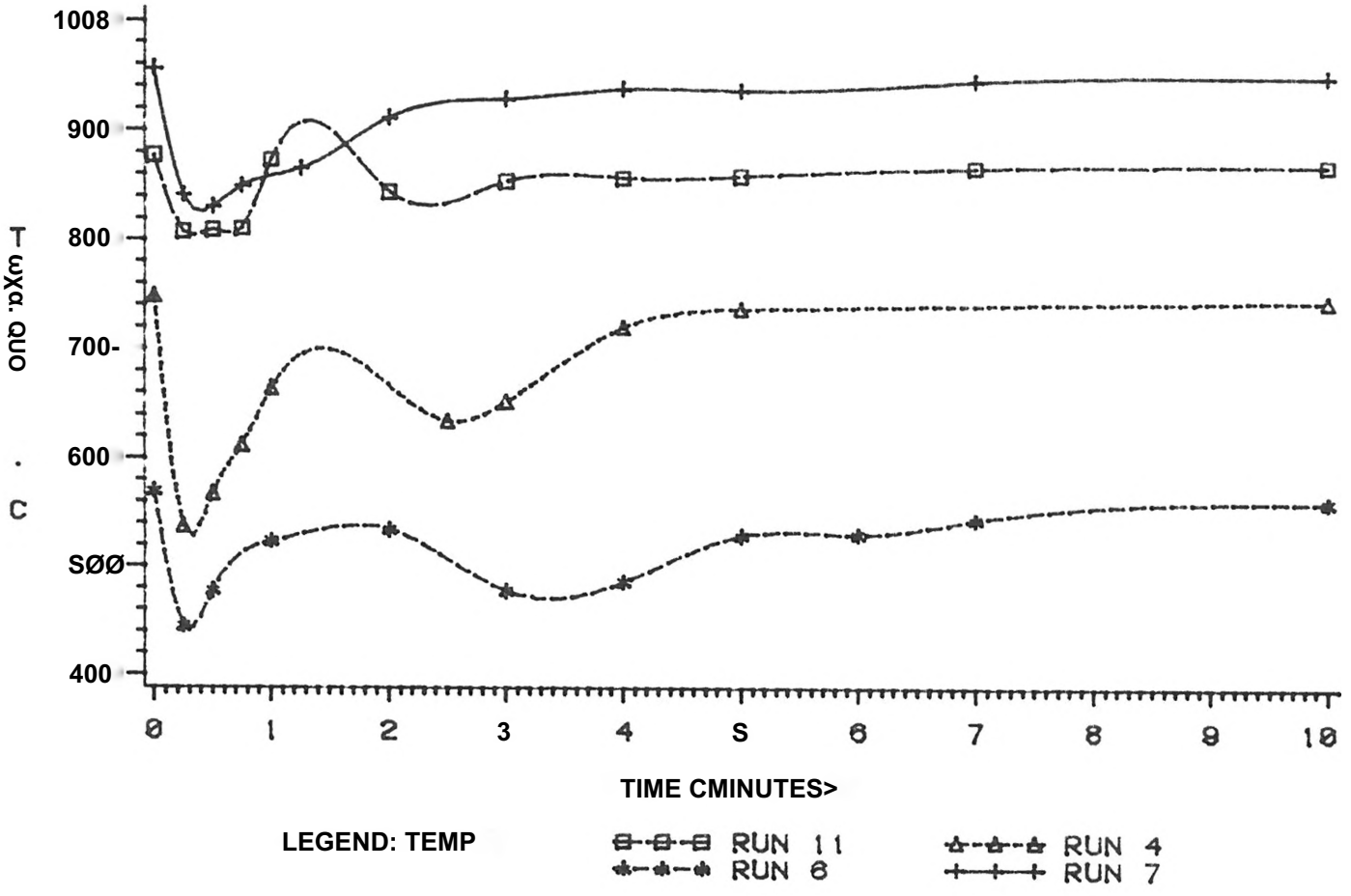

Figure 30. Reactor Temperature vs. Time

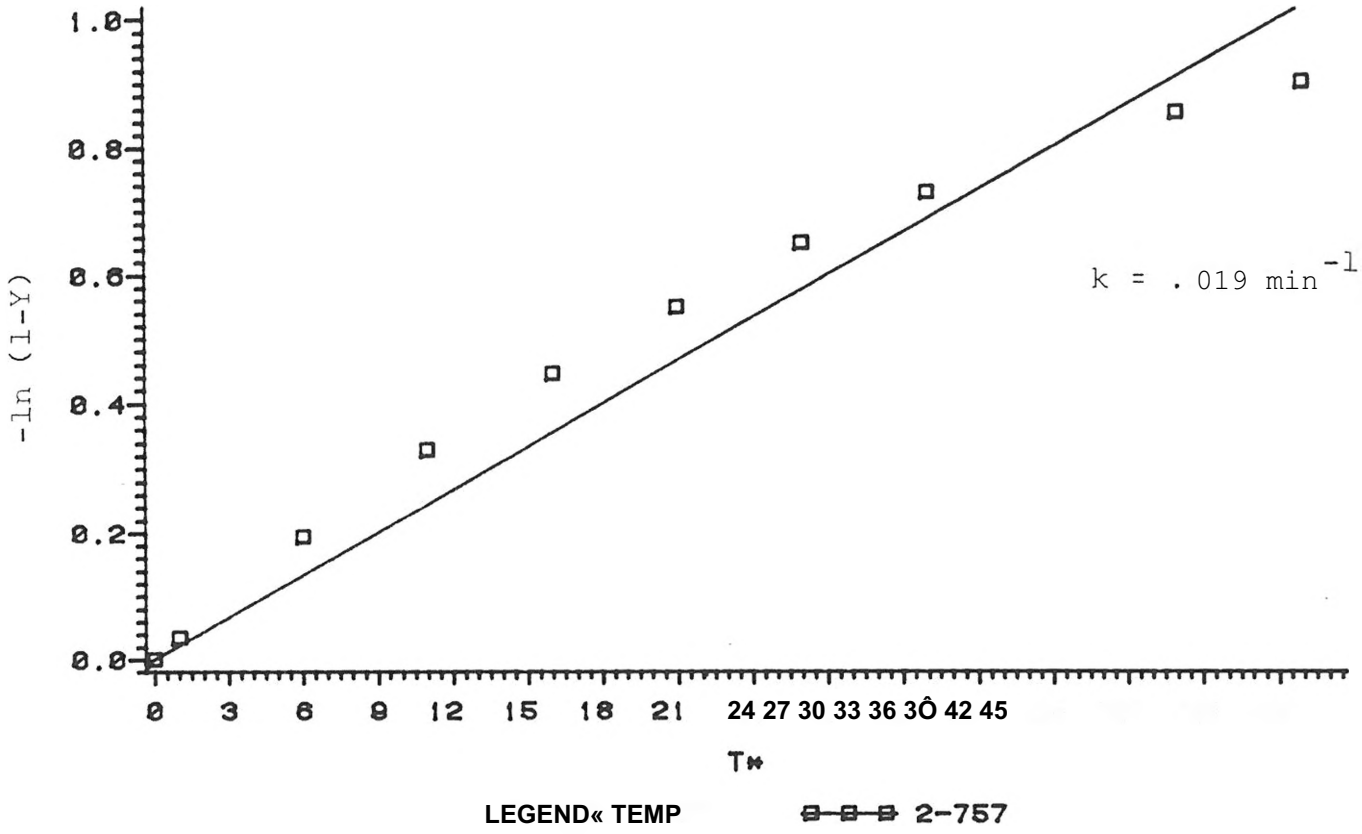

Figure 31. -ln(1-Y) vs t* - 757°C

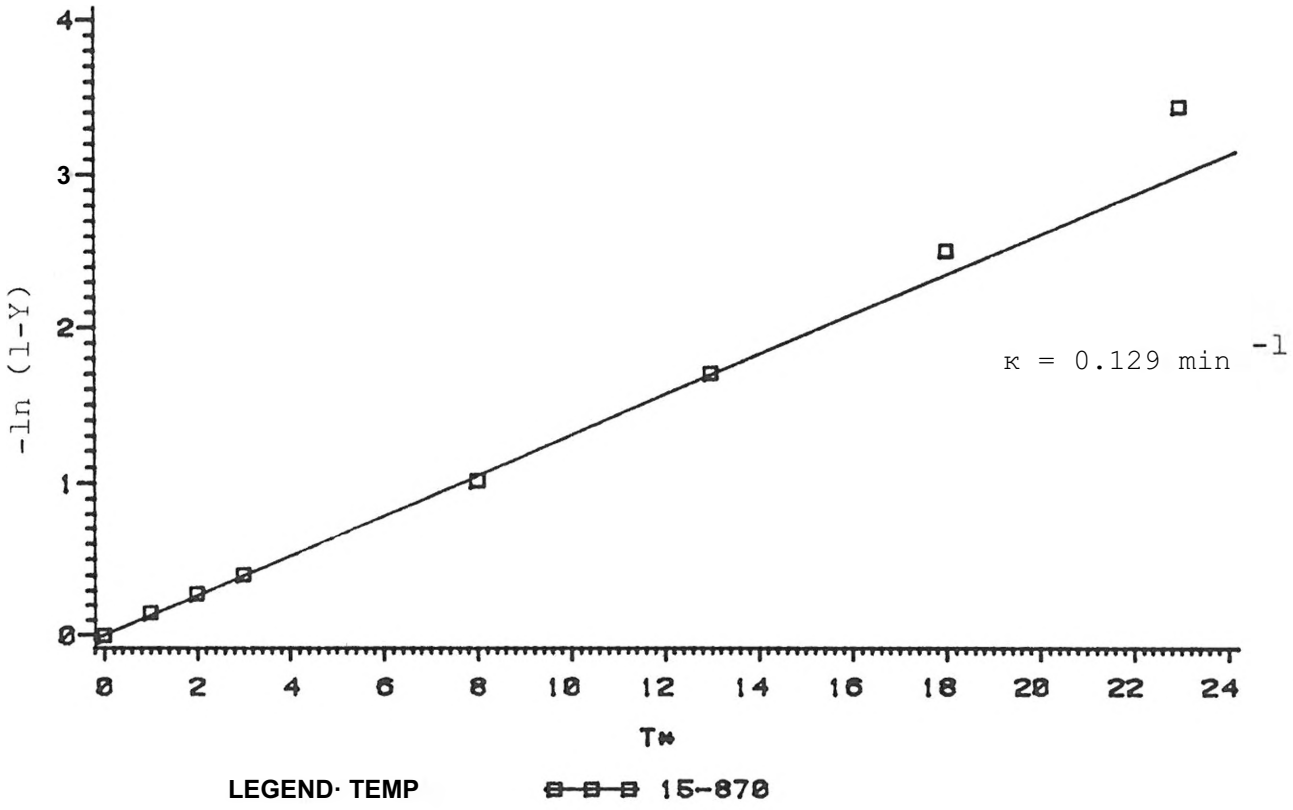

Figure 32. -ln(1-Y) vs t^* - 870°C

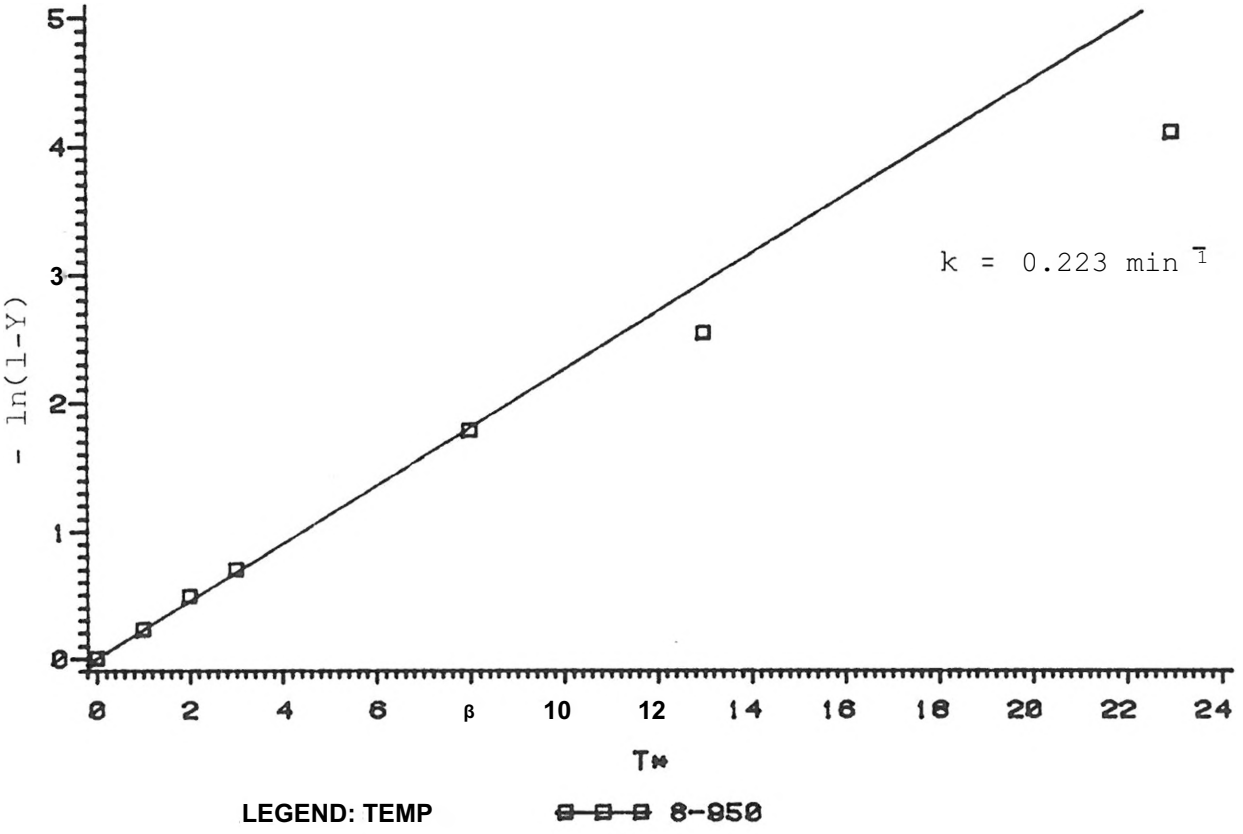

Figure 33. -ln(1-Y) vs t* - 950°C

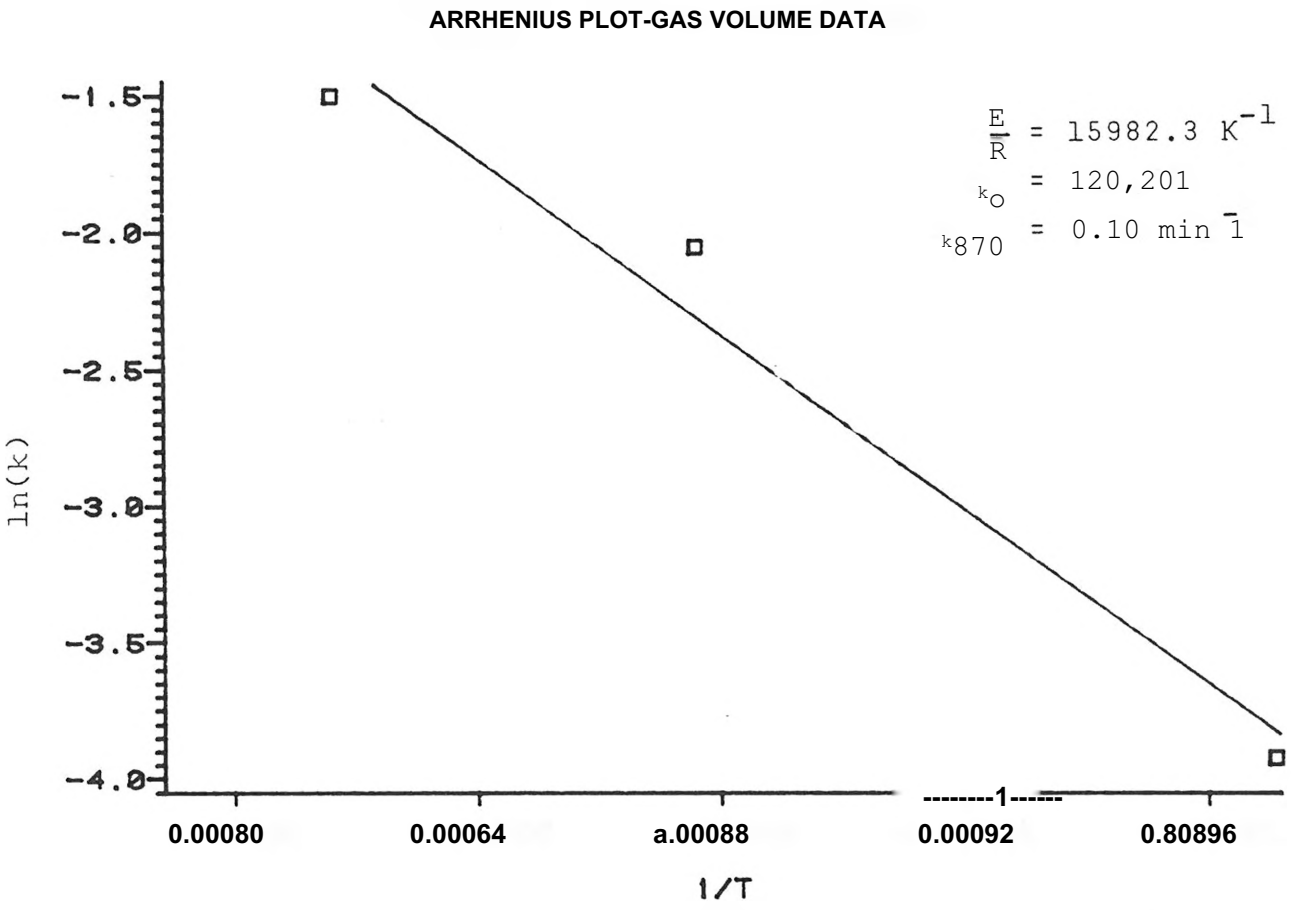

Figure 34. Arrhenius Plot - Gas Volume Data

PART B

RAPID PYROLYSIS OF MISSISSIPPI LIGNITE

CHAPTER I

INTRODUCTION

Coal has emerged as the principal potential source of the synthetic pipeline gas and fuel gases that may be needed to supplant our rapidly dwindling natural gas reserves; and to provide fuel alternatives for electrical utilities and other industries. Coal research pertinent to gasification is not new, and considerable experimental data are dispensed throughout the scientific and technical literature. Unfortunately, the phenomenon are so complex that no unifying theory has evolved. The type of coal, the nature of the experiment, and the apparatus each profoundly influence the results, hence, only restricted interpretations have been possible. (1)

Coal represents approximately 70% of the recoverable fossil fuel resources in the United States and may eventually become our principal source of hydrocarbon fuels and feedstocks (1). National recognition of the enormous, immediate and long-range potential of coal has resulted in substantial efforts toward the development of economically and environmentally viable coal utilization technologies. Coal conversion to clean gaseous and liquid product is especially attractive with respect to minimal impact on existing consumption patterns. The approaches now under extensive development in the United States include gasification, liquifaction and devolatilization (1).

Interest in clean gaseous fuels from coal has been stimulated by the introduction of environmental constraints and the significant decline of proven and recoverable U.S. natural gas reserves.

Present coal gasification efforts are directed toward low Btu, intermediate Btu, and high Btu (pipeline quality, essentially methane) gas. Choice among these options and other possible fuels from coal will be decided locally and will be strongly influenced by required fuel characteristics and distribution considerations (1).

It has been estimated that the Gulf Coast region of the United States contains a total of 22.5 billion tons of recoverable lignites. Of this total, Mississippi with 5 billion tons ranks second only to Texas with an estimated 11.5 billion tons. Currently about 20 million tons of lignite are mined annually in Texas for use as a boiler fuel. No commercial utilization of Mississippi lignites has been practical so far (2).

Coal is the product of very slow decomposition of organic matter deposited in prehistoric times. The age of coal is indicated by its carbon content or rank, for example, lignite, bituminous, anthracite, and the nature of the original matter is reflected by the material composition of the coal (1). The decomposition can be accelerated artifically by elevating the temperature. Upon being heated at a more or less conventional rate, coal begins to decompose at 350° to 400°C into a carbon rich residue and a hydrogen rich volatile fraction (1). The decomposition continues until a temperature typically around 950°C is reached which, if maintained for an extended time, results in a residue of nearly pure carbon possessing a structure approaching that of graphite.

The accumulated volatiles are comprised of various gases and liquids, the relative proportions of which depend on the coal type and the manner of heating (1).

In the early 1960's investigators in Germany (Peters, et al., 1960, 1965), France (Loison and Chauvin, 1964), England (Badzioch, 1961), and the United States (Jones, et al., 1964) found that rapid heating techniques for coal, permit substantially more volatiles than traditional slow heating methods. Furthermore, the liquid or tar fraction seemed most strongly influenced, resulting in considerable excitement over the prospects of renovating the obsolete coal carbonization industry. Much work has since focused on the kinetics, mechanism, and product distribution in order to provide a basis for choosing and optimizing a commercial scheme (1).

One of the most intriguing avenues of research centers on the direct production of methane from the reaction of hydrogen and raw coal rather than the more costly and less efficient catalytic methanation of hydrogen and carbon monoxide (3)

Quantitative understanding of coal devolatilization or thermal decomposition is essential to the efficient development of better coal combustion and gasification processes. Through the subject of many investigators, the kinetics and mechanism of rapid devolatilization of pulverized coal are not satisfactorily understood. The actual phenomena are complex and possibly cannot be modeled exactly (4) . Attempts have been made to correlate devolatilization rates with the first-order expression

$$dV/dt = K(V^* - V) \quad [1]$$

where V is the mass of volatiles per mass of original coal, evolved at time t and V* is the value of V at t = The rate constant K is usually assumed to have the Arrhenius form

$$K = K\theta \exp(-E/RT) \quad [2]$$

where Kθ and E are the apparent frequency factor and activation energy, R is the ideal gas constant, and T is the absolute T (4). Correlations such as [Eq. 1] have proven applicable only for the limited experimental conditions upon which they were based. For a given set of conditions values of K from various authors may differ by several factors of 10 and E may vary from several K Cal/mole to nearly 50 KCal/mole. Furthermore, V* depends upon both the experimental temperature and the technique. Thus, it was found that rapid devolatilization of pulverized coal dispersed in carrier gas can result in considerably larger V* values than those obtained by the relatively slow heating of a small bed of pulverized coal in a crucible (standard proximate analysis) (4). A mechanism or model compatible with all these diverse results has not been reported. The lack of consistent data for a wide range of well-defined conditions has been a major difficulty. The present work was conducted in order to better characterize Mississippi lignite. The objective was to determine the rate and extent of devolatilization of the Mississippi lignite under a wide range of controlled conditions in an apparatus similar to that of Anthony, et al. (1) and Suuberg, et al. (8). This apparatus was constructed and used for the measurement of weight loss from small

captive samples of pulverized coal devolatilized in inert gas under various conditions of heating rate, temperature, and particle size. The data gathered was then compared to data from the literature on other lignites and to data gathered on Texas lignites in the same apparatus.

CHAPTER II

LITERATURE SURVEY

Coal represents approximately 70 percent of the recoverable fossil fuel resources in the United States. National recognition of the enormous immediate and long-range potential of coal has resulted in substantial efforts toward the development of economically and environmentally viable coal utilization technologies. Coal conversion to clean gaseous and liquid product is especially attractive with respect to minimal impact on existing consumption patterns (1).

Coal is an intermediate product of the very slow decomposition of organic matter deposited in prehistoric times. The final product would be pure carbon. This natural carbonization can be artificially accelerated by elevating the temperature. Although most of the carbon remains in the solid form when a relatively massive sample of coal is heated, it is often possible to volatilize 50 percent or more of the initial carbon by rapidly heating a finely ground and well-dispersed sample and by rapidly quenching the products. Furthermore, if this rapid heating takes place under sufficient hydrogen pressure, nearly all of the carbon in the coal can be converted to methane in fractions of a second (1).

Much evidence supports the hypothesis that the devolatilization of coal is a chemical decomposition reaction. Coal is a complex organic polymer consisting of aromatic clusters of several fused rings strung together by assorted hydrocarbon and heteroatom (O,N,S) linkages (1).

Heating causes the structure to decompose, the weaker bonds rupturing at lower temperatures and the stronger ones at higher temperatures, and the fragments that are volatile attempt to escape from the particle. Some of the fragments are highly reactive free radicals subject to a variety of secondary reactions sudi as cracking and repolymerization (1). Generally such secondary reactions are undesirable in practice, since they deposit a portion of the volatile matter as a solid or char and diminish gas and liquid yields. The extent of secondary reactions can be reduced by enhancing the transport of volatile fragments away from the reactive environment, such as by operating at reduced pressures with smaller and more widely dispersed particles (1).

The complexity of this phenomena has handicapped the development of models suitable for design and scale-up (1).

Hydrogen will react with devolatilizing coal several orders of magnitude faster than with the residual char (1). The short lived period of high reactivity lasts only a few seconds or less at temperatures of interest in gasification. The so called rapid-rate carbon species is not clearly identified, though convincing evidence suggests that hydrogen interferes with the char forming secondary reactions presumably by hydrogenating reactive fragments sufficiently to stabilize them during their escape (2).

Physical and Chemical Changes in Coal Pyrolysis

A series of consecutive and parallel reactions occur during the rapid stage of pyrolysis of coal. The effect of initial heating is to

release the secluded gases and moisture from the coal. For coking coals, as temperature increases, the coal particle softens to form a metastable plastic intermediate, metaplast, which depolymerizes to yield the primary volatile products and the semi-coke (5).

Table II-1 shows the possible chemical reactions which take place during the pyrolysis in an inert atmosphere, at the conditions of moderate heating rates and temperatures and at an atmospheric pressure. At the conditions of long vapor residence time and/or extremely rapid heating rates and temperatures, for example, in flash heating, considerable amounts of acetylene, other unsaturated hydrocarbons and cracked carbon are formed by the vapor cracking of the primary products of gaseous hydrocarbons (5).

Volatiles Yield, Product Distribution, and Kinetics of Coal Pyrolysis

A knowledge of the kinetics of coal pyrolysis is essential in predicting the yield and product distribution in a coal gasifier. The understanding of coal pyrolysis is very important in view of the potential of the process to take advantage of (a) the phenomena of rapid pyrolysis and (b) obtaining higher yields of gaseous and liquid hydrocarbons by the application of pressure and hydrogen atmosphere (5).

It has been confirmed that volatile matter significantly higher than those indicated by the proximate analysis can be obtained from coal by rapid heating. Pilot plant studies have demonstrated that about 30-35 percent conversions of coal to oil is possible in pyrolysis by rapid heating of coal at comparatively lower temperatures and with the minimum

TABLE II-1

The Chemical Processes Of Coal Pyrolysis

Product	Source	Process
1. Tar + Liquid	Weakly bonded ring-clusters	Distillation + decomposition
2. CO_2	Carboxyl groups	Decarboxylation
3. CO (<500°C)	Carbonyl groups and ether linkages	Decarbonylation
4. CO (>500°C)	Hetero-oxygens	Ring rupture
5. H_2O	Hydroxyl groups	Dehydroxylation
6. $CH_4 + C_2H_e$.	Alkyl groups	Dealkylation
7. Hj	Aromatic C-H bonds	Ring rupture

Volatiles are reteased from coal "approximately" in the following order: H_2O, CO_2, CO, C_2H_t, CH tar + liquid, H,.

residence time of the volatile matter. It has again been shown by the pilot plant studies of Union Carbide that production of both the gaseous and liquid hydrocarbon is improved significantly under high partial pressure of hydrogen (5).

Figure II-1 shows, qualitatively, the effects of heating rate and temperature on (a) the relative total yields of volatiles, (b) the relative rates of liqud (liquid and tar) to gaseous volatiles and (c) the gas composition. In this Figure it is assumed that the solid is held at the final temperatures until complete decompositions, while the vapor residence time is held at the minimum (5). Thus, at a particular heating rate both the total yield of volatiles and the ratio of gaseous to liquid hydrocarbons increases with the increase in temperature. On the other hand, if the heating rate is increased, keeping the final temperature constant at a low level (around 500°C) the yield of total volatiles increases but the ratio of gaseous to liquid hydrocarbon decreases. However, at a much higher level of temperature (around 1000°C) and rapid heating rate both the total yield and the ratio of gaseous to liquid hydrocarbons increase again (5). Among the gaseous products, as the temperature rises, the total amount of CO and CO_2 decreases while the amount of hydrogen increases. The total amount of CH_4 and C_2H_6 reaches a peak value at around 500°C and decreases on further increase in temperature (5). According to Anthony, et al., the primary volatiles formed by decomposition within the coal particles are of two categories, reactive and non-reactive.(6)

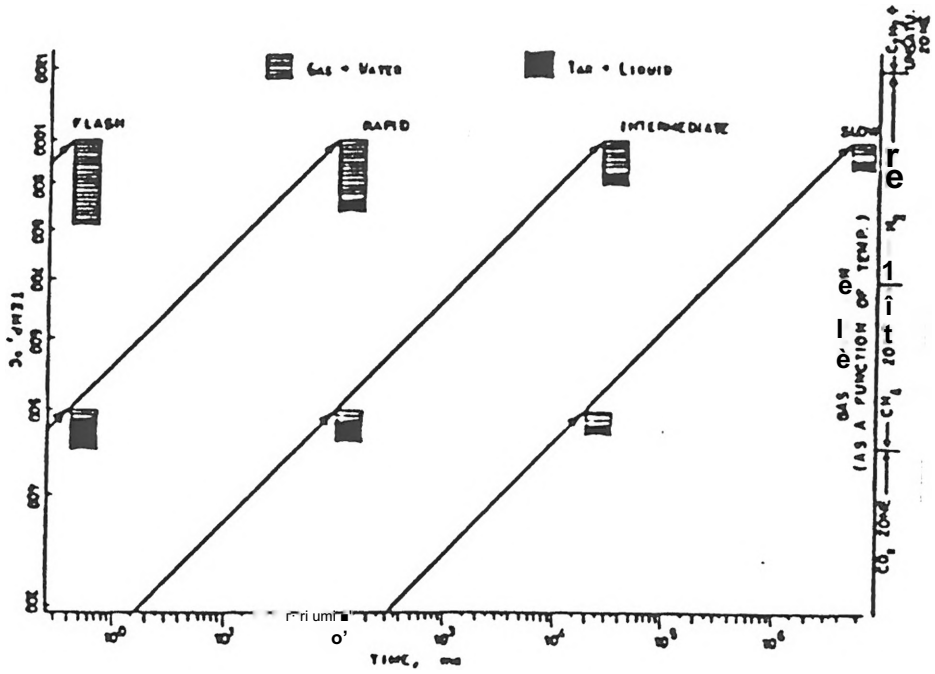

Figure II-1. Relative Yields and Product Distributions Of Pyrolysis In Inert Atmosphere As Functions of Temperature, Time and Heating Rate.

The non-reactive volatiles escape out of the particle as such, whereas a part of the reactive volatiles deposits inside the particles by polymerization and/or cracking.

Thus, only a part escape out. This is believed to be the main reason for higher volatiles yield in rapid heating compared to that in slow heating. In rapid heating the residence time of the primary decomposition products within the coal particles is shortened, lessening the chance of the secondary reactions within the coal matrix (5).

Based on the available data it can be said that similar to the pyrolysis by slow heating, the yield of tar and liquid in the pyrolysis by rapid heating does not increase beyond a temperature around 650-700°C. The yield of remaining fraction, which consists of higher hydrocarbons, acetylene and other unsaturated hydrocarbons, is significantly higher in rapid pyrolysis than that in slow pyrolysis. However, this fraction diminishes with the increase of temperature (5). The yield, product distributions and the duration of decomposition reactions would be affected if the particle size and/or sample size are large (5).

General Characteristics of Char-Gas Reactions

The char-gas reactions that take place during the second stage following the pyrolysis reaction may be classified into two distinct categories, namely volumetric reactions and surface reactions. Whether it is volumetric reaction or surface reaction, char-gas reaction takes place on external or internal surface of the char. Thus, diffusion is an important step in heterogeneous char-gas reactions (5).

in the case of volumetric reaction, the reacting gas diffuses into the interior of the particles and the reaction zone spreads throughout the body of the solid (5) .

In the case of surface reaction, on the other hand, the reacting gas can hardly penetrate into the interior of the solid particles and the reaction is therefore confined only to the surface of the "shrinking zone of unreacted solid". In such a case, therefore, the reaction interface is sandwiched between the inner non-reacted zone of solid and the outer product solid layer (ash) (5).

Figures II-2 and II-3 show typical concentration profiles of carbon and the reacting gas in surface reaction and volumetric reaction as a function of carbon conversion. Generally speaking, surface reaction occurs when the chemical reaction is very fast such as combustion reaction and diffusion is the rate controlling step. Volumetric reaction, on the other hand, is the characteristic of slow reactions and porous solids (5).

Hydrogasification By Rapid Heating

Experimental studies, for example by Graff, et al., indicate that higher heating rate foavors higher carbon conversion (5).

The experiments of Squires, et al., show that there is practically no liquid and tar in the volatiles at temperatures above 900°C, when the gasification was done in a hydrogen partial pressure of 100 atmosphere and at a rapid rate. At 1000°C, all the carbon gasified was found to appear as almost pure CH_4. The data of Moseley and Patterson shows that

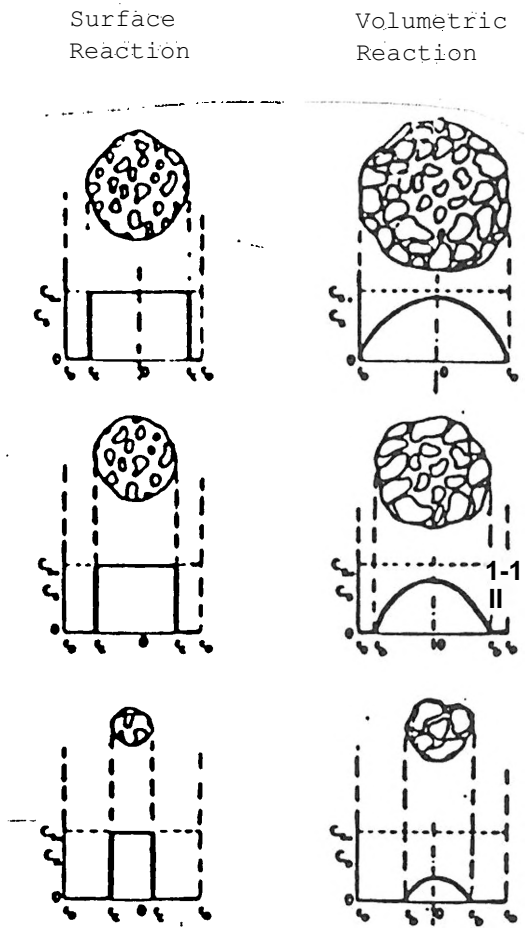

Figure II-2. Carbon Concentration Profile

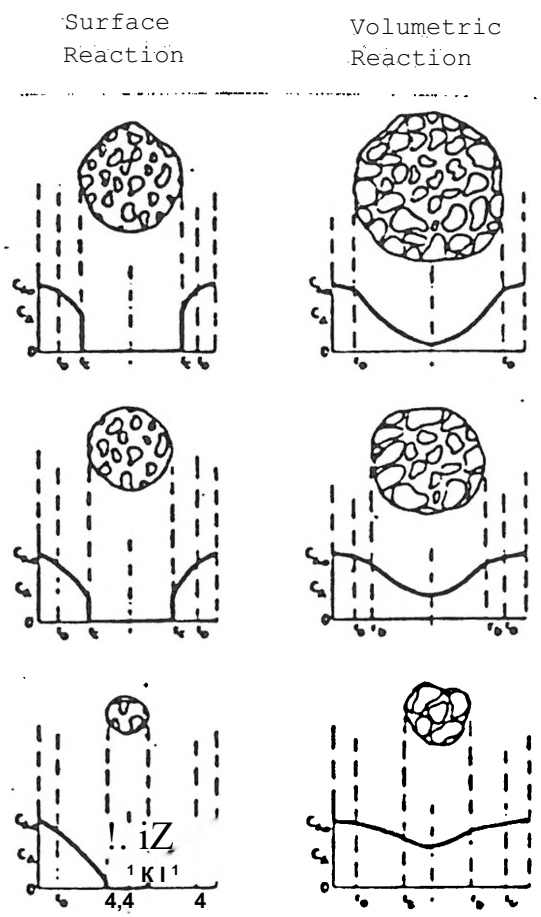

Figure II-3. Gas Concentration Profile

percentage of CO_x decreases and that of CH_4 and C_2H_6 increases in the gaseous products, as the hydrogen partial pressure is raised (5). In another study by Anthony and Howard, et al., rapid devolatilization and hydrogasification of a Pittsburgh Seam bituminous coal were studied and an appropriate coal conversion model was developed that accounts for thermal decomposition of the coal, secondary char-forming reactions of volatiles, and homogeneous and heterogeneous reactions involving hydrogen (6). Approximately monolayer samples of coal particles supported on wire mesh heating elements were electrically heated in hydrogen, helium and mixtures thereof. Coal weight loss (volatiles yield) was measured as a function of residence time (0-20s), heating rate (65 - 10,000°C/second), final temperature (400 - 1100°C), total pressure (0.0001 - 7 MPa), hydrogen partial pressure (9-7 MPa) and particle size (70 - 100 μm). Volatiles yield under these conditions increases significantly with decreasing pressure, decreasing particle size, increasing hydrogen partial pressure and increasing final temperature, but only slightly with increasing heating rate (6). The data supports the view that coal conversion under these conditions involves numerous parallel thermal decomposition reactions forming primary volatiles and initiating a sequence of secondary reactions leading to char. Intermediates in this char-forming sequence can escape as tar if residence time in the presence of hot coal surface is sufficiently short (e.g. low pressures and small particles well dispensed). Hydrogen at sufficiently high partial pressure can interrupt the char-forming sequence thereby increasing volatile yield (6). Rate of total product generation is largely controlled by

coal pyrolysis. Competition between mass transfer, secondary reactions, and rapid hydrogenation affects only the relative properties of volatile and solid products formed (6).

Although the residual 'fixed carbon' in char reacts with hydrogen to produce methane, the reported rates are relatively slow, in the range 0.6 - 30 percent of carbon mass/hour-atmosphere at H_2 927°C. Early work, by Dent showed that a substantial portion of the carbon in raw coal can be converted to methane more rapidly than can the carbon in char (6). Numerous subsequent experiments indicated the existence of a short-lived period of high reactivity which was first believed simply to reflect hydrogenation of the coal's volatile matter. In a 1962 patent, however, Schroeder pointed out with ample subsequent support that the non-catalytic hydrogenation of raw coal can involve yields significantly exceeding the proximate volatile matter (6).

Moseley and Patterson proposed the first mechanistic description of rapid hydrogasification of coal. They postulated the formation of a highly reactive species, probably in the solid phase, as an early stage in coal heating, which then participates in each of two simultaneous competing reactions: (a) decomposition to relatively unreactive char, (b) hydrogenation to methane. It is then assumed that increased hydrogen partial pressure has no effect on the rate of (a) but increases the rate of (b) (6). Obviously, devolatilization is assumed to proceed and be independent of hydrogenation (6).

The following questions pertinent to process development were of particular interest: can higher heating rates increase yields?

Some investigators conclude that high heating rates lead to pyrolysis yields exceeding the proximate volatile matter, in some cases by as much as 80 percent.

Typical variations of weight loss with time for runs in hydrogen and in helium are shown in Figure II-3 using data obtained at 7 bfPa. The data points represent residence time up to current cutoff and total weight loss including the small but significant amount occuring during sample cooling (6). Much of the weight loss occurs during the heat-up period, even at the highest heating rates. After a short time, e.g. 2-3s at 900°C (Figure II-4), no observable further weight loss appears to occur in runs lasting to 20 or 30 seconds. Moreover, the weight loss in hydrogen remains identical with that in helium until the latter approximately reaches its final value, after which the weight loss in hydrogen increases to higher values than in helium. At 7 MPa (Figure II-4), the final weight loss in hydrogen is 17-18 percentage points greater than in helium. The main contribution of hydrogen to weight loss thus appears with regard to its time and rate of occurrence, like an extension of the devolatilization observed in helium (6).

The weight losses attained in 5-20 S at 1000°C, different rates are shown as data points in Figure II-5. In helium weight loss decreases with increasing pressure and reaches asymptotic values of 54.2 and 37.2 percent of the original coal at low and high pressures, respectively. Weight loss in hydrogen exhibits a peculiar minimum (48-50%) in the pressure range of about 0.1-2 MPa and then rises with increasing pressure to about 60 percent of the original coal at 7 MPa. The increase

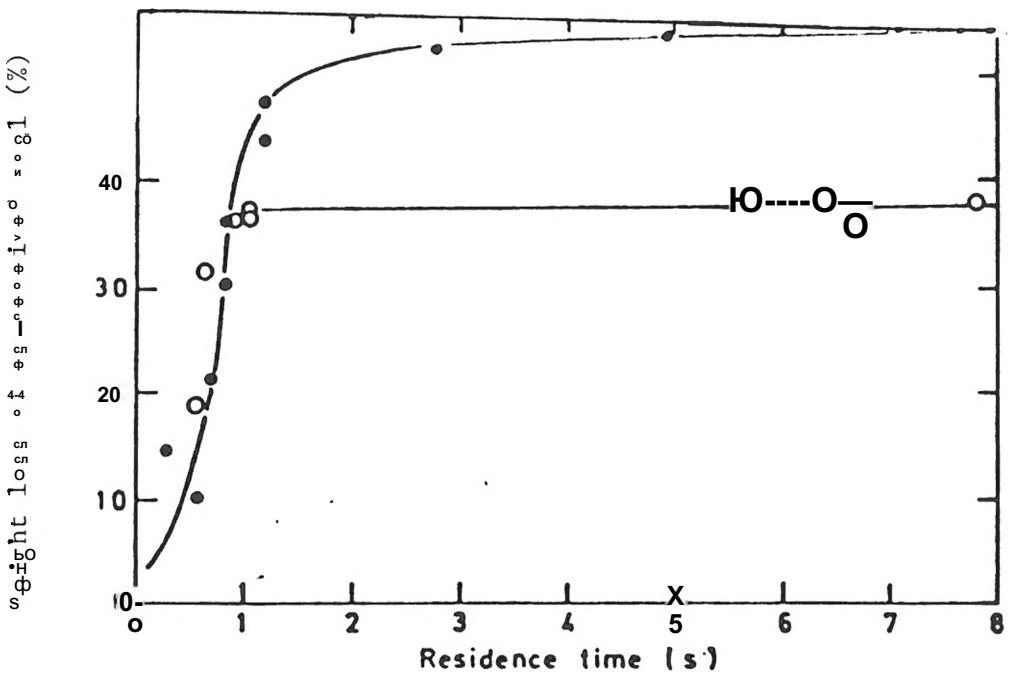

Figure II-4. Effect of Time On Weight Loss From Coal Heated In Helium and Hydrogen Atmospheres

(Final temperature 900°C; nominal heating rate 750°C/s; mean particle diameter 70 µm; pressure ≈ 7 MPa; O helium; ϕ hydrogen)

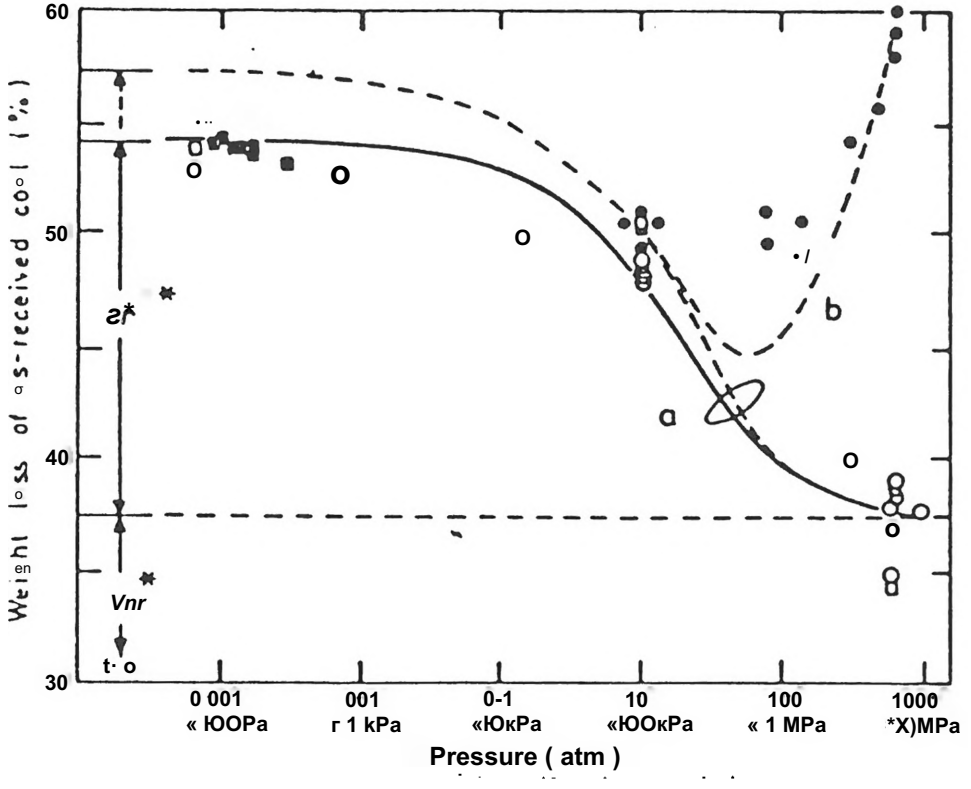

Figure II-5. Effect of Pressure On Weight Loss From Coal Heated In Helium and Hydrogen Atmospheres.

(Final temperature = 1000°C; residence time = 5-20x; mean particle diameter = 70 m; helium, nominal heating rate = 10,000°C/s; ■ helium, nominal heating rate = 3000°C/s; o helium, nominal heating rate = 650-750°C/s; · hydrogen, nominal heating rate = 750°C/s, Curves: (a) equation (5); (b) equation (10); (solid) V_r** = 17.0% of original coal; (dashed) V_r** = 20.0% of original coal, corrected for cracking deposition on screens; V_{nr}* = 37.2% of original coal)

of heating rate from 750-10^4 °C/s increases yields only by about 2 percentage points at 0.1 MPa and has no effect on yield at the pressure extremes. The weight loss of 48-50 percent here attained in 5-20s at 0.1 MPa is considerably larger than the volatile matter plus moisture (41.4%) determined by proximate analysis, which is carried out in 420s. To explore results of longer runs, several of the sample residues from the present apparatus were reheated in an proximate analysis apparatus for 420s. An additional weight loss of 4.5-70 percent of original coal was observed, suggesting that further weight losses would occur if the present runs were extended beyond 20-30s, and that the yield from the present apparatus at 0.1 MPa and 420s would exceed that of proximate analysis by 11-15 percent of the original coal (6). Tar condensation was observed in the reactor. The amount of tar deposited in helium atmospheres follows the same trend as weight loss, decreasing with increasing pressure and essentially disappearing at about 7 MPa. In hydrogen, tar deposition also decreases with increasing pressure and disappears at about 7 MPa despite the increased weight losses. Some darkening of the screens, assumed to be deposits from the cracking of volatiles, and observed at low pressures.

The effect of temperature on weight losses attained in 5-20s in hydrogen at 7 MPa, helium at 7 MPa, and nitrogen or helium at 0.1 MPa is shown in Figure II-6. Inspection shows that yields increase equally under the different conditions up to about 600°C, above which (a) yields at 7 MPa become much greater in hydrogen than in inert gas, (b) yields

in inert gas become much greater at 0.1 MPa than at 7 MPa, and (c) yields at 7 MPa in inert gas are almost independent of temperature (6). Two samples of char from low temperature runs at 7 MPa were reheated to high temperatures at 7 MPa (Figure II-6). The cumulative weight loss in each case was essentially identical with that for raw coal heated directly to the same high temperature (6).

The effect of particle size on yields is substantial for hydrogen atmosphere but small for helium (Figure II-7) at 7 MPa and H_2 1000°C, reduction of particle size from 1000 to 70 μm increases the weight loss attained in 5-20s from 44 to 59 percent of the original coal. The observed trend indicates that this larger increases in yield would result from further reduction of particle size (6). In another study, also by Anthony, et al., lignite and bituminous coal were heated so rapidly that most of the weight loss occurred during heat up even in the cases of the largest initial heating rate (nominal heating rates of 3000 to 10,000°C/s) (4). Typical variations of weight loss with time at different heating rates are given in Figure II-8, using the lignite data obtained at 1.0 atmosphere. The weight-loss versus time histories were obtained by a series of runs, each represented here by a data point, at the same heating rate but of increasing duration. Small but significant weight loss occuring during sample cooling was determined with an iterative computer procedure that both calculated this contribution, using the kinetic model developed from the data, and accounted for it in the kinetic analysis (4). The weight loss shown in Figure II-8 includes

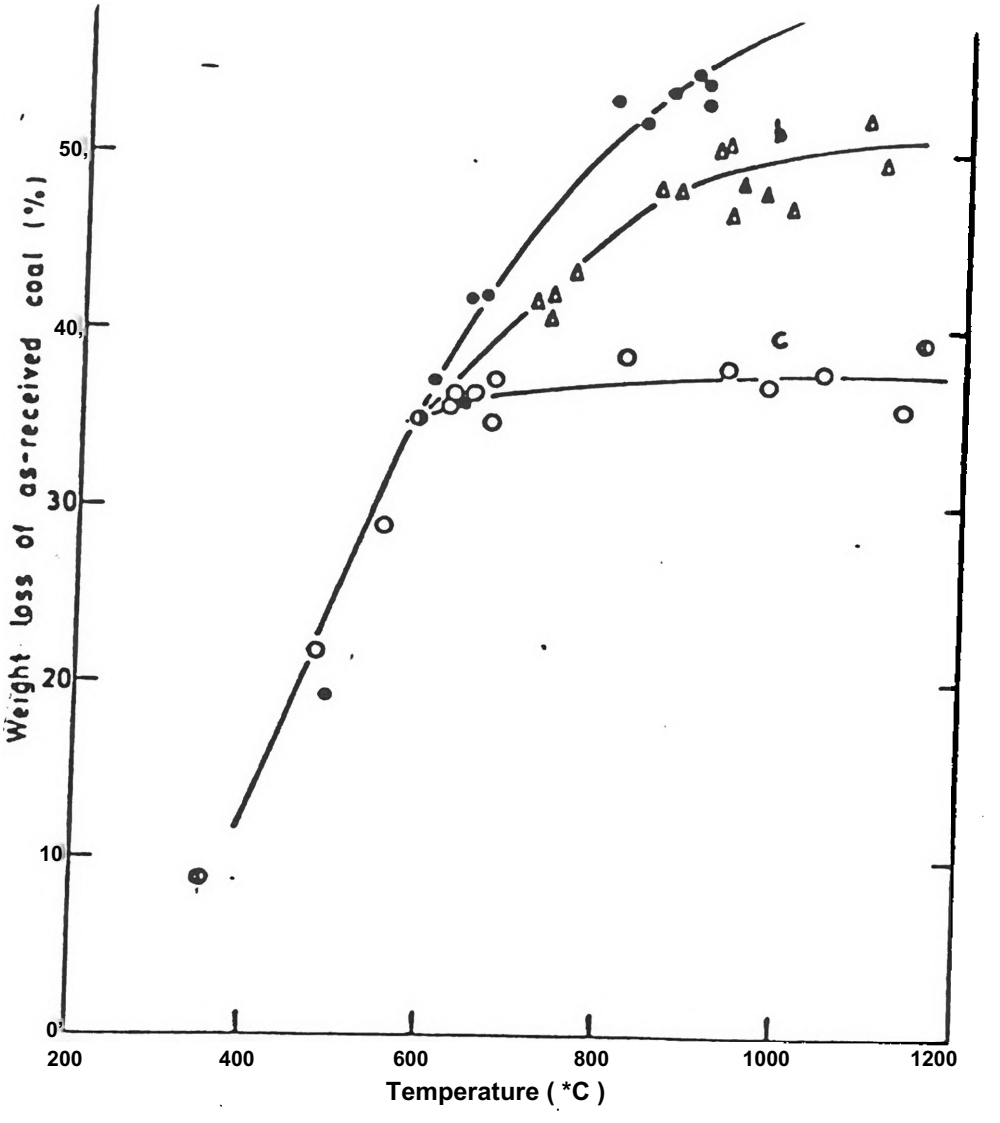

Figure II-6. Effect of Temperature on Weight Loss From Coal Heated In Hydrogen and Inert Atmospheres at High and Low Pressure

(Nominal heating rates = 65-750°C/s; mean particle diameter = 70 pm; residence time = 5-20s; · hydrogen, « 7 MPa; A helium and nitrogen, latm;O helium, * 7 MPa; Φ two-step heating, helium ~ 7 MPa; G two-step heating, hydrogen, ~ 7 ~ MPa. Curves, equation (14) with parameter values given in text: (a) P = P * 7 MPa; (b) P = 1 am, P = 0; (c) P * 7 MPa, $P_{u_{H2}}$ = 0).

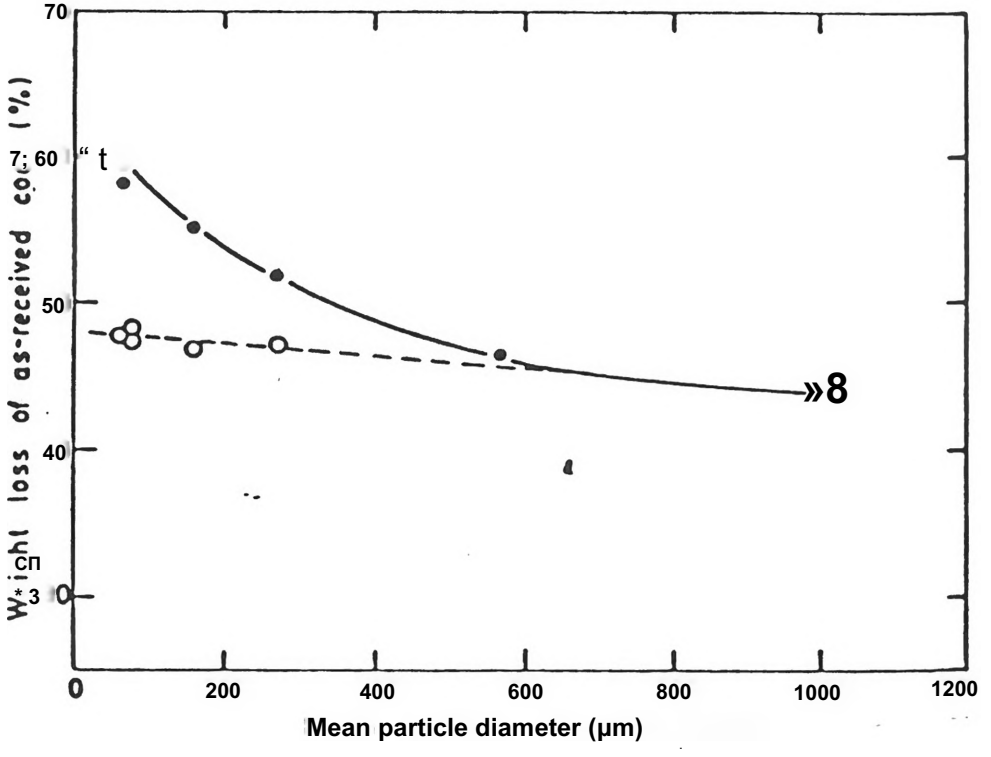

Figure II-7. Effect of Particle Size On Weight Loss From Coal Heated In Helium and Hydrogen Atmospheres.

(Final temperature = 1000°C; residence time = 5-20 s; nominal heating rate = 650-750°C/s; · hydrogen, * 7 MPa; O helium, 1 atm.

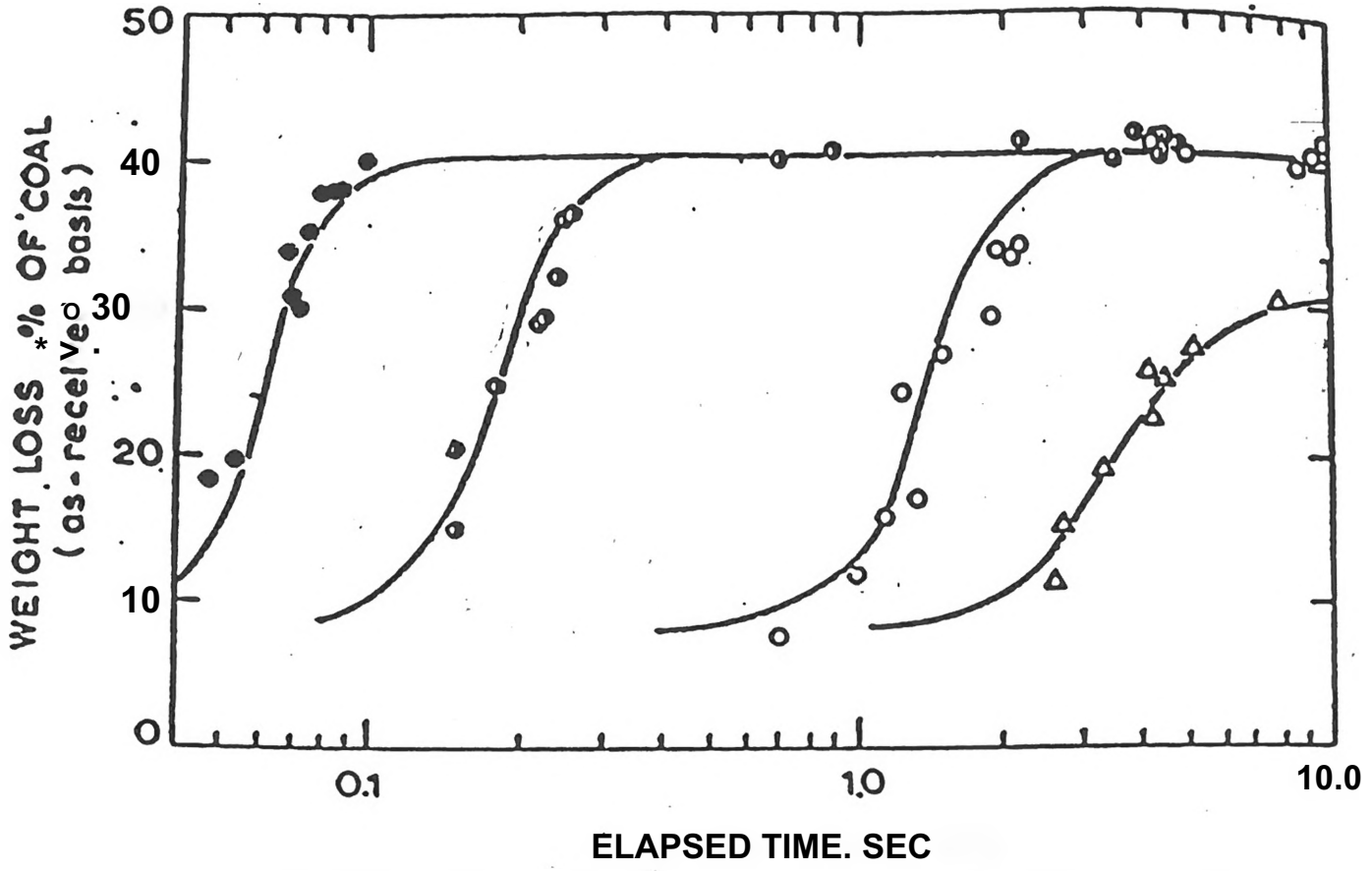

Figure II-8. Effect of Time On Devolatilization Weight Loss From Montana Lignite at Different Heating Rates And Final Temperatures

(t = 0 at initiation of heating; pressure = 1.0 atm helium; mean particle diameter = 70 pm; final temperature (if attained) - 1000°C (>, 0 , O), 700°C (Δ); nominal heating rate (°C/sec) - 10,000 (·), 8000 (O), 650 (O), 180 (Δ) ; curves

a small reduction for that loss estimated to have occurred during the cooling period and time is consequently the duration of a run upto the point of current cut-off (Figure II-9).

Final weight loss from the lignite, independent of heating rate, was 41 percent at 1000°C and 31 percent at 700°C (Figure II-8). The increase, with increasing final temperature, of final weight loss (residence time at final temperature >5 sec) became negligible at 900-950°C (Figure 11-10). The largest weight losses from lignite are smaller than the 44.7 percent obtained by proximate analysis (950°C, 7 minute duration) (4). Therefore, although the rate of weight loss became negligible after a few seconds, a small additional weight loss would have occurred if the runs had been extended for several minutes. Weight loss from the lignite was not affected by pressure in the range studied (0.001-100 atm.)(4).

Weight loss from the bituminous coal increased with increasing temperature in a manner similar to lignite. However, contrary to the lignite behavior, weight loss from the bituminous coal decreased substantially with increasing pressure (Figure 11-11) and at pressures below about 5 atm, exceeded that obtained by proximate analysis (41.5%) (4). Figure 11-11 shows that higher heating rates increased the weight loss at pressures from 1.0 atm down by about 2 percentage points, but the effect of heating rate was trivial at high pressure. Tar condensation was observed with the bituminous coal but not with the lignite. The amount of tar deposited in the reactor followed the same trend as

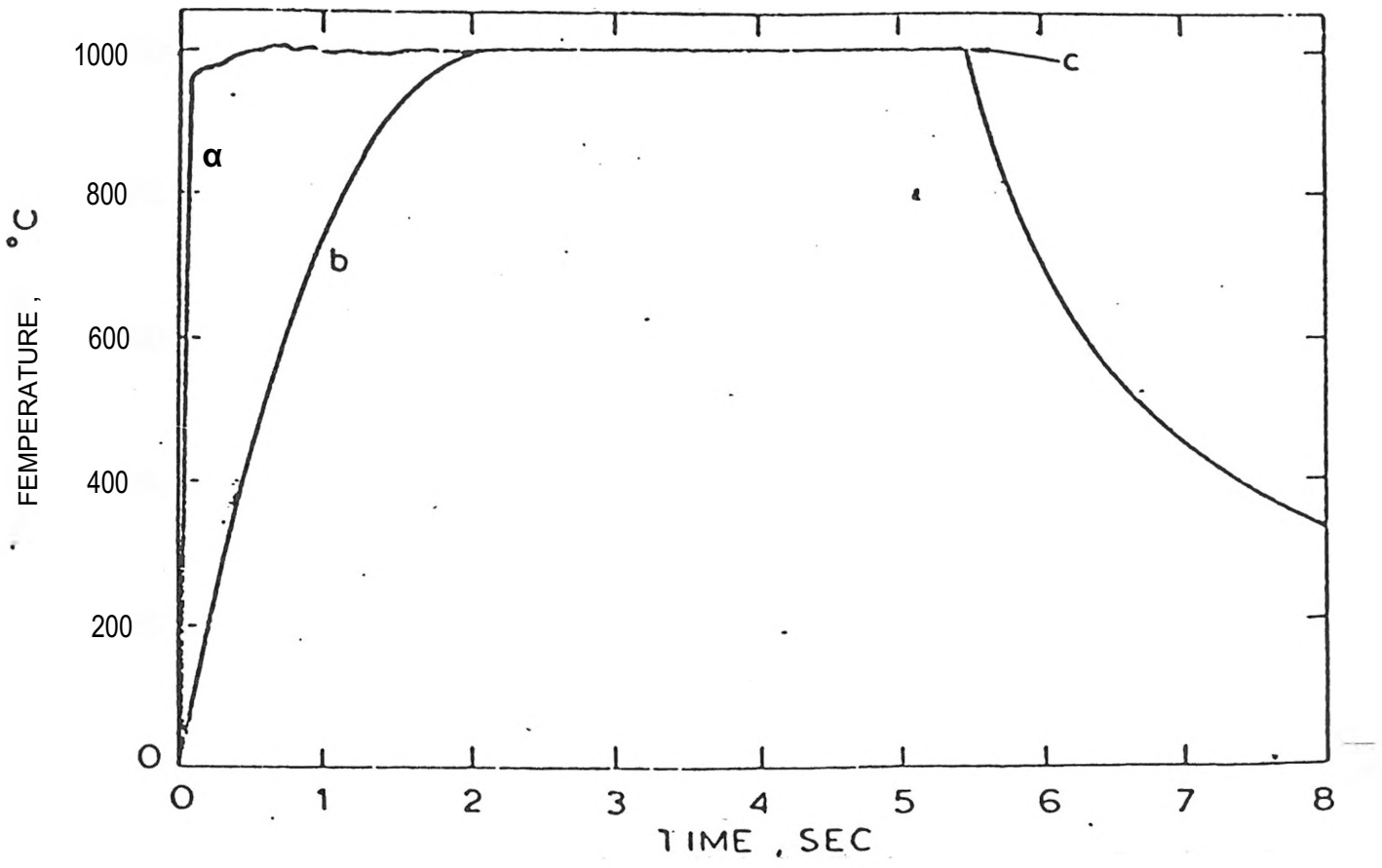

Figure II-9. Typical Time-Temperature Histories of Coal Samples

[pressure = 1 atm; nominal heating rate (85% of final temperature divided by time to reach 85% of final temperature) - 10,000°C/sec (a), 650°C/sec (b); current cutoff (c)].

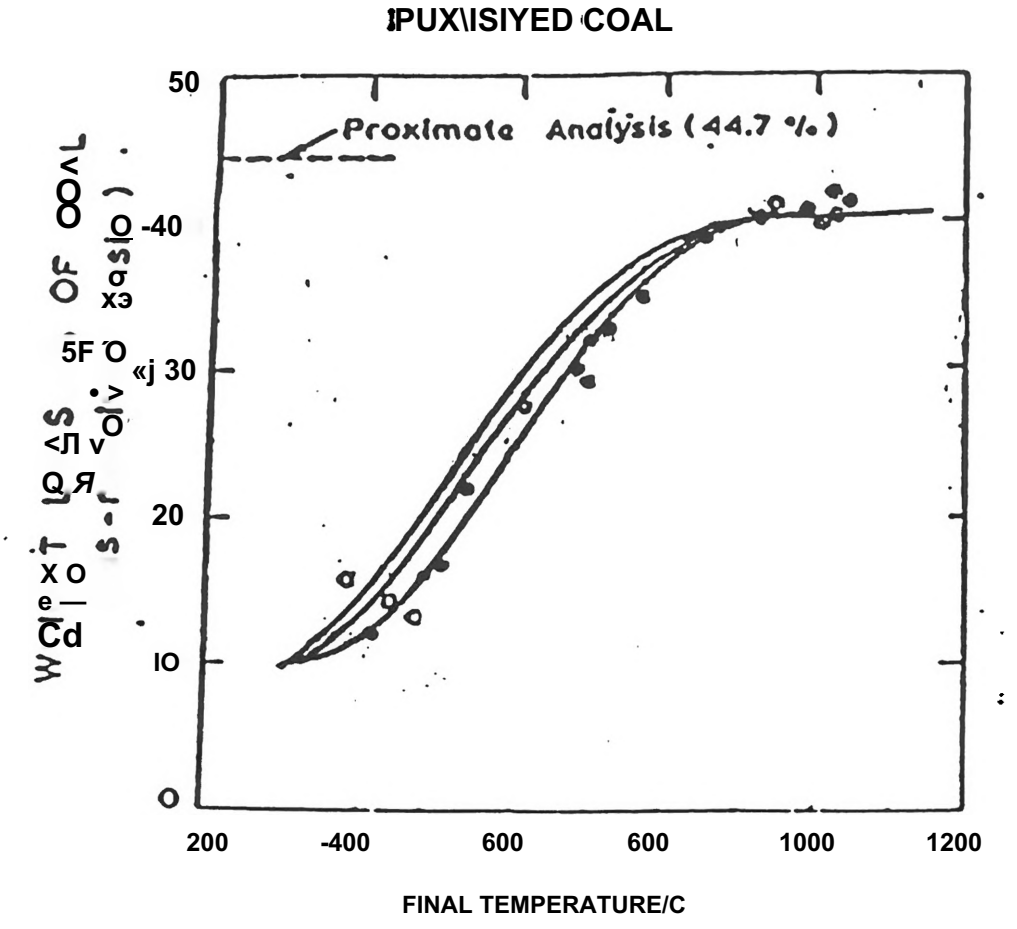

Figure II-IO. Effect of Final Temperature On Devolatilization Weight Loss From Montana Lignite

(points — data experimental time - 5 to 20 sec, mean particle diameter = 70 µm, atmosphere = helium).

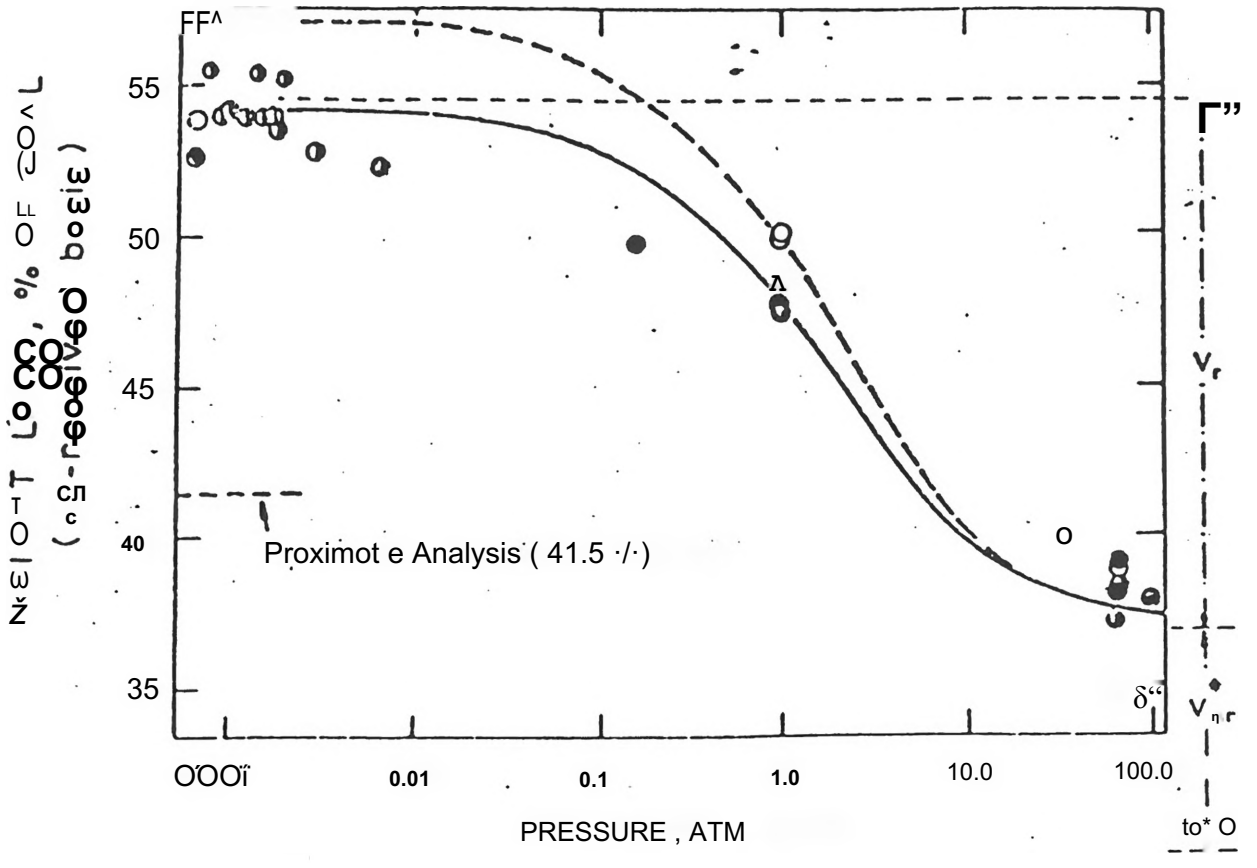

Figure II-ll. Effect of Pressure on Devolatilization Weight Loss From Pittsburgh Seam Bituminous Coal

(Final temperature = 1000 C; experimental time = 5 to 20 sec; mean particle diameter = 70 pm; atmosphere = helium; nominal heating rate (°C/sec) - 10,000 (O), 3000 (Э), 650 to 750 (O); curves (solid-uncorrected for cracking deposition; dashed-corrected for cracking deposition)

weight loss, decreasing with increasing pressure and essentially disappearing at about 69 atm. Deposition on the heating screens resulting from volatiles cracking decreased the apparent weight loss from the coal. This effect was measured by weighing the screens without the coal residue (Figure 11-11) (4).

Suuberg, et al., (7), showed the effect of hydrogen on the total yield of volatiles by direct measurements of weight loss from the coal and by summing the yields of all volatile products. Weight loss results are shown in Figures 11-12 and 11-13, for the lignite and the bituminous coal respectively, for experiments in which the coal was heated at 1000°C s^{-1} to a peak temperature and then cooled at 200°C s^{-1} with zero holding time at the peak temperature.

Comparing first the methane yields from the lignite or I atm He pyrolysis and 69 atm H_2 hydropyrolysis (Figure 11-14), it is apparent that the hydrogen has a substantial effect at temperatures as low as 600°C (7).

The data in Figure 11-15 compares the yields of methane from atmospheric pressure pyrolysis and 69 atm hydropyrolysis of bituminous coal. Figure 11-16 shows that the combined yield of hydrocarbon gases other than methane and ethylene generally follows the trend displayed by the methane yield (7). This combined yield is enhanced by the presence of hydrogen.

The yields of ethylene from pyrolysis and hydropyrolysis of lignite are compared in Figure 11-17 while the variations in inert gas pressure seems to have no effect on this product, an increase in hydrogen

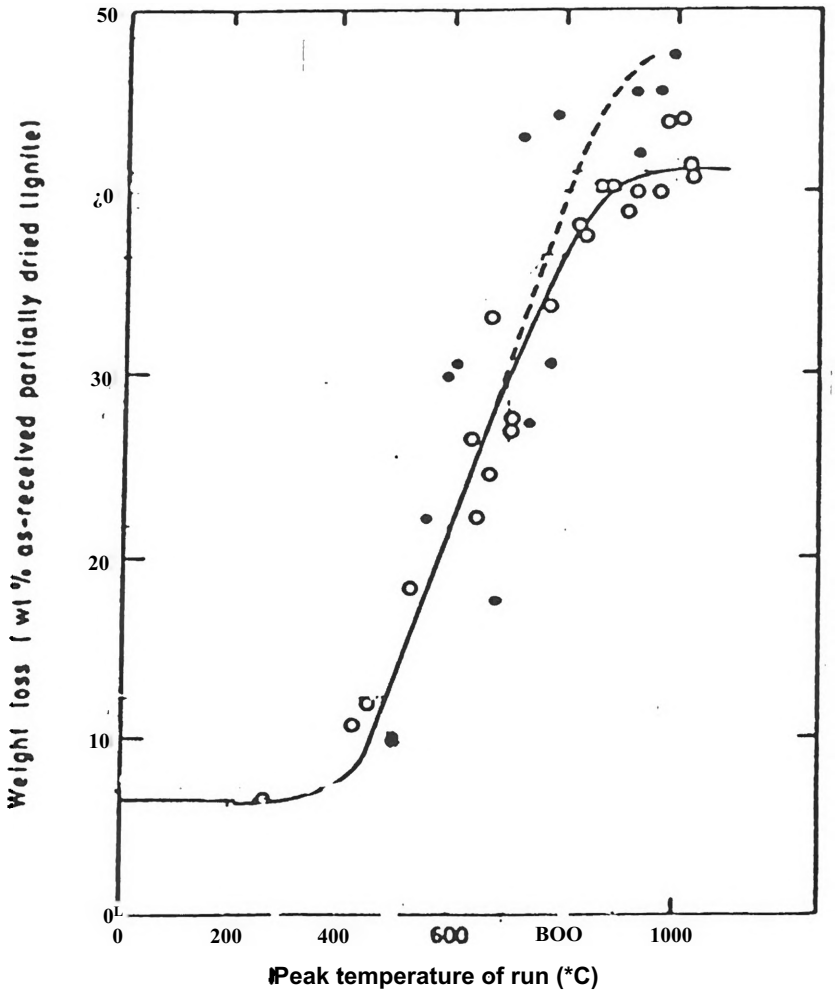

Figure 11-12. Comparison of Total Weight Loss From Pyrolysis and Hydropyrolysis of Lignite To Different Peak Temperatures.

(· , 69 atm H_2; O 1 atm He; heating rate, 1000°C s-) ;

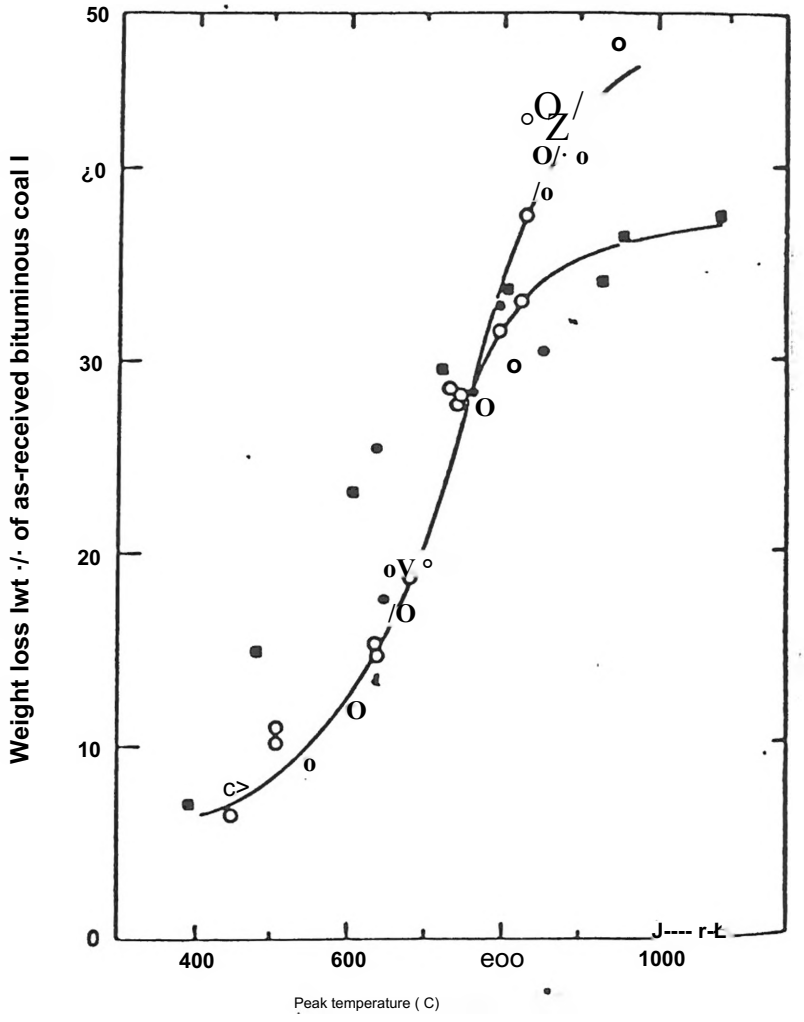

Figure 11-13. Comparison of Total Weight Loss From Pyrolysis And Hydropyrolysis of Bituminous Coal To Different Peak Temperatures.

(· , 69 atm H_2; o , 1 atm He; ■ , 69 atm He)

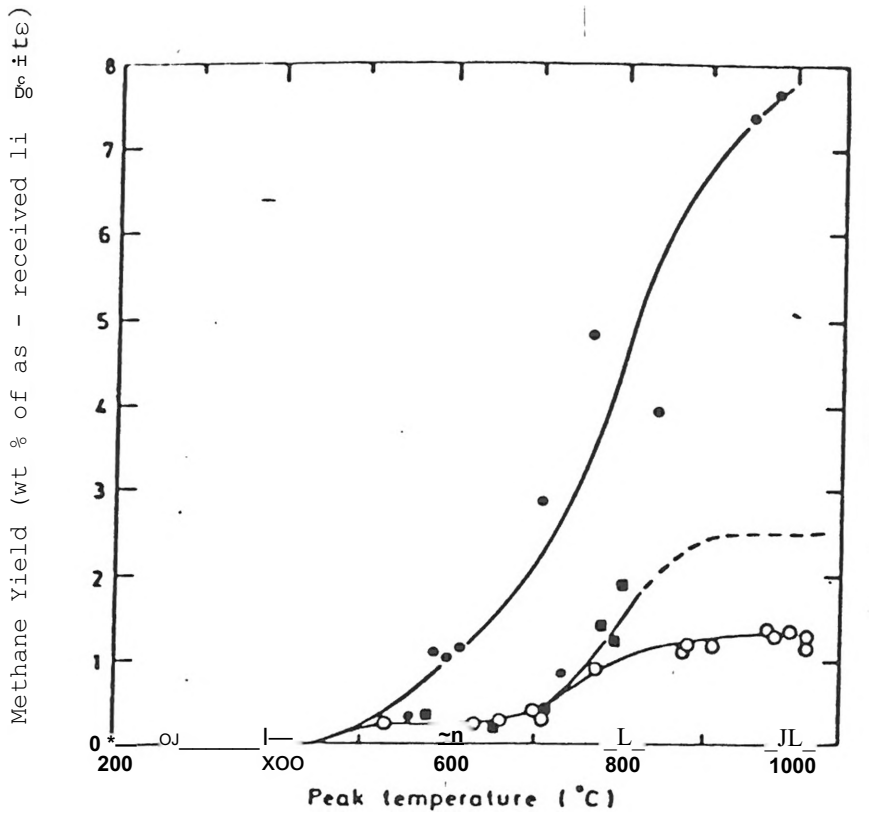

Figure 11-14. Comparison of Methane Yields From Hydropyrolysis And Pyrolysis of Montana Lignite to Different Peak Temperatures.

(Average particle diameter, 74 pm; heating rate, 1000°C s \
Asymptote for 69 atm helium (----) established by runs with holding times 2-10s at the peak temperature) · , 69 atm ; H_2 O 1 atm He; ■ 69 atm He.

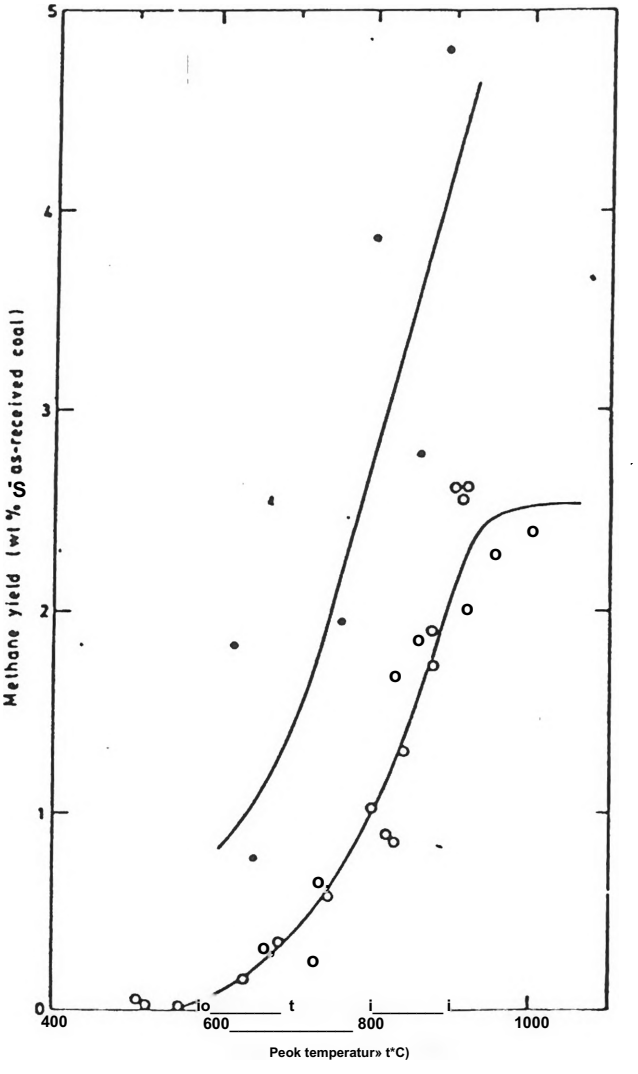

Figure 11-15. Comparison of Methane Yields From Hydropyrolysis and Pyrolysis of Pittsburgh Seam Bituminous Coal To Different Peak Temperatures.

(Average particle diameter, 74 µm; heating rate, 1000°Cs^{-1})
• , 69 atm H_2; 1 atm He

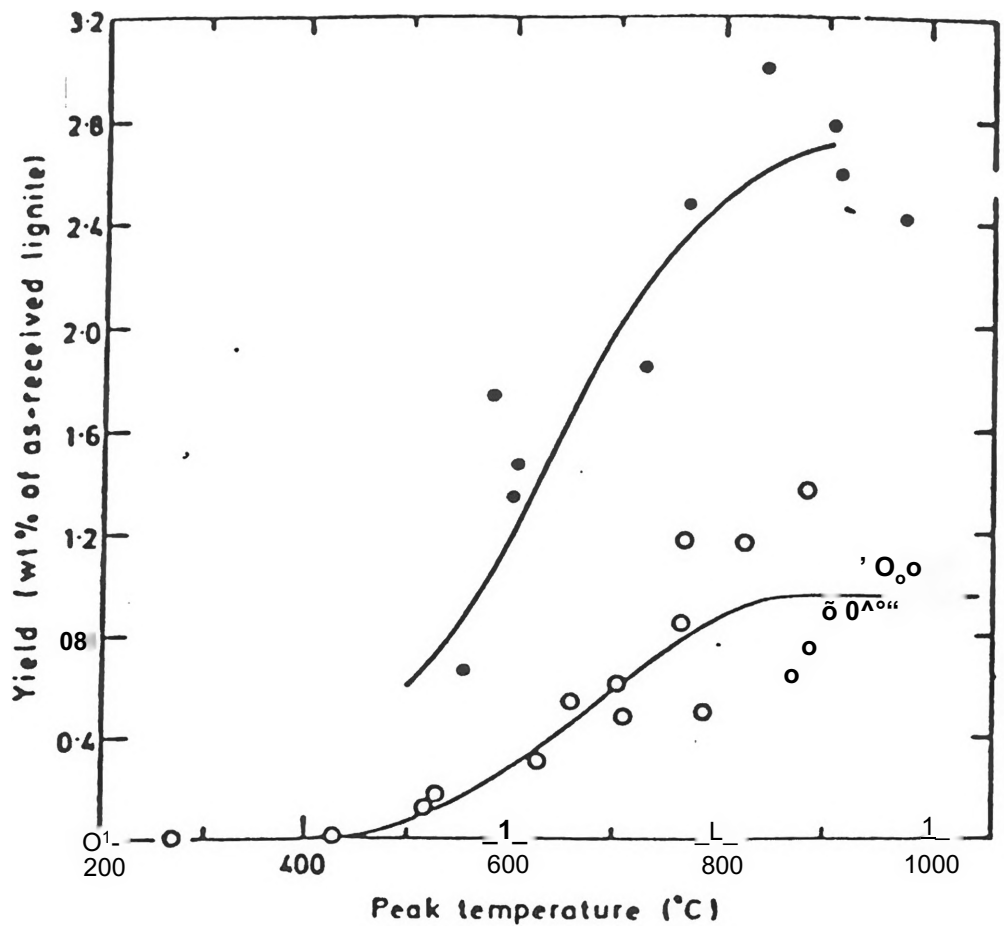

Figure 11-16. Comparison of Yields of Hydrocarbon Gases Excluding Methane and Ethylene From Hydropyrolisis and Pyrolysis of Montana Lignite To Different Peak Temperatures.

(Average particle diameter, 74 pm; heating rate, 1000°C s S $^{-}$
● , 69 atm H_2; Q , 1 atm He

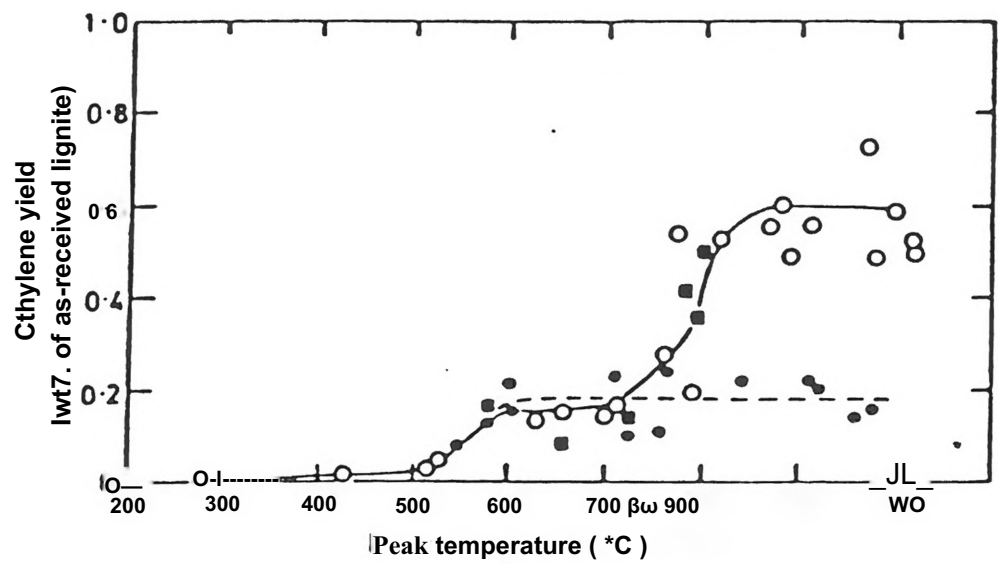

. Figure 11-17. Comparison of Ethylene Yields From Hydro-
pyrolysis and Pyrolysis of Montana Lignite
to Different Peak Temperatures

(Average particle diameter, 74 pm; heating rate, 1000°C s^{-1})
• , 69 atm H,; » 1 atm He; ■ , 69 atm He

pressure appears to suppress formation of ethylene at temperatures above 700°C. An even more dramatic decrease is found in the tar product produced from bituminous coal (Figure 11-18). This tar is any material condensible at room temperature, left in the reactor or on a filter in the reactor exit after a purge with 10 reactor volumes of helium. The tar yield has previously been shown to be a sensitive function of both external (inert) gas pressure and particle diameter. In the present case, the ultimate yield of tar from atmospheric pressure pyrolysis is ≃24 percent by weight of the coal; this yield drops to = 12 percent during pyrolysis under 69 atm of He (7). Changing from 69 atm of helium to 69 atm of hydrogen has no effect on the ultimate yield of tar. In the case of this product, hydrogen appears to have a physical effect, like that of inert gas. Limiting the rate of escape of tar from the particle and allowing the occurrence of tar destruction by secondary reactions. However, the secondary reactions will include hydrocracking and therefore the products formed by tar destruction differ from those of the cracking reactions occuring in the helium case (7).

A comparison of yields of light oxygenated products from pyrolysis and hydropyrolysis of lignite is presented in Figure 11-19. Ultimate analyses of chars produced by pyrolysis and hydropyrolysis of the lignite are compared in Figure 11-20. Carbon conversion is of course higher during hydropyrolysis.

In summary, Tables II-2 and II-3 present comparative yield data from the Montana lignite and Pittsburgh seam bituminous coal. In contrast to the data in Figure II-12 thru 11-19 which for the most part

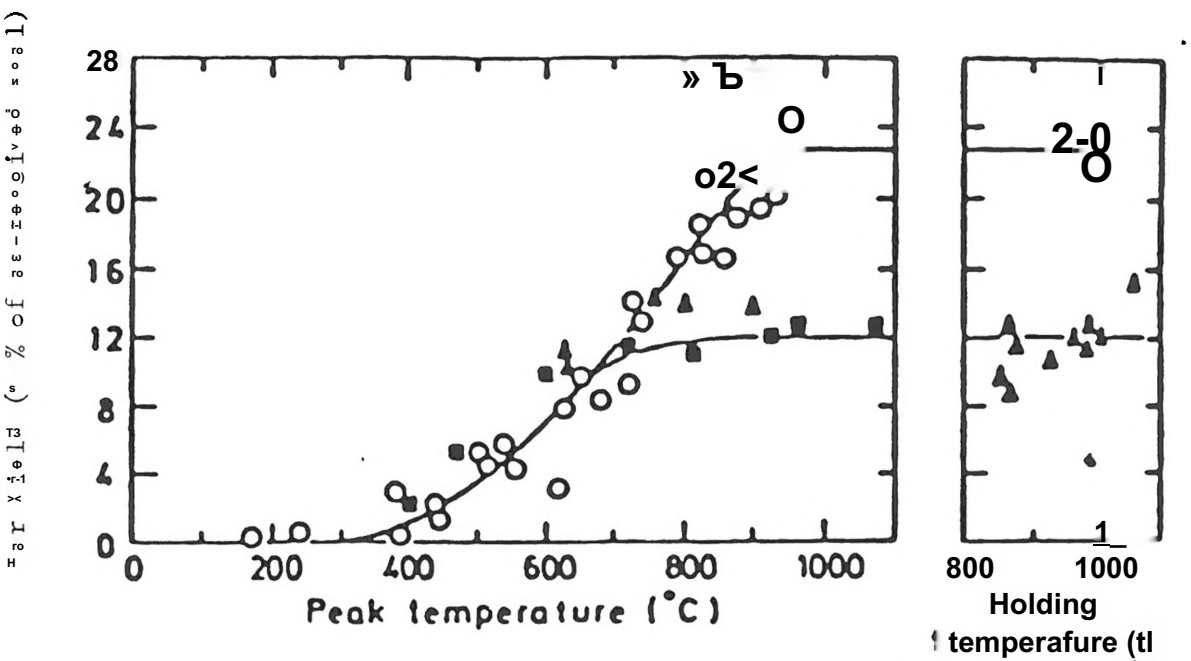

Figure 11-18. Comparison of Tar Yields From Hydropyrolysis and Pyrolysis of Pittsburgh Seam Bituminous Coal

(Average particle diameter, 74 pm; heating rate, 1000°C s^{-1}; Holding time at peak temperature 2-20 seconds for right-hand graph, zero for left-hand graph), o , 1 atm He; ■ , 69 atm He; ▲ 69 atm H_2

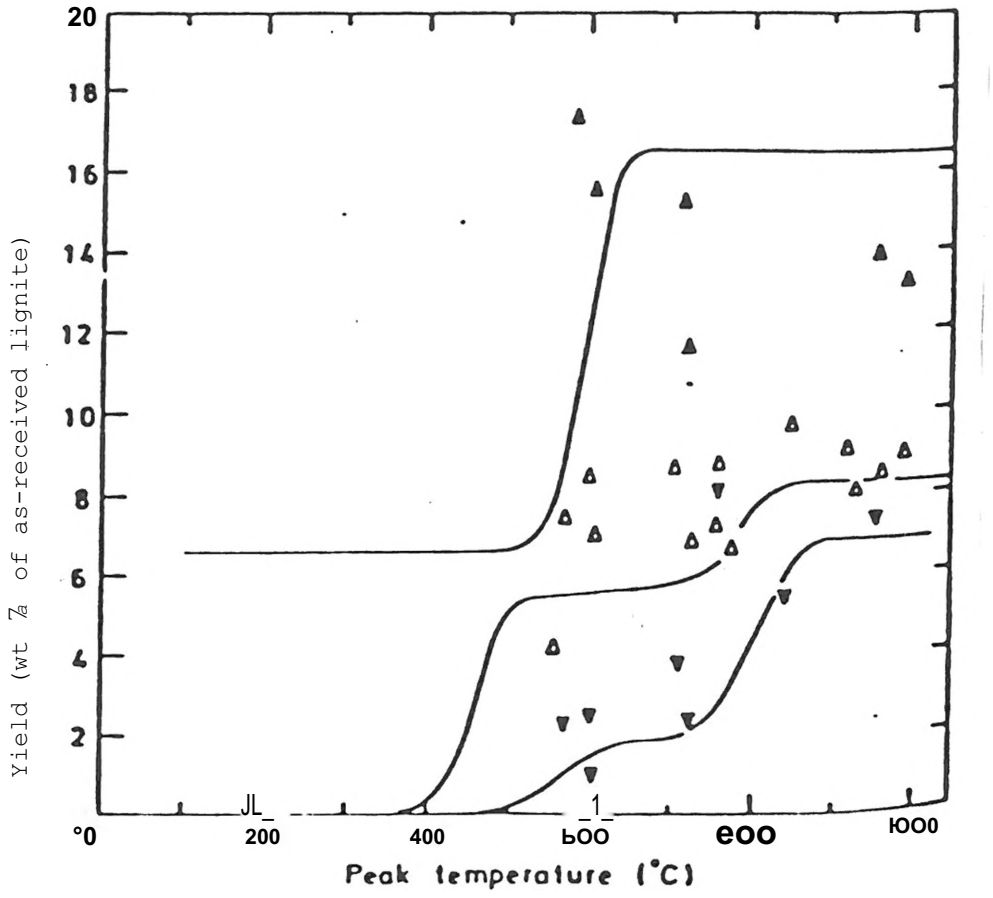

Figure 11-19. Comparison of Yields Of Water (A), Carbon dioxide (Δ) and Carbon Monoxide (V) From Hydropyrolysis And Pyrolysis Of Montana Lignite to Different Peak Temperatures.

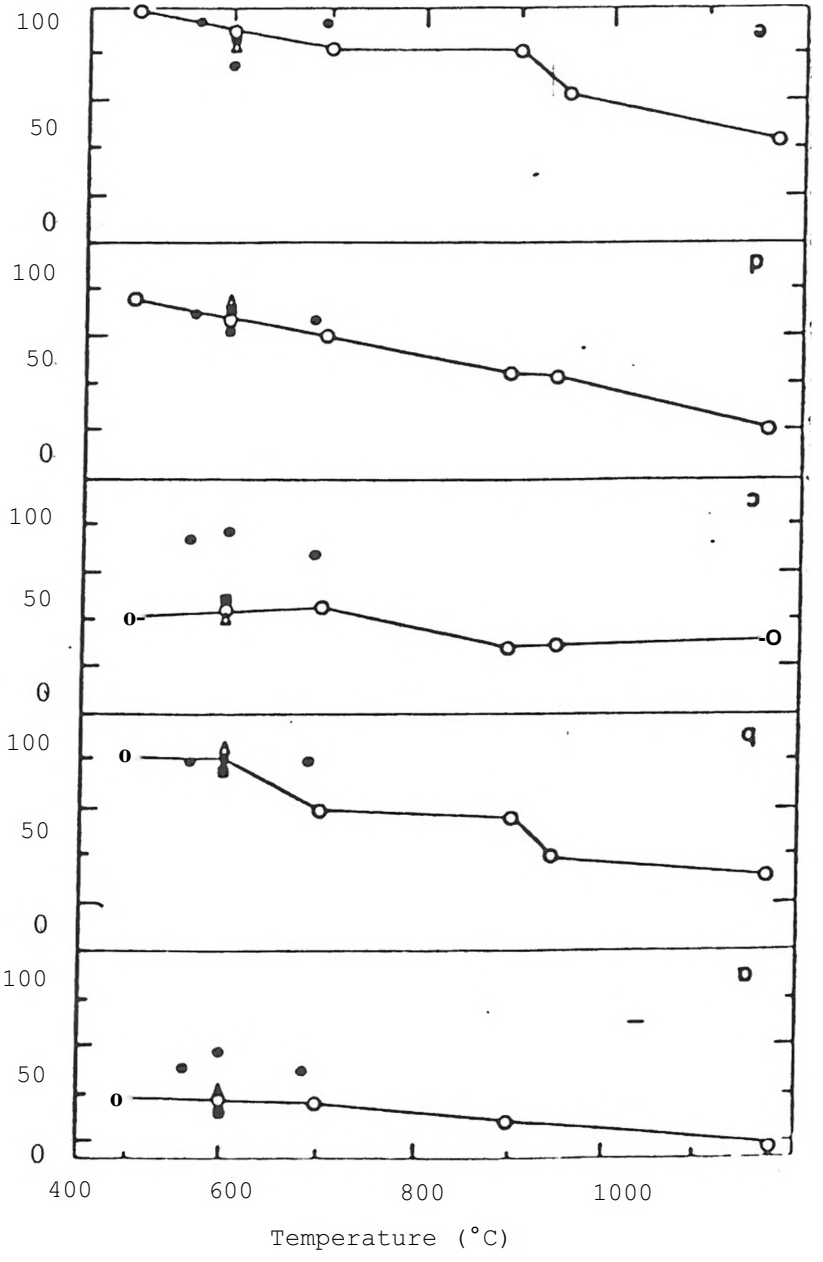

Figure 11-20. Comparison of Elemental Retentions In Chars From Pyrolysis and Hydropyrolysis of Lignite: Q , 1 atm He, zero residence time (a) at peak temperature; V,1 atm He, 5-20s residence time; ■ ,69 atm He 5-10s residence time; · ,69 atm H^ 2-30s residence time, (a) carbon; (b) hydrogen; (c) nitrogen; (d) sulphur; (e) oxygen

TABLE II-2

Comparison of Yields From Pyrolysis And Hydropyrolysis of Montana Lignite. Heating rate, 1000°C s"l; average particle diameter, 74 µm; holding time and temperature; pyrolysis under 1 atm He, 3-10 s at -900-1000°C; pyrolysis under 69 atm He, -10 s at 875-1070°C; hydropyrolysis under 69 atm H_2, :10s at 850-1000°C.

Product	Yield (w! % of Lienite «-received)		
	1 atm He	69 atm He	69 atm H_2
CO	9.4	9.0	7.1
CO_2	9.5	10.6	8.5
H_2O	16.5	12.9	16.0
CH_4	1Л	2.5	9.5
C_2H_4	0.6	0.6	0.2
C_2H_4	0.2	0.2	1.4
Other hydrocarbons	0.8	1.7	4.1
Tar	5.4	*3	*8
Char	56.0	59 £	48.5

TABLE II-3

Comparison of Yields From Pyrolysis and Hydropyrolysis of Pittsburgh Seam Bituminous Coal. Heating rate, 1000°C s-; average particle diameter, 74 pm; holding time and temperature; pyrolysis under 1 atm He, 2-10 s at 850-1000°C; pyrolysis under 69 atm He, 2-10 s at 850-1070°C; hydropyrolysis under 69 atm H_2 14-20 s at 870-930°C.

	Yield (wt % of coal as-received)		
Product	1 atm He	■69 atm He	69 atm H_2
CO	2.4	2.5	N.M.*
CO_2	13	1.7	13
H_2O	6.8	9.5	N.M.
CH_4	2.5	3.2	233
$^H_4$	0.8	0.5	0.4
C_2H_6	0.5	OS	23
$C_3H_6+C_3H_8$	13	0.7	0.7
Other hydrocarbon gases	13	1.6	2.0
Light HC liquids	2.4	2.0	53
Tar	23	12	12
Char	53.0	62.4	403

[3] N.M. — Not measured

presented yields from runs with no isothermal holding period, Tables II-2 and II-3 present data from runs in which the samples were maintained isothermally at the indicated temperatures for periods of several seconds (7). Table II-3 shows that hydropyrolysis of the lignite under 69 atmosphere of hydrogen gives ~7.5 weight percent increase in total volatiles but only a small increase in tar yield, over these obtained at 1 atmosphere. For both the lignite and the bituminous coal, 69 atmosphere hydropyrolysis causes substantial relative increases over the yield from pyrolysis at atmospheric pressure (7).

Effect of Particle Diameter

The absolute pyrolysis and hydropyrolysis conversions are somewhat larger than those previously published but confirm that total weight loss in hydrogen decreases dramatically with increasing particle diameter. Similarly extrapolation to smaller particle diameters suggests opportunity for significant improvements in total conversion (7). Table II-4 shows the effect of particle diameter on the yields of several important products from hydropyrolysis under the conditions stated above. A part from an apparent decline in the yields of ethane and other hydrocarbon gases with increasing particle diameter, which may reflect an increased contribution of secondary cracking reactions, no clear trends are indicated (Figure 11-21) (7).

TABLE II-4

Effect Of Particle Diameter On Product Compositions From The Rapid Hydropyrolysis of Pittsburgh Seam Bituminous Coal. Heating rate, 1000°C s-; holding time and temperature, 10-20 s, 900-1050°C; total pressure, 69 atm of hydrogen.

	Avg. particle diameter (μm)		
Product	74	570	910
Tar	12	13	12
CH_4	23	19	20
C_2H_6	23	1.7	1b
Other HC gases *	3.1	1.4	13
Light HC liquids	53	3.6	53
CO_2	13	1.0	1.4

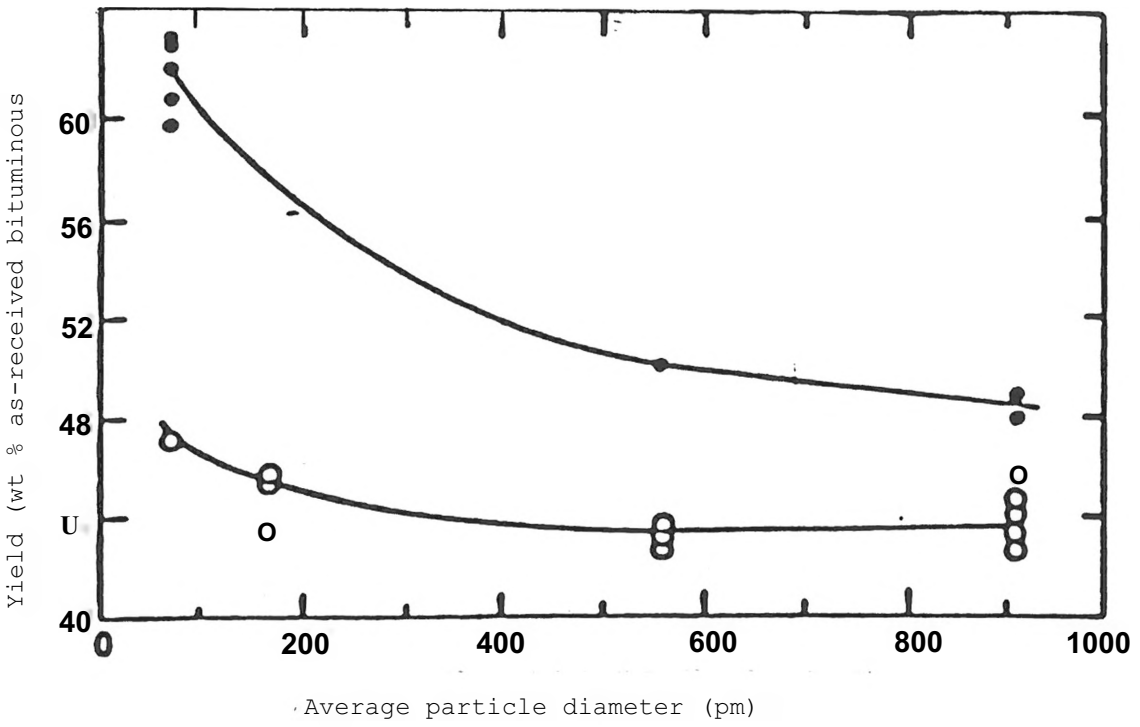

Figure 11-21. Effect of Particle Diameter On Total Yields From Pyrolysis and Hydropyrolysis of Bituminous Coal.

(· , hydropyrolysis, 69 atm $H_{2>}$ Q , pyrolysis, 1 atm He)

CHAPTER III

APPARATUS

The apparatus is similar to that described by Suuberg et al. (8). It consists of four components: the reactor, designed to contain a coal sample in a gaseous environment of known pressure and composition; the electrical system, used to expose the sample to a controlled time-temperature history; the time-temperature monitoring system and the product analysis system (Figure III-1).

The reactor, designed for atmospheric pressure pyrolysis work consists of a six inches long, four inch diameter pyrex glass.

The coal sample is held and heated in the vessel by a folded strip of 325 mesh stainless steel screen positioned in between two relatively massive brass electrodes. These brass electrodes are based on a 0.3 inch thick teflon plate which allows for evacuating, filling the system with helium, conducting electricity to the screen, thermocouple entrance to the system and volatile matter's pathway to the gas chromatograph (Figures III-1 and III-2). The elctrical system consists of two Sears Die Hard automobile batteries connected in series to the reactor electrodes through a timer controlled relay switch which connects the batteries for a predetermined time. This circuitry permits control of sample holding time and final temperature.

The temperature-time history of the coal is measured by a chromel-alumel thermocouple (250 μm in diameter) with time constant of about 0.25

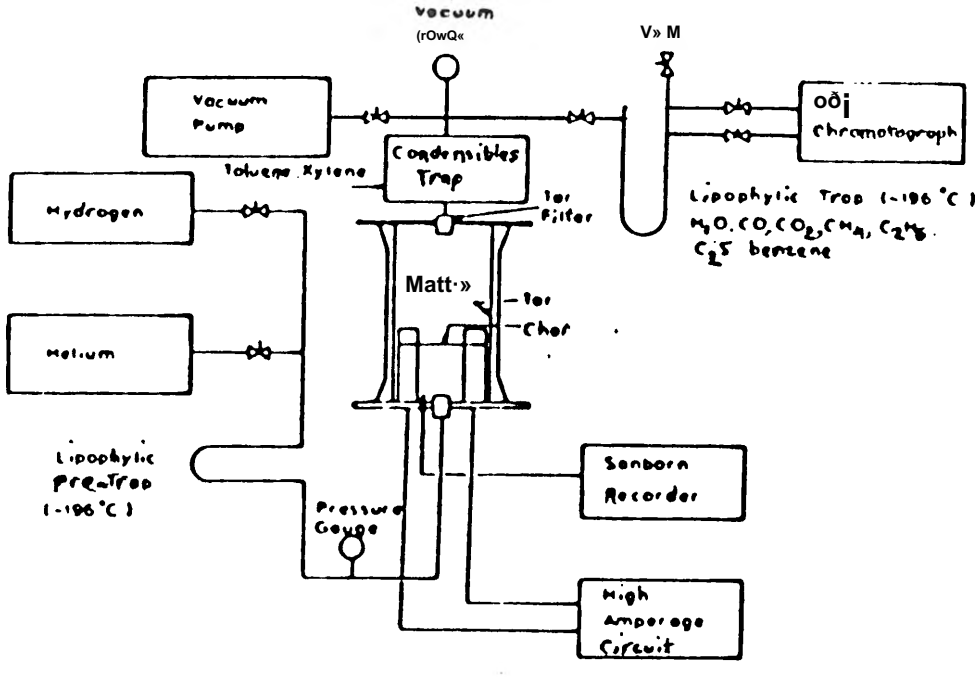

Figure III-1. Captive Sample Apparatus and Analysis System

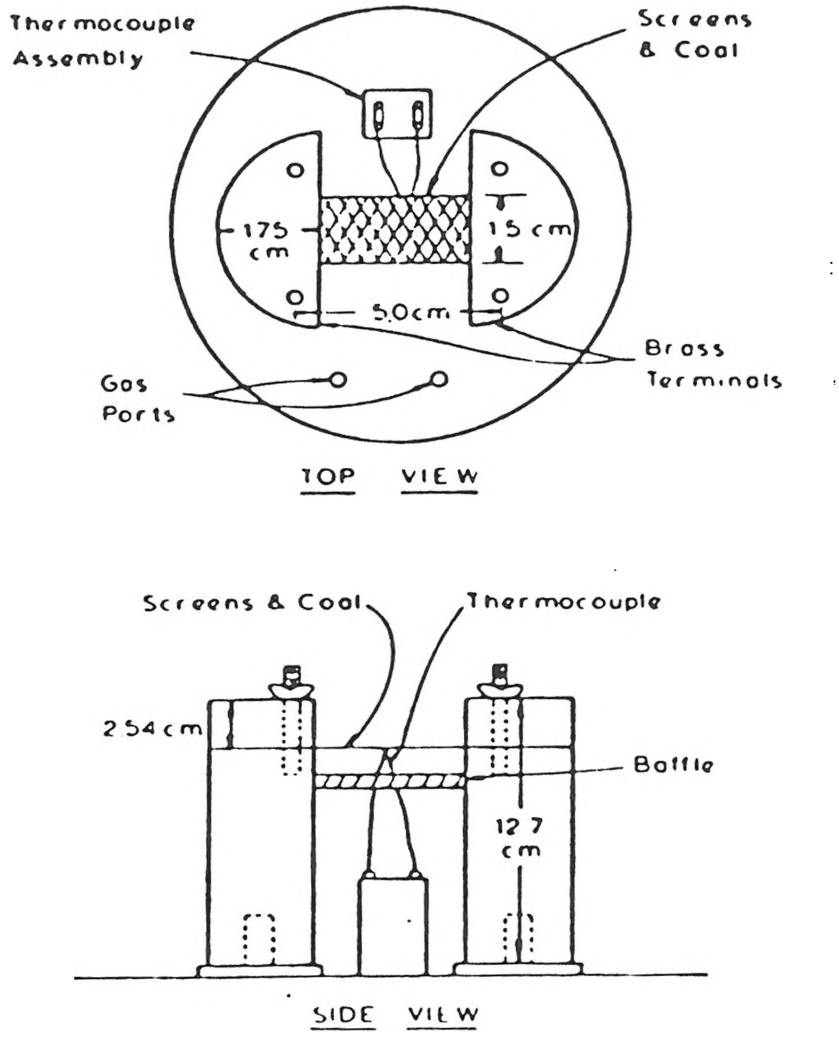

Figure III-2. Sample Holding and Heating Assembly.

second, placed within the sample between the folded screen and connected to a LINSEIS high speed stripchart recorder.

Procedure

A sample of 0.1 to 0.2 grams of powdered coal is spread in a layer on a preweighed screen which is reweighed after adding the coal, and is placed between the brass electrodes. The thermocouple head is inserted between the folded screen. The reactor is evacuated and flushed with helium three to five times to remove trace quantities of oxygen (air), and then repressurized at 5 psig helium.

A single throw double pole switch is thrown which puts the full power of batteries to the screen and starts a Cole-Parmer timer which is set for a predetermined amount of time (0.1-0.40 sec). At the end of indicated time another relay is tripped by the timer and the current passes through a plate resistor which causes the temperature to level off. After five seconds at the ultimate temperature the circuit is broken. Sample cooling by convection and radiation then occurs rapidly. The yield of char, which remains on the screen is determined gravimetrically. Gaseous products are analyzed by Gas Chromatograph.

The weight of the coal and screen was determined to within + 0.0005 gram, hence the uncertainty of the total weight loss measurement is about 0.05 percent by weight of the coal. The products quantitated chromatographically are subject to calibration uncertainties.

The inherent uncertainty of the thermocouple measurements is about $\pm$ 10°C over the present range of temperature.

The weight loss is divided by the weight loss obtained by ASTM analysis for that particular coal using Fisher Coal Analyzer (Model 490). The ratio is plotted against the temperature each set of 25 - 35 experiments were performed for 3 different sizes of Mississippi lignite and one size of Texas lignite.

CHAPTER IV

RESULTS

Pyrolysis is a series of thermal decomposition reactions resulting in volatiles and char-forming intermediates. These intermediates can escape as tar or liquid if their residence time inside the coal particle are sufficiently short as in the case of low pressures and small particles well dispersed (6).

During our experiments, Mississippi lignite was heated at a relatively rapid rate and it was determined that as temperature increased and particle size decreased more volatiles were released. In Table IV-1, the ASTM proximate analysis of the experimental samples are shown. In Table IV-2 through IV-5, the data collected on each sample is shown.

In Figures IV-1 to IV-9, we can see the weight loss with respect to temperature for three sizes of Mississippi lignite and one size of Texas lignite.

Figure IV-1 shows temperature versus weight loss for 30-60 mesh Mississippi lignite and we observe only loss of moisture up to 500-550°C. Above this range a rise in the weight loss indicates release of volatiles and this loss continues to increase upto about 850-900°C, after which no more weight loss is observed indicating the maximum volatile loss for this type of coal, apparatus and procedure.

TABLE IV-1

ASTM Proximate Analysis Of The
Experimental Lignite

ASTM PROXIMATE ANALYSIS

COAL TYPE	PARTICLE SIZE MESH (PM)	X* MOISTURE	X· VOLATILES	C7# fa ASH	X* FIXED CARBON
MISSISSIPPI	80-100 (177-149)	9.27	38.11	26.5	25.4
MISSISSIPPI	12-20 (1680-841 ;	8.1	42.1	28.8	18.1
MISSISSIPPI	30-60 (595-250)	7.04	33.50	39.86	19.6
TEXAS	30-60 (595-250)	19.93	37.74	10.11	32.2

* WET BASIS VALUES

TABLE IV-2

Collected Data On 30-60 Mesh
Mississippi Lignite

30 - 60 MESH MISSISSIPPI LIGNITE

Run Number	T (°C)	Sample Weight(g)	Char Weight(g)	Fractional Weight Loss (%)	(Fr. Wt. Loss / ASTM Wt. Loss)*	Heating Time (Sec)
S-17	320	0.1465	0.1380	5.8	14.3	0.1
S-3	342	0.5411	0.4937	9.6	23.7	0.2
S-I 6	481	0.1685	0.1567	7.0	17.3	0.1
S-12	648	0.1508	0.1321	17.9	31.9	
S-20	730	0.116	0.0875	24.0	59.0	0.4
S-7	750	0.3721	0.2700	27.9	67.6	0.3
S-4	775	0.226	0.1887	16.5	40.7	0.3
S-10	819	0.1478	0.0884	40.2	99.0	0.4
S-22	855	0.1661	0.1089	34.4	85.0	0.3
S-5	910	0.1714	0.1120	35.0	86.0	0.3

* ASTM Weight Loss - (Volatile Matter + Moisture) Wet Basis

TABLE IV-3

Collected Data On 12-20 Mesh
Mississippi Lignite

12-20 MESH MISSISSIPPI LIGNITE

RUN Number	T(°C)	Sample Weight(g)	Char Weight(g)	Weight Loss(%)	(Wt. Loss / ASTM Wt. Loss)*	Time Heated
S"2	320	0.2011	0.1913	4.87	9.7	0.5
S"5	367	0.2715	0.256	5.7	11.3	0.5
S"42	440	0.1062	0.0967	8.95	17.8	0.1
S"27	510	0.2586	0.2274	12.06	24.0	0.2
S"43	575	0.1008	0.0916	9.17	18.0	0.2
S"28	603	0.270	0.240	11.1	22.1	0.3
S"6	626	0.1812	0.1606	11.37	22.6	0.7
S"51	630	0.1000	0.0757	24.3	48.4	0.2
S"49	708	0.1000	0.0676	32.4	64.5	0.2
S"50	750	0.1048	0.0837	20.13	40.0	0.3
S"48	772	0.1060	0.0915	13.7	27.3	0.3
S"41	794	0.1010	0.0732	27.5	55.0	0.1
S"44	794	0.1030	0.0748	27.38	54.5	0.3
S"55	794	0.1020	0.0747	26.7	53.2	0.4
S"56	820	0.0988	0.0631	36.1	72.0	0.4
S"59	820	0.0995	0.0581	41.6	82.8	0.4
S"54	843	0.1013	0.0639	36.9	73.5	0.3
S"61	843	0.1255	0.0925	26.29	52.4	

* ASTM Weight Loss =(Volatile Matter + Moisture) Dry Basis

TABLE İV-4

Collected Data On 80-100 Mesh
Mississippi Lignite

80 - 100 MESH MISSISSIPPI LIGNITE

Run Number	T (°C)	Sample Weight (g)	Char Weight(g)	Fractional Weight Loss (%)	Fr. Wt. Loss / ASTM Wt. Loss *	Heating Time (sec)
S*-44	295	0.6215	0.1149	5.4	13.5	0.1
S*-2	386	0.1357	0.1196	11.86	23.1	0.1
S*-3	386	0.1252	0.1085	13.33	26.0	0.1
S*-43	462	0.1043	0.0932	10.6	20.6	0.1
S*-37	473	0.1318	0.1183	10.24	20.0	0.2
S*-52	532	0.1092	0.0836	2.34	45.7	0.2
S*-54	550	0.0976	0.0765	21.61	42.2	0.2
S*-40	697	0.1081	0.8855	22.75	44.4	0.2
S*-45	709	0.1017	0.064	37.0	72.0	0.2
S*-35	720	0.1107	0.075	32.2	62.8	0.2
S*-38	720	0.1062	0.0854	19.58	38.2	0.2
S*-51	722	0.1028	0.0777	24.4	47.6	0.1
S*-32	730	0.1051	0.0644	38.7	75.5	0.2
S*-56	767	0.1033	0.0720	30.30	59.0	0.2
S*-42	768	0.0994	0.0642	35.4	69.0	0.2
S*-39	780	0.1000	0.0692	30.8	60.0	0.3
S*-49	794	0.1000	0.0621	37.9	74.0	0.2
S*-48	794	0.1037	0.0685	33.9	66.0	0.2
S*-33	843	0.1197	0.0697	41.79	81.5	0.3

* ASTM Weight Loss = (Volatile Matter + Moisture) Dry Basis

TABLE IV-5

Collected Data On 30-60 Mesh
Mississippi Lignite

30 - 60 MESH TEXAS LIGNITE

Run Number	T (°C)	Sample Weight(g)	Char Weight(g)	Fractional Weight Loss (%)	/ Fr. Wt.\ ƒ Loss U \ ASTM Wt/" ' Loss *	Heating Time (Sec)
S^T-4	320	0.0912	0.0771	15.4	23.0	0.1
S^T-12	320	0.1037	0.0878	15.3	23.0	0.1
S^T-22	410	0.0978	0.0802	18.0	26.8	0.1
S^T-36	450	0.0916	0.0741	19.1	28.5	0.2
S^T-35	533	0.1067	0.0883	17.2	25.6	0.2
S^T-53	556	0.1030	0.0738	28.3	42.2	0.2
S^T-41	690	0.0788	0.0547	30.6	45.6	0.1
S^T-32	720	0.1000	0.0718	28.2	42.0	0.1
S^T-42	733	0.1005	0.0613	30.0	58.0	0.2
S^T-31	740	0.0900	0.051	43.2	64.4	0.3
S^T-28	747	0.1110	0.0753	32.2	48.0	0.3
S^T-43	747	0.1037	0.0605	42.0	62.6	0.3
S^T-33	760	0.1129	0.0712	37.0	55.0	0.3
S^T-51	765	0.1040	0.0575	44.7	66.6	0.4
S^T-45	770	0.1015	0.0589	41 .9	62.4	0.3
S^T-50	770	0.1059	0.060	43.0	64.0	0.3
S^T-47	786	0.0994	0.0612	38.43	57.3	0.4
S^T-38	794	0.1010	0.0595	41.10	61.3	0.2
S^T-30	830	0.0926	0.0633	32.0	47.7	0.2

* ASTM Weight Loss =(Volatile Matter + Moisture) Dry Basis

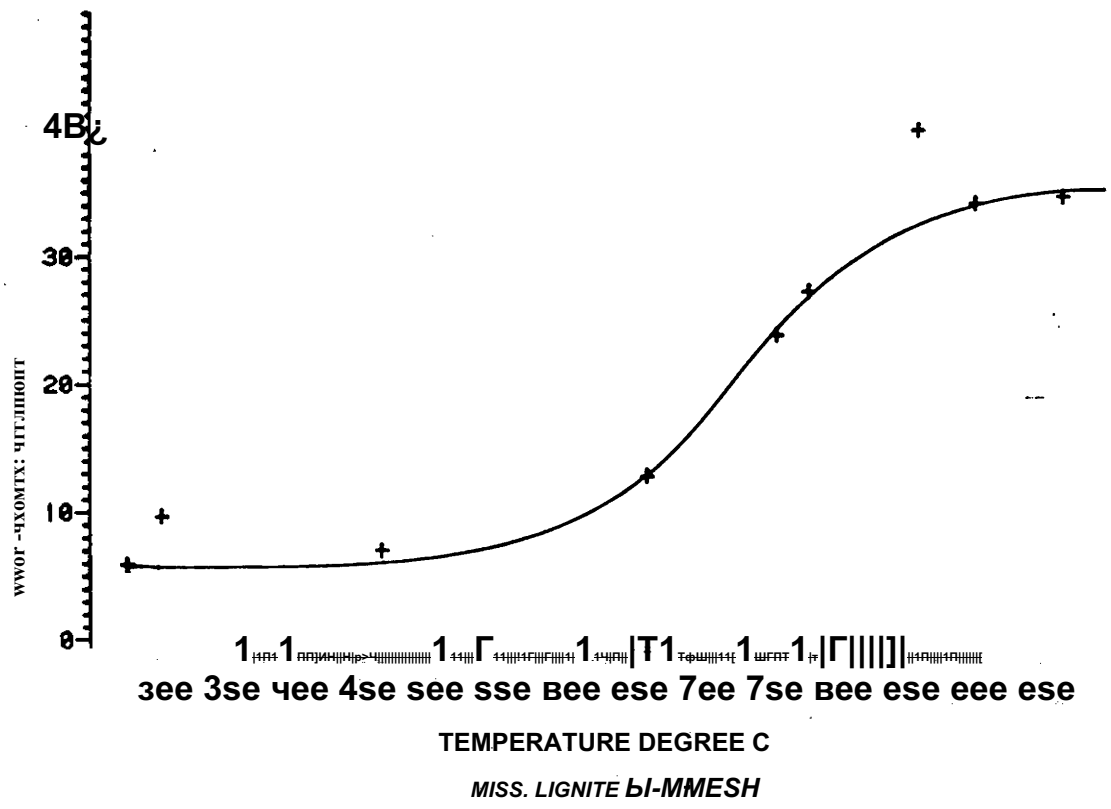

Figure IV-1. Weight Loss vs. Temperature For 30-60 Mesh Mississippi Lignite

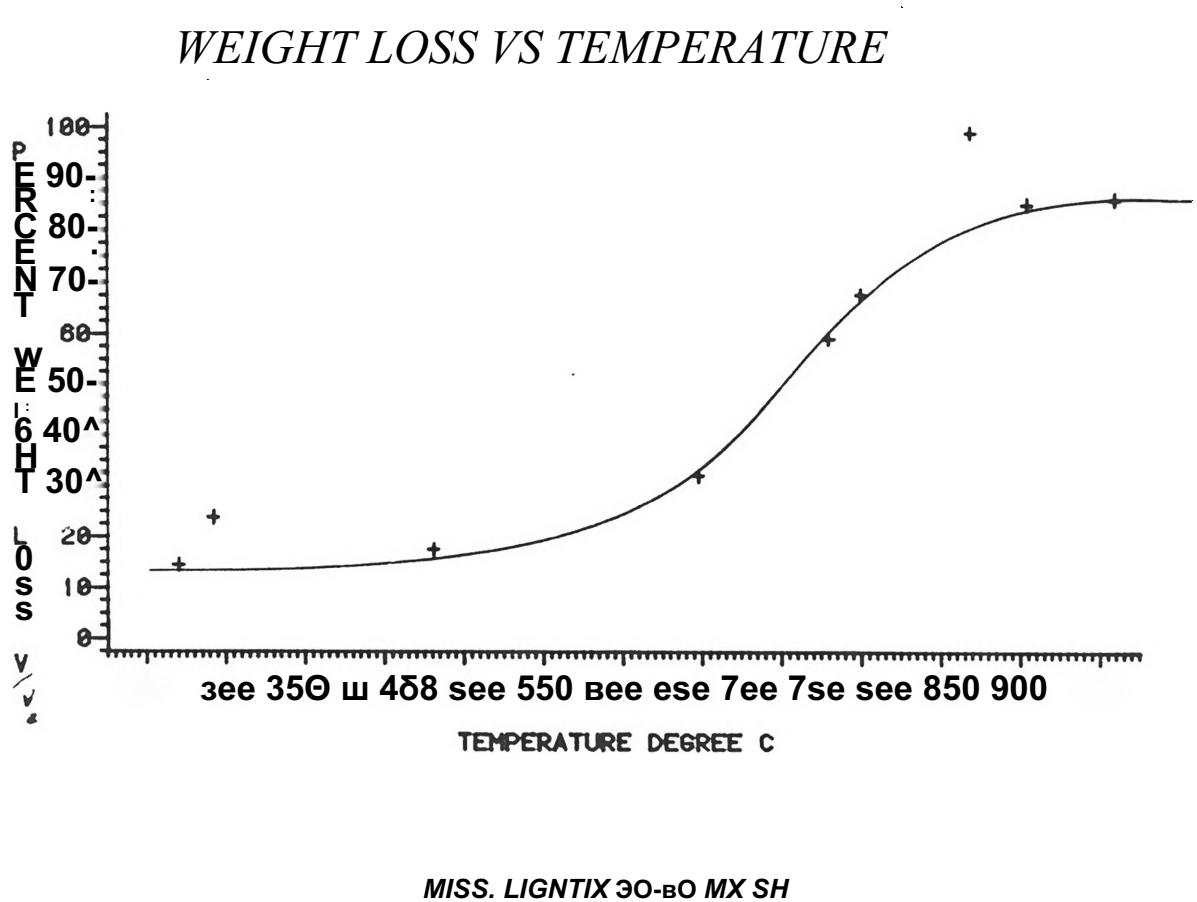

Figure IV-2. ASTM Weight Loss vs. Temperature for 30-60 Mesh Mississippi Lignite

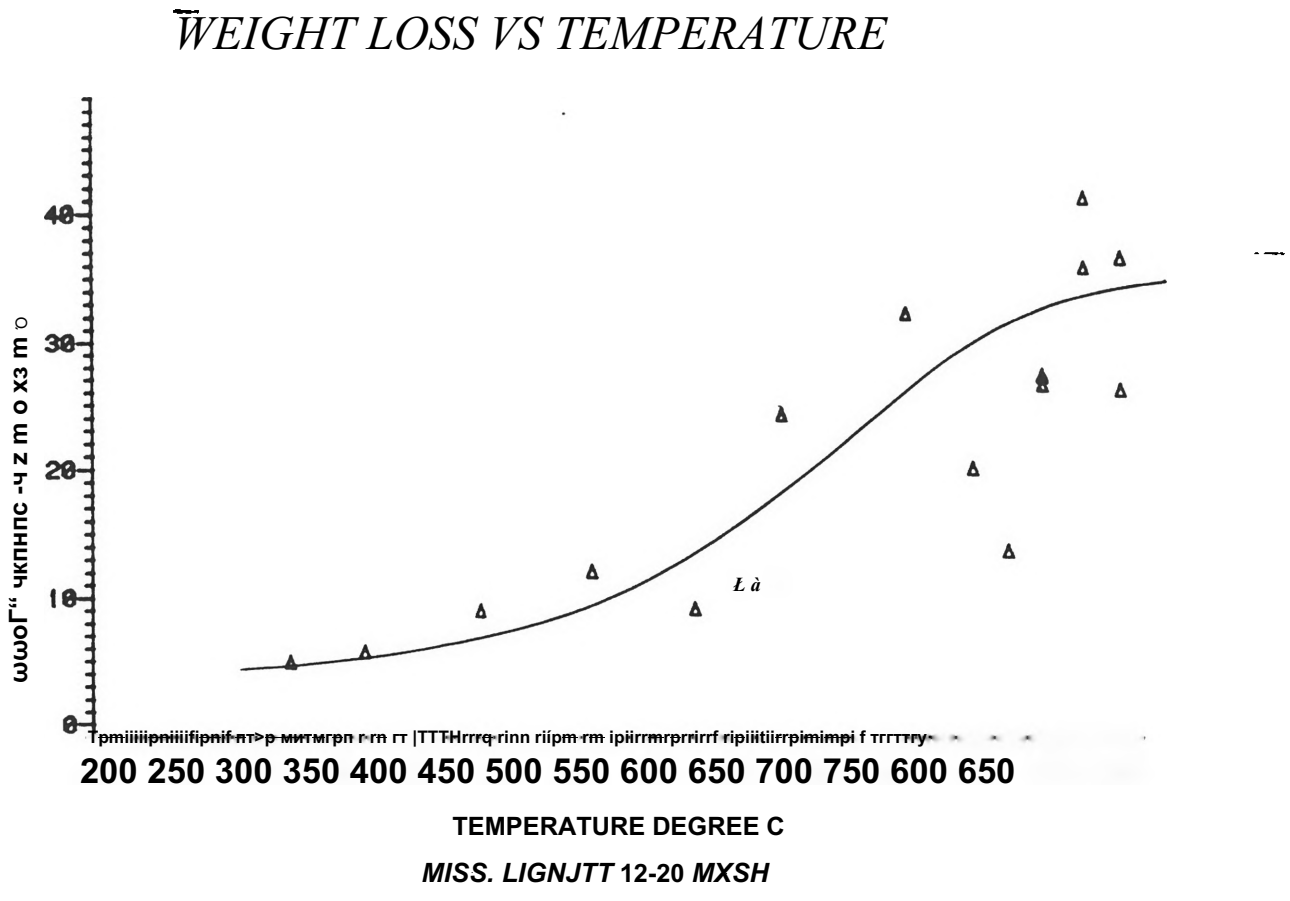

'Figure IV-3. Weight Loss vs. Temperature For 12-20 Mesh Mississippi Lignite

WEIGHT LOSS VS TEMPERATURE

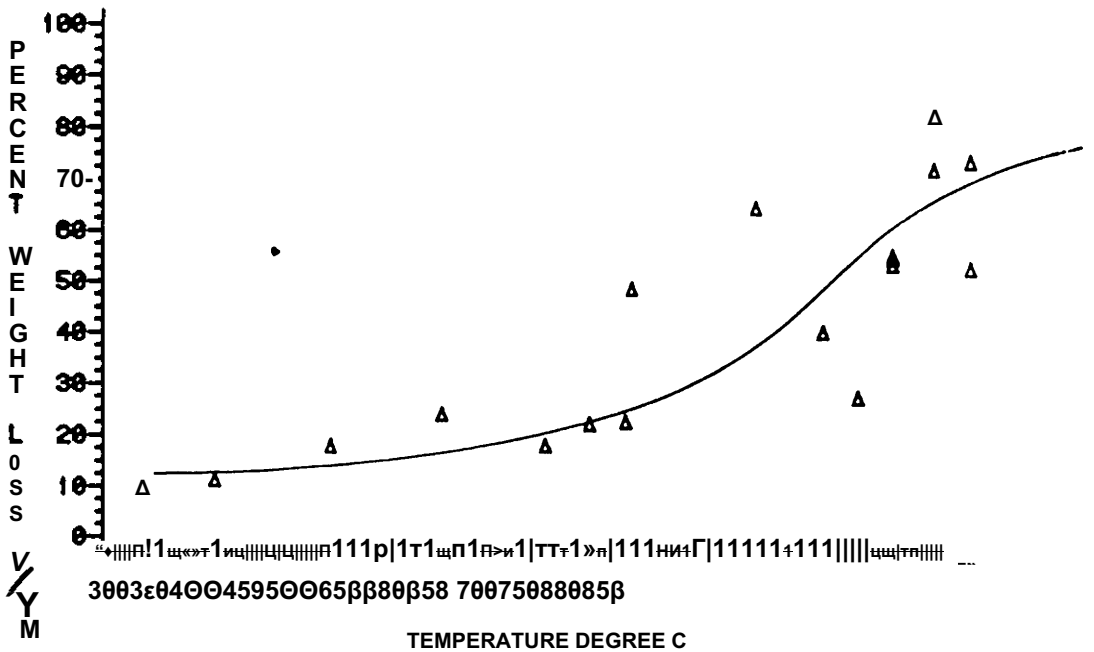

MISS. LIGNITI* 12-20 *MESH

Figure IV-4. ASTM Weight Loss vs. Temperature For 12-30 Mesh Mississippi Lignite

In the 12-20 mesh Mississippi lignite, Figures IV-3 and IV-4, loss of volatile matter also begins at 500-550°C, but 80-100 mesh Mississippi lignite begins to lose volatiles at 400-500°C.

The maximum, volatile release occurs at 800-850°C in the larger particles, but at lower temperature 750-800°C in the 80-100 mesh (Figures IV-5 and IV-6), As is shown the rate of weight loss increases as the particle size decreases due to the shorter residence time for secondary char-forming reactions to take place in the smaller particles.

Figures IV-7 and IV-8 show weight loss versus temperature for 30-60 mesh Texas lignite and Figure IV-9 shows the Texas lignite in comparison to the Mississippi lignites. The Texas lignite began losing volatile matter at 400-500°C and the maximum volatile loss occurred at 700-750°C. Because of the high moisture content of the Texas lignite it appears to release more volatile matter but about half of the 43 percent weight loss is water.

In Figure IV-10, the weight loss of 30-60 mesh Mississippi lignite is compared under two different heating rates and reaction holding time. The weight loss of the experiments performed by Don Farage (9) at lower heating rate but longer reaction holding time is higher than the shorter holding time.

Figure IV-10 shows that the data of Farage (9), Cox (10) and Agarwal (11) are reasonably consistent. Farage took data at an unknown heating rate in a 1 inch tubular fixed bed reactor over 20 minutes. Agarwal's data was obtained over 37 minutes in a proximate analyzer furnace which has been estimated to heat at 35°C/minute (11). Cox

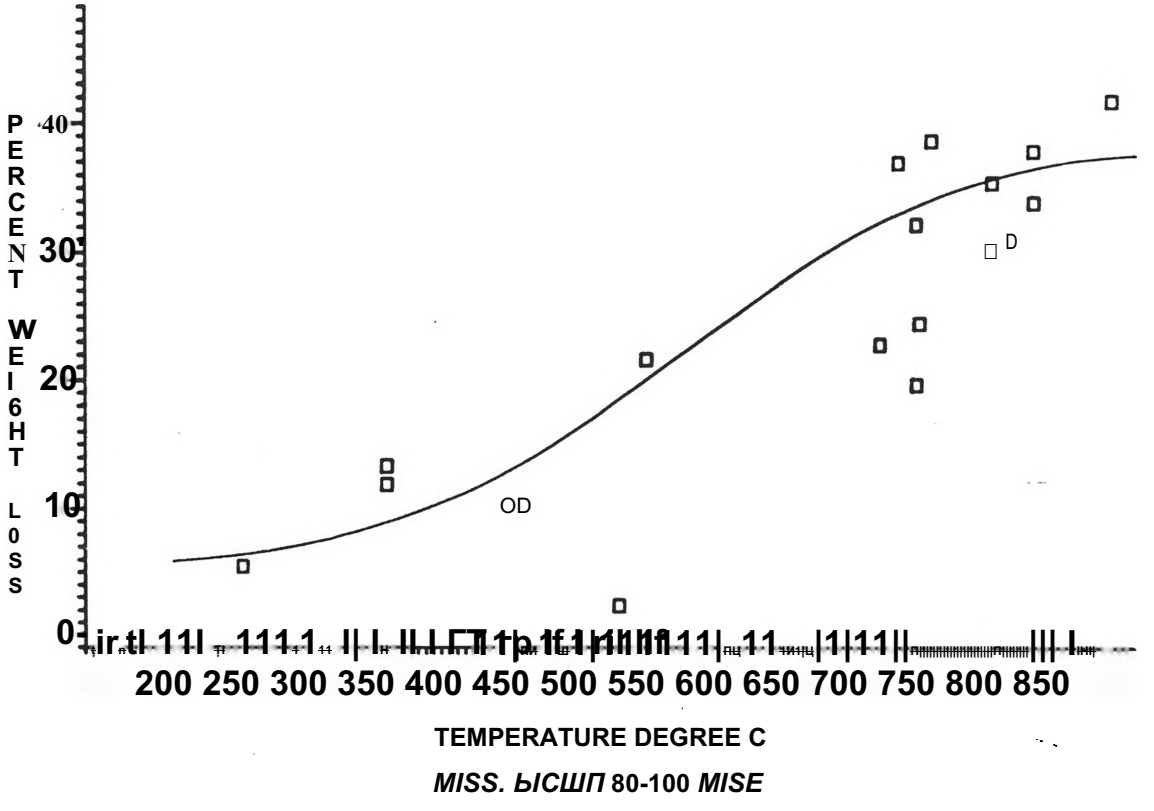

Figure IV-5. Weight Loss vs. Temperature For 80-100 Mesh Mississippi Lignite

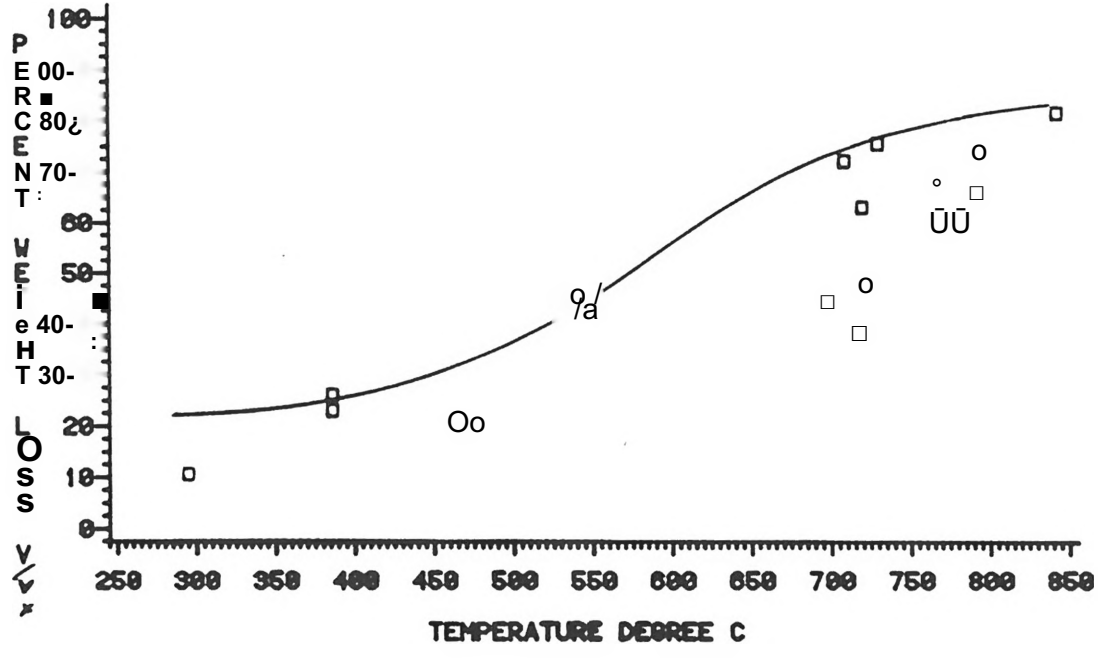

Figure IV-6. ASTM Weight Loss vs. Temperature For 80-100 Mesh Mississippi Lignite

WEIGHTLOSS VS TEMPERATURE

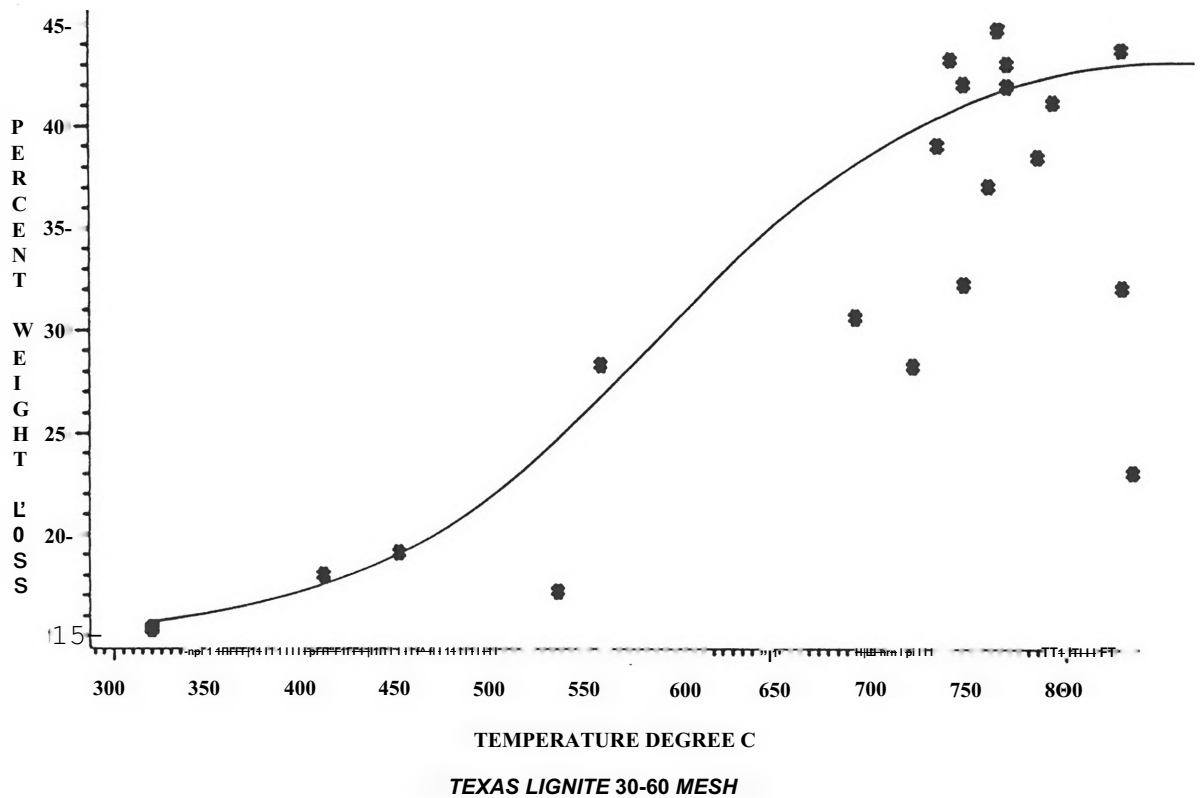

Figure IV-7. Weight Loss vs. Temperature For 30-60 Mesh Texas Lignite

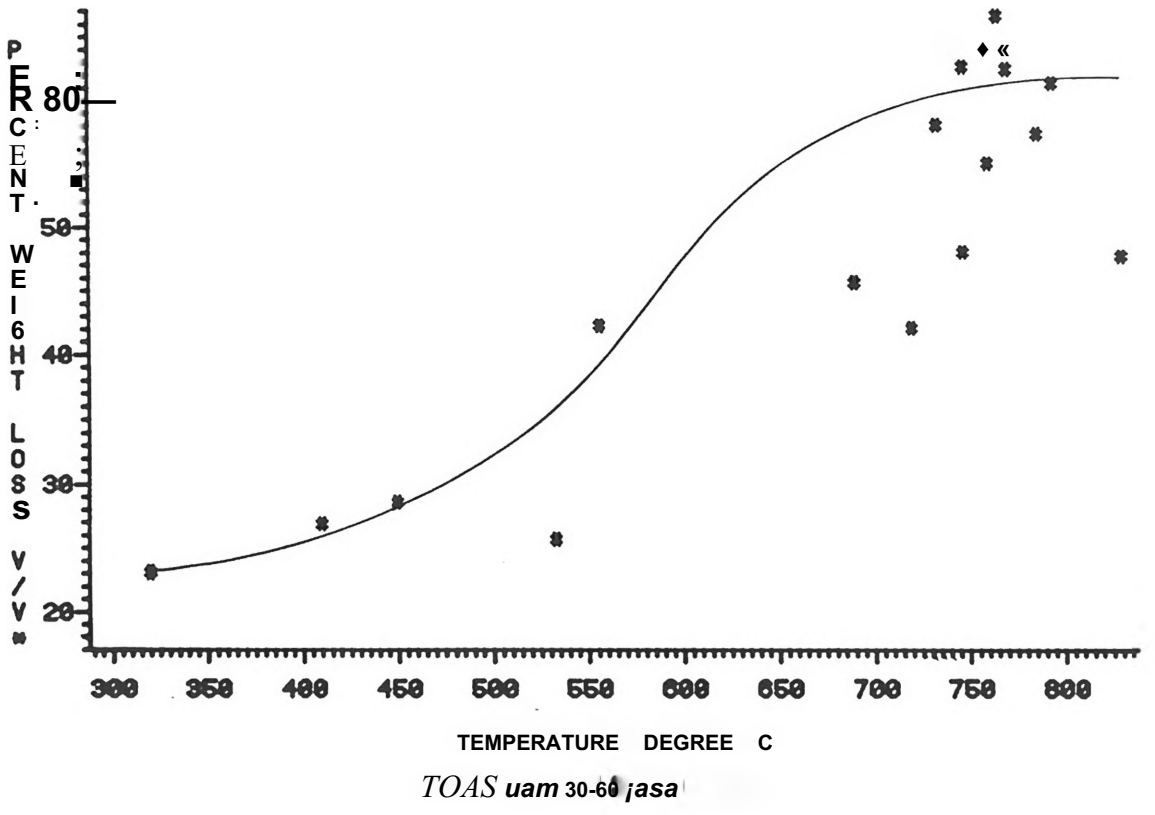

Figure IV-8. ASTM Weight Loss vs. Temperature For 30-60 Mesh Texas Lignite

WEIGHT LOSS VS TEMPERATURE

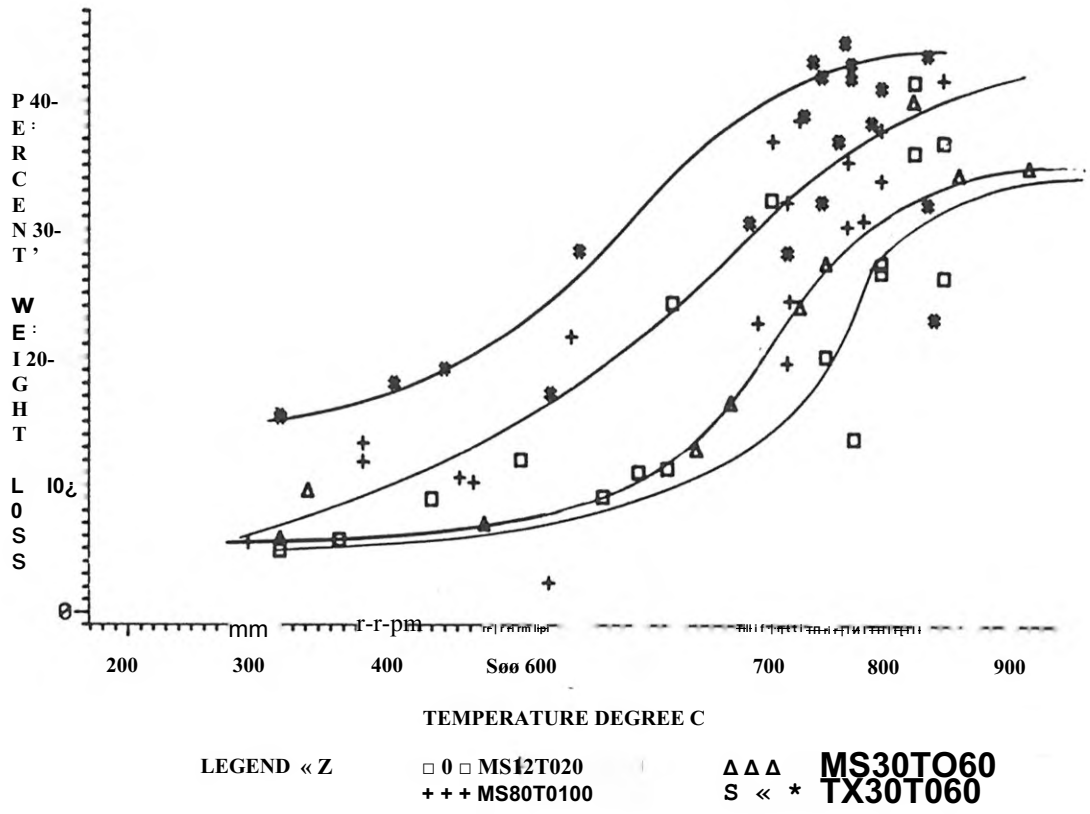

Figure IV-9. Weight Loss vs. Temperature For Three Different Sizes Of Mississippi Lignite and One Size of Texas Lignite

PERCENT OF ASTM VOLATILES RELEASED VS. TEMPERATURE

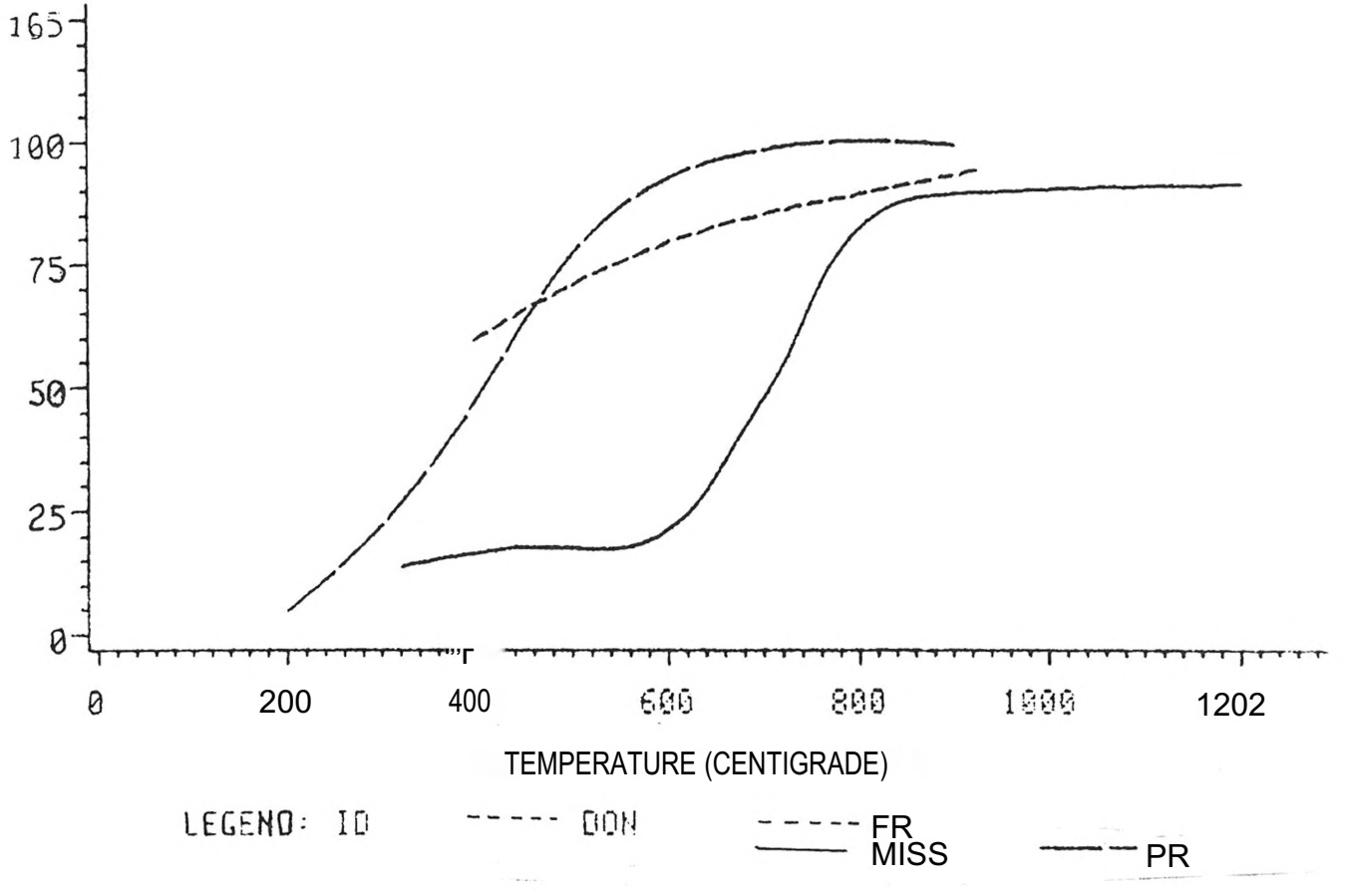

Figure IV-10. ASTM Weight Loss vs. Temperature for Mississippi Lignite Obtained By Different Holding Time and Heating Rate.

collected data at a heating rate of about 175°C/second with a reaction time of about 15 seconds. Figure IV-10 shows higher weight loss is obtained by the longer reaction holding time.

Figure IV-11 shows weight loss by Mississippi lignite compared to Texas (14), North Dakota (13) and Australian Brown Coal (12) from the literature. Our weight loss data is consistent with other data from the literature.

In Figure IV-12 the weight loss of Mississippi lignite is compared to Montana lignite.

Figure IV-13 shows the weight loss of Montana lignite versus temperature (7). As we can see there is a similar scattering in this data with those obtained on Mississippi and Texas lignite. These scatterings are due to the wide range of heating rates (about 500-2000°C), the thermocouple and unknown complexities.

PERCENT OF VOLATILES RELEASED VS. TEMPERATURE

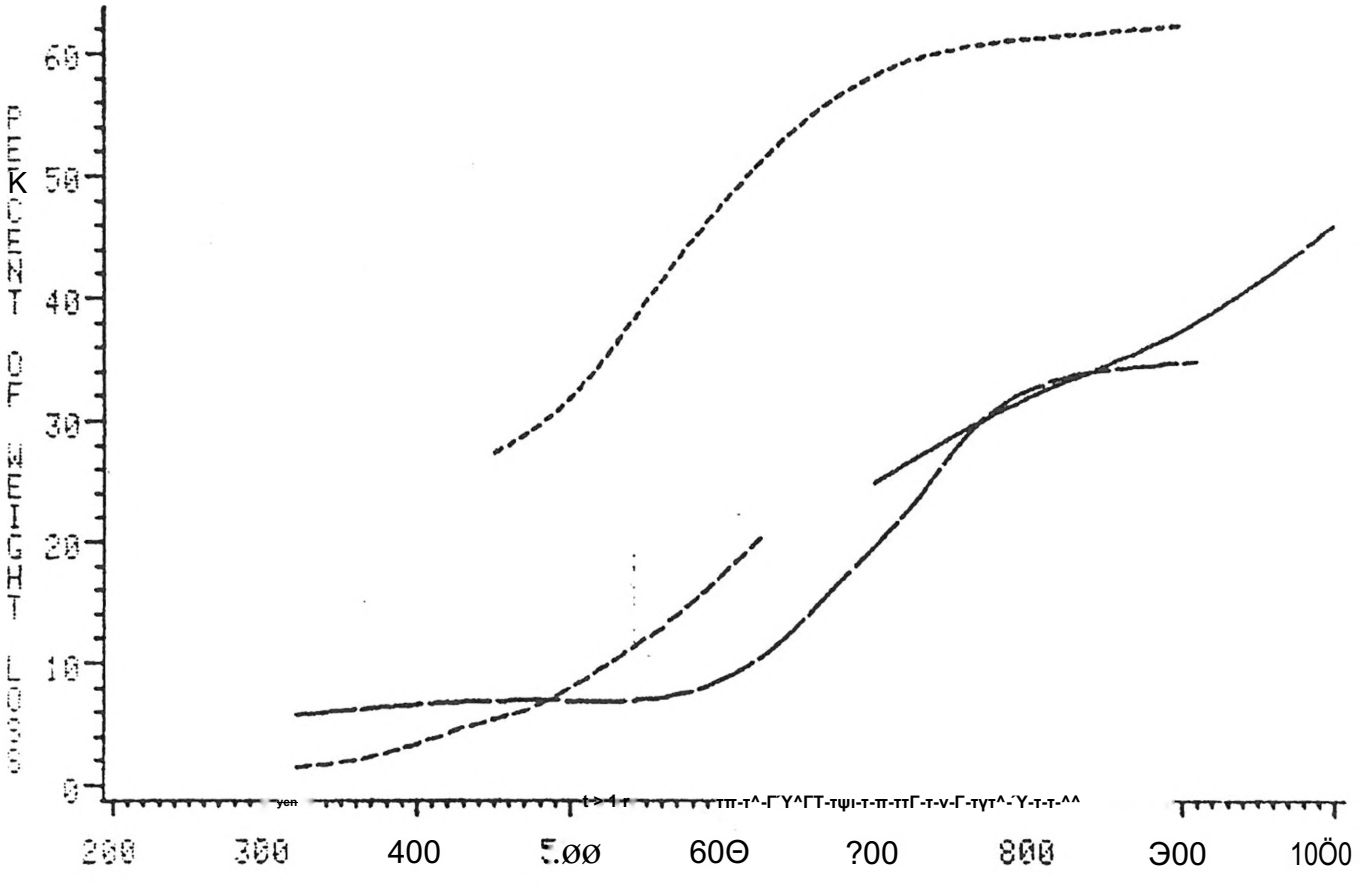

Figure IV-11. Weight Loss vs. Temperature For Mississippi Lignite As Compared To Australian Brown Coal, North Dakota Lignite and Texas Lignite

PERCENT OF ASTM VOLATILES RELEASED VS. TEMPERATURE

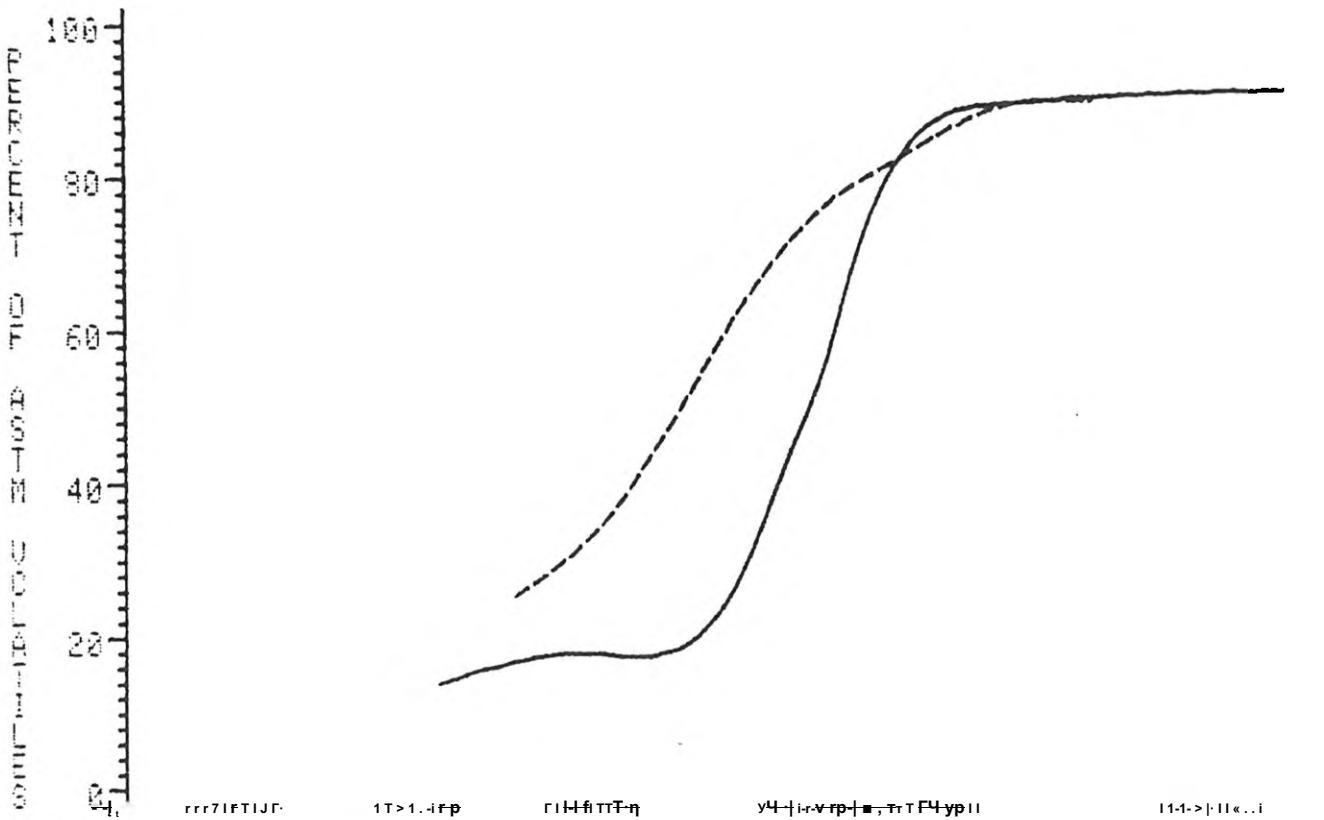

Figure IV-12. ASTM Weight Loss vs. Temperature For Mississippi Lignite Compared To Montana Lignite

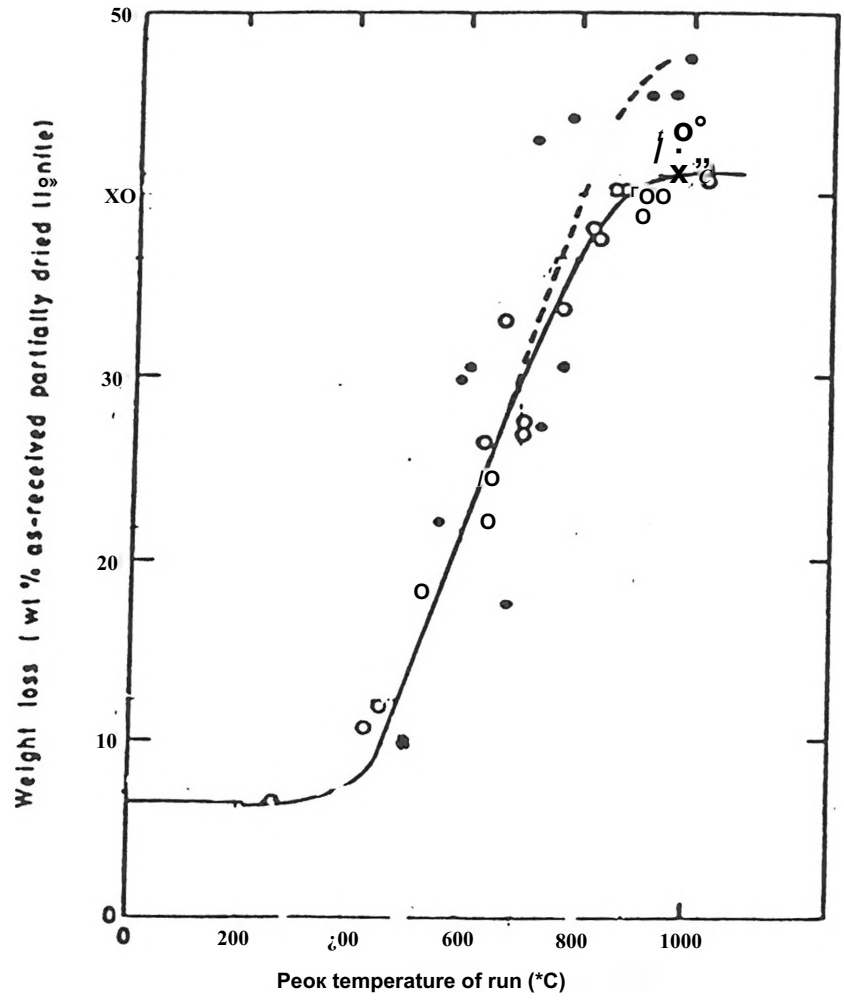

Figure IV-13. Comparison of Total Weight Loss From Pyrolysis and Hydropyrolysis of Lignite To Different Peak Temperatures.

(£ ,69 atm H; O, 1 atm He; heating rate, 1000°C s -1)

REFERENCES

1. Anthony, D.B. and Howard, J.B., "Coal Devolatilization and Hydrogasification", AIChE Journal, Vol. 22, No. 4, July 1976, p. 625.

2. Haynes, Henry W., Dr., "Gasification of Mississippi Lignites", University of Mississippi, University, Mississippi

3. Anthony, D.B., Howard, J.B., Meissner, H.P. and Hottel, H.C., "Apparatus For Determining High Pressure Coal. Hydrogen Reaction Kinetics Under Rapid Heating Conditions", Rev. Sei. Instrum., Vol. 45, No. 8, August 1974, p. 992.

4. Anthony, D.B., Howard, J.B., Hottel, H.C. and Meissner, H.P., "Rapid Devolatilization of Pulverized Coal", p. 1303.

5. Wen, C.Y. and Dutta, S., "Solid Gas Reactions in Coal Conversion Processes", West Virginia University, Morgantwon, WV, p. 40.

6. Anthony, D.B., Howard, J.B., Hottel, H.C. and Meissner, H.P., "Rapid Devolatilization and Hydrogasification of Bituminous Coal", Fuel, 1976, Vol. 55, April, p. 121.

7. Suuberg, E.M., Peters, W.A. and Howard, J.B., "Product Composition In Rapid Hydropyrolysis of Coal", Fuel, 1980, Vol. 59, June, p. 405.

8. Suuberg, E.M., Peters, W.A. and Howard, J.B., "Product Composition And Kinetics of Lignite Pyrolysis", Ind. Eng. Chern. Process Des. Dev., Vol. 17, No. 1, 1978, p. 37.

9. Farage, Donald L., Thesis, University of Mississippi, 1984.

10. Cox, Frank W. , Dissertation, University of Mississippi, (in progress).

11. Agarwal, Pradeep K., Dissertation, University of Mississippi, 1983.

12. Tyler, R., Fuel, Vol. 58, 1979, p. 680.

13. Suuberg and Scelza, Fuel, Vol. 61, 1982, p. 198.

14. Torrest, Robert S. and VanMeura, P., "Laboratory Studies of the Rapid Pyrolysis and Desulphurization of a Texas Lignite", Fuel, 1980, Vol. 59, July, p. 458.